
Air-Sea Interactions of Natural Long-Lived Greenhouse Gases (CO₂, N₂O, CH₄) in a Changing Climate

3

Dorothee C.E. Bakker, Hermann W. Bange, Nicolas Gruber, Truls Johannessen, Rob C. Upstill-Goddard, Alberto V. Borges, Bruno Delille, Carolin R. Löscher, S. Wajih A. Naqvi, Abdirahman M. Omar, and J. Magdalena Santana-Casiano

Abstract

Understanding and quantifying ocean–atmosphere exchanges of the long-lived greenhouse gases carbon dioxide (CO₂), nitrous oxide (N₂O) and methane (CH₄) are important for understanding the global biogeochemical cycles of carbon and nitrogen in the context of ongoing global climate change. In this chapter we summarise our current state of knowledge regarding the oceanic distributions, formation and consumption pathways, and oceanic uptake and emissions of CO₂, N₂O and CH₄, with a particular emphasis on the upper ocean. We specifically consider the role of the ocean in regulating the tropospheric content of these important radiative gases in a world in which their tropospheric content is rapidly increasing and estimate the impact of global change on their present and future oceanic uptake and/or emission. Finally, we evaluate the various uncertainties associated with the most commonly used methods for estimating uptake and emission and identify future research needs.

3.1 Introduction

Carbon dioxide (CO₂), nitrous oxide (N₂O) and methane (CH₄) are long-lived atmospheric greenhouse gases, whose global budgets are substantially determined by

the marine system. Understanding and accurately predicting the evolution of the marine CO₂ sink and the marine emissions of N₂O and CH₄ is of great importance for future climate change scenarios as used in studies for the Intergovernmental Panel on Climate Change (Denman et al. 2007).

The tropospheric dry mole fractions of these three greenhouse gases (Box 3.1) have been increasing since the industrial revolution, principally reflecting anthropogenic inputs, but also comparatively small fluctuations in the balance of natural sources and sinks. The tropospheric abundance of CO₂ has been regularly monitored since the late 1950s, and those of N₂O and CH₄ since the 1970s (<http://agage.eas.gatech.edu/index.htm>; <http://www.esrl.noaa.gov/gmd>) (Fig. 3.1). Table 3.1 summarises the tropospheric abundances, lifetimes, and radiative forcings of CO₂, N₂O and CH₄ for 2005

D.C.E. Bakker (✉)
e-mail: d.bakker@uea.ac.uk

H.W. Bange (✉)
e-mail: hbange@geomar.de

N. Gruber (✉)
e-mail: nicolas.gruber@env.ethz.ch

T. Johannessen (✉)
e-mail: truls.johannessen@gfi.uib.no

R.C. Upstill-Goddard (✉)
e-mail: rob.goddard@ncl.ac.uk

Box 3.1

Atmospheric gases are quantified by their dry mole fraction, given in units of ppm or $\mu\text{mol mol}^{-1}$ for CO₂ and in units of ppb or nmol mol^{-1} for N₂O and CH₄. In this chapter we report annual fluxes in Pg C year⁻¹ for CO₂, in Tg C year⁻¹ for CH₄ and in Tg N year⁻¹ for N₂O. One Pg (Petagram) is equivalent to 10¹⁵ g and one Tg (Teragram) is equivalent to 10¹² g. The troposphere is the lower part of the atmosphere and extends from the Earth's surface to the tropopause at 10–15 km height. In this chapter we are mainly concerned with the troposphere, unless specified otherwise.

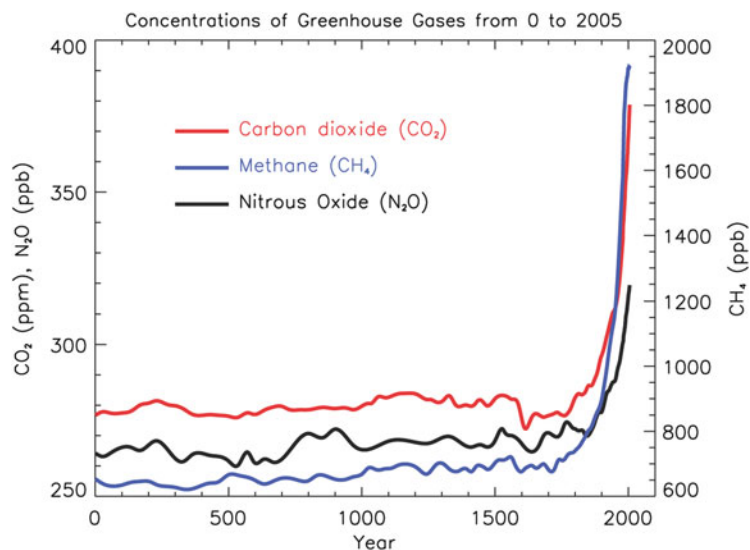


Fig. 3.1 Atmospheric concentrations of carbon dioxide, methane and nitrous oxide over the last 2,000 years (Reproduced from Forster et al. (2007) by permission of the IPCC)

Table 3.1 The tropospheric dry mole fractions, radiative forcings (RF) and lifetimes (adjustment time) of CO₂, N₂O and CH₄ (After Forster et al. 2007; WDCGG 2012)

Gas	Abundance in 2010	Abundance in 2005	RF in 2005 (W m^{-2})	Lifetime (years)
CO ₂	389.0 ppm	379 ± 0.65 ppm	1.66	See below ^a
N ₂ O	323.2 ppb	319 ± 0.12 ppb	0.16	114
CH ₄	1,808 ppb	$1,774 \pm 1.8$ ppb	0.48	12

^aNo single adjustment time exists for CO₂ (Joos et al. 2001), as the rate of removal of CO₂ from the troposphere is determined by the removal rate of carbon from the surface ocean (Annexe I in IPCC 2007). An approximate value of 100 years may be given, while decay constants of 172.9 to 18.51 and 1.186 years have been used in models (Forster et al. 2007).

(Forster et al. 2007). An increase in the dry mole fractions (Box 3.1) of these long-lived greenhouse gases leads to tropospheric warming and stratospheric cooling, which may impact on chemical reaction rates and atmospheric dynamics (Wayne 2000). Other effects of changes in the dry mole fractions of these gases are listed in Table 3.2.

Global CO₂ emissions are currently increasing exponentially, primarily reflecting the accelerating development of large emerging economies such as

China and India (Friedlingstein et al. 2010). If sustained, this recently rapid growth in tropospheric CO₂ may precipitate critical climate and other global environmental changes, possibly faster than previously identified (e.g. IPCC 2007).

Given its current tropospheric growth and the ongoing decline in chlorofluorocarbon (CFC) emissions, N₂O may soon replace CFCs as the fourth most important greenhouse gas after water vapour (H₂O), CO₂ and CH₄ (Forster et al. 2007). The major sink of N₂O is

Table 3.2 Air-sea exchange and impact of the long-lived greenhouse gases CO₂, N₂O and CH₄ in a changing climate, as discussed in this chapter. See Table 3.1 for the radiative forcings and atmospheric lifetimes

Gas	Role in atmospheric chemistry	Oceanic contribution to contemporary atmospheric budget	Impact of environmental change on air-sea gas exchange in the twenty-first century
CO ₂	Inert	Net ocean sink for about 30 % of CO ₂ emissions from human activity partly mitigates climate change; the ocean ultimately controls atmospheric CO ₂ content	Global warming The net ocean sink likely to decrease by 2100 Coastal CO ₂ sink likely to increase
N ₂ O	Largely inert in the troposphere; depletion of stratospheric O ₃	Open ocean natural N ₂ O source, coastal regions (incl. rivers) anthropogenic N ₂ O source, equivalent to 20 % and 10 % of the global N ₂ O emissions	Ocean acidification Small effect on ocean CO ₂ sink Unknown Increase of subsurface production Negligible or small increase in the open ocean N ₂ O source Large increase in the coastal N ₂ O source
CH ₄	Regulates tropospheric O ₃ and OH radical; affects stratospheric O ₃ chemistry; CO ₂ source	Natural open ocean and coastal CH ₄ sources equivalent to 10 % of the global, natural CH ₄ sources; continental CH ₄ seeps poorly known	Global warming Increased CH ₄ release from CH ₄ hydrates and increased CO ₂ release upon oxidation of hydrate-derived CH ₄ Unknown Negligible or small increase in the open ocean CH ₄ source Negligible or small increase in coastal CH ₄ source

Table 3.3 Sources and sinks of tropospheric CH₄. Ranges are derived from estimates for the period 1983–2004, as compiled by Denman et al. (2007)

	CH ₄ sources and sinks (Tg C year ⁻¹)
Natural sources:	
Wetlands	75–173
Termites	15–22
Oceans, incl coastal regions	3–11
Hydrates	3–4
Geological sources	3–11
Wild animals	11
Wildfires	2–4
Total natural sources	109–195
Anthropogenic sources:	
Energy	56–58
Coal mining	23–36
Gas, oil, industry	36–68
Landfills and waste	26–52
Ruminants	57–142
Rice agriculture	23–84
Biomass burning	11–66
Vegetation	27
Total anthropogenic sources	198–321
Total sources:	377–458
Sinks:	
Tropospheric OH radical	321–383
Soils	20–26
Stratospheric loss	22–34
Total sinks	386–436

the stratosphere where it photochemically decomposes via reaction with O(¹D) (oxygen singlet D) to form nitric oxide (NO) radicals. The latter represent a major removal pathway for stratospheric ozone (O₃) (Crutzen 1970; Ravishankara et al. 2009). Indeed, N₂O is expected to become the dominant O₃ depleting compound during the twenty-first century (Ravishankara et al. 2009).

CH₄ is the most abundant organic species in the troposphere, where it influences oxidising capacity and regulates levels of O₃ and OH (hydroxyl free radical). Oxidation of CH₄ by OH to CO₂ and CO (carbon monoxide) is its major tropospheric sink (Table 3.3). In the stratosphere photo-oxidation of CH₄ is a major source of stratospheric H₂O, which influences both tropospheric warming and stratospheric cooling (Michelsen et al. 2000), and a small source of stratospheric CO₂. CH₄ plays a complex role in stratospheric O₃ chemistry (Wayne 2000). Additional stratospheric

CO₂ arises from rapid CO oxidation. However, these two CO₂ sources are minor and as there are no recognised stratospheric sinks for CO₂ (Hall and Prather 1993); any variation in stratospheric CO₂ principally reflects the inflow of tropospheric air masses.

3.1.1 Atmospheric Greenhouse Gases from Ice Cores

Analysis of the composition of fossil air trapped in ice cores has extended the tropospheric histories of all three gases, to ~800,000 years before present (YBP) for CO₂ (Petit et al. 1999; EPICA community members 2004; Lüthi et al. 2008) and to ~650,000 YBP for N₂O and CH₄ (Spahni et al. 2005). These data show that during the last 650,000 years CO₂ has varied from ~170 ppm during glacials to ~280 ppm during interglacials, while during the preceding 100,000 years the range was somewhat smaller. For comparison, tropospheric CO₂ increased from 280 ppm pre-industrially to 389 ppm in 2010 (Forster et al. 2007; WDCGG 2012). Changes in ocean circulation and biology and the feedbacks between them have been invoked to explain the glacial/interglacial fluctuations of tropospheric CO₂ but understanding the precise mechanistic details remains a substantial challenge (Jansen et al. 2007). Over the last 420,000 years, tropospheric CO₂ has tracked reconstructed changes in Antarctic temperature with a time lag of several hundred to a thousand years (Mudelsee 2001), implying that changes in the physical climate system such as temperature and the extent of glaciers have initiated changes in the global carbon cycle and tropospheric CO₂. The carbon cycle then has responded by amplifying these initial perturbations through positive carbon-climate feedbacks. Today the situation is fundamentally different in that the increasing greenhouse gas content drives changes in climate and environment.

Variation in stratospheric N₂O between 200 and 280 ppb during the past 650,000 years (Spahni et al. 2005) can be attributed to concurrent natural changes in both the terrestrial and the oceanic sources (Sowers et al. 2003; Flückiger et al. 2004). Since the pre-industrial era the mean tropospheric N₂O dry mole fraction has increased from 270 ± 7 to ~323 ppb. The current tropospheric N₂O growth rate of about 0.7 ppb year⁻¹ can primarily be attributed to the continued increased use of nitrogen fertilisers (Forster et al. 2007; Montzka et al. 2011).

The tropospheric dry mole fraction of CH₄ has varied from ~400 ppb during glacials to ~700 ppb during interglacials. The current average tropospheric CH₄ dry mole fraction is ~1,808 ppb, reflecting large and growing anthropogenic CH₄ fluxes since the pre-industrial era (Table 3.3). Even so, tropospheric CH₄ growth is temporally quite variable. High annual growth rates of ~20 ppb year⁻¹ during the 1970s were followed by growth rates of ~9–13 ppb year⁻¹ through the 1980s, 0–13 ppb year⁻¹ through most of the 1990s, almost zero growth during the late 1990s to early 2000s (Dlugokencky et al. 2003) and renewed growth rates of ~10 ppb year⁻¹ during the late 2000s (Rigby et al. 2008). This complex behaviour reflects short-term source variability that has been variously ascribed to decreased fossil fuel output following the economic collapse of the former Soviet Union, volcanic activity, wetland and rice paddy emissions, biomass burning, changes in the global distributions of temperature and precipitation, and reduced microbial sources in the Northern Hemisphere (Denman et al. 2007; Dlugokencky et al. 2009; Aydin et al. 2011; Kai et al. 2011).

A consequence of this ocean CO₂ uptake is a decrease in ocean pH, known as ocean acidification (Sect. 3.5.2) (Feely et al. 2004; Raven et al. 2005). If anthropogenic CO₂ emissions were to cease now, the oceans would eventually absorb 70–80 % of the anthropogenic CO₂ so far added to the troposphere, but this would take several hundred years (Archer et al. 1997; Watson and Orr 2003). Dissolution of calcium carbonate (CaCO₃) in deep ocean sediments and on land would further reduce tropospheric CO₂ to within 8 % of its pre-industrial level over thousands of years (Archer et al. 1997). Given the importance of the oceans in moderating human-induced climate change, quantifying net oceanic CO₂ uptake and estimating its long-term evolution are of critical importance. Although much progress has been made in quantifying CO₂ air-sea fluxes over the past decade, considerable uncertainties remain, in particular relating to inter-annual variability and long-term trends. The current state of knowledge is discussed here for the open ocean (Sect. 3.2.3) and for coastal seas (Sect. 3.2.4), with emphasis on the principal uncertainties (Sect. 3.6).

3.2 Surface Ocean Distribution and Air-Sea Exchange of CO₂

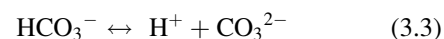
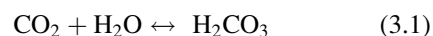
3.2.1 Global Tropospheric CO₂ Budget

In 2010 alone the tropospheric CO₂ increase was equivalent to 5.0 ± 0.2 Pg C (Box 3.1), principally due to the release of 9.1 ± 0.5 Pg C from fossil fuel burning and cement manufacture and 0.9 ± 0.7 Pg C from land use change (Fig. 3.2) (Global Carbon Project 2011; Peters et al. 2012). The ocean absorbs a substantial fraction of CO₂ emissions to the troposphere. From pre-industrial times to 1994 the oceans are estimated to have taken up 118 ± 19 Pg C from the troposphere, corresponding to roughly 50 % of fossil fuel CO₂ or about 30 % of the total anthropogenic emissions that include CO₂ emissions from land use change (Fig. 3.2; Table 3.2) (Sabine et al. 2004). Scientists are debating whether regional and global ocean CO₂ uptake has increased, remained constant or decreased in recent decades (Le Quéré et al. 2007, 2010; Schuster and Watson 2007; McKinley et al. 2011; Ballantyre et al. 2012).

3.2.2 Processes Controlling CO₂ Dynamics in the Upper Water Column

The air-sea exchange fluxes of CO₂ show high spatial and temporal variability, reflecting a complex interplay between the biological and physical processes affecting surface water fCO₂ (Box 3.2) (Takahashi et al. 2002; Sarmiento and Gruber 2006). In addition, observations show surface water fCO₂ to rarely be in equilibrium with tropospheric fCO₂ (see below and Box 3.3). Key to understanding the behaviour of CO₂ with regard to equilibration is CO₂ chemistry, which we briefly review next. We also discuss the key processes controlling the CO₂ dynamics of the upper ocean.

Dissolved CO₂ in seawater chemically equilibrates with carbonic acid (H₂CO₃) and the bicarbonate (HCO₃⁻) and carbonate (CO₃²⁻) ions:



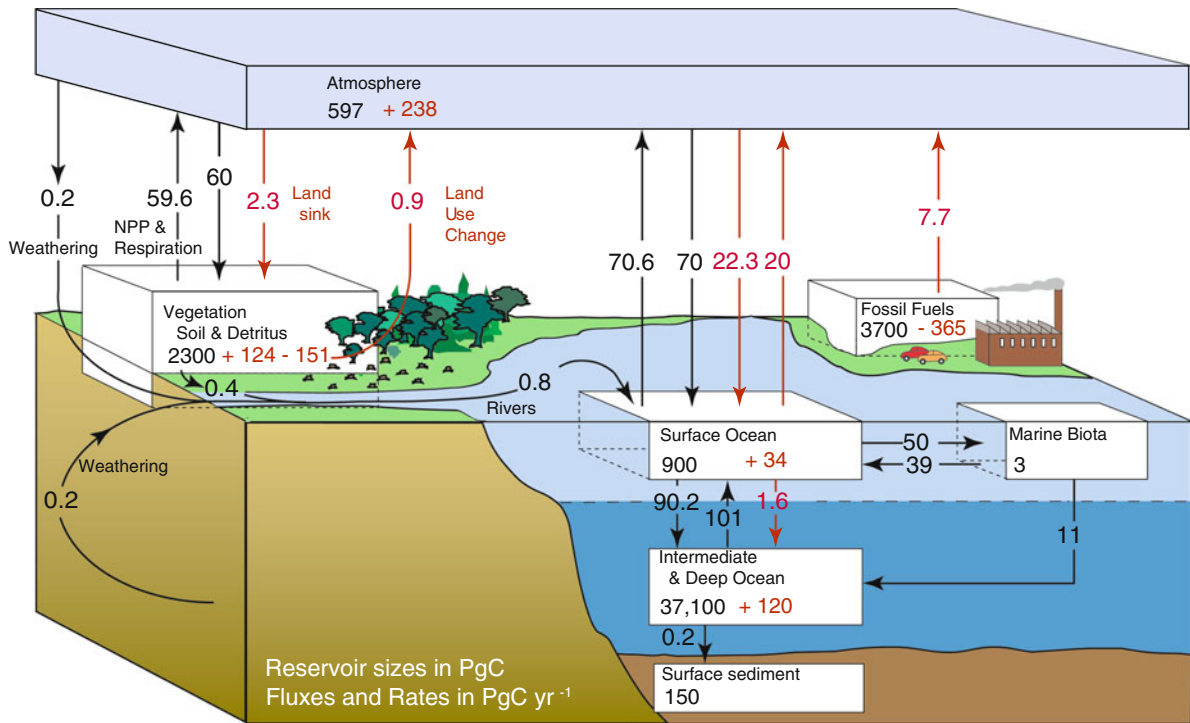


Fig. 3.2 The global carbon cycle with annual fluxes (in PgC year⁻¹) for the years 2000–2009. Pre-industrial, natural fluxes are in *black* and anthropogenic fluxes are in *red*. Integrated fluxes and standing stocks are from 1850 to 2011. NPP is annual

net terrestrial primary production. Cumulative changes are for end 2011 (The figure updates those in Sarmiento and Gruber (2002) and Denman et al. (2007)). Figure courtesy of N Gruber)

Box 3.2

Whereas the amount of CO₂ dissolved in seawater is generally reported in terms of its partial pressure pCO₂ (unit: μatm or 0.101325 Pa) or fugacity fCO₂ (unit: μatm), N₂O and CH₄ are more commonly presented in concentration units (nM or nmol kg⁻¹ seawater) or as percent (%) saturation. The latter is calculated from the ratio of the measured concentration to the theoretical equilibrium concentration, as determined by ambient water temperature, salinity and air pressure, and the atmospheric dry mole fraction corresponding to the time of last atmospheric contact. A surface saturation of 100 % indicates a water mass in equilibrium with overlying air, values below 100 % indicate undersaturation and values above 100 % indicate supersaturation. For all three gases, deviations from the air-sea equilibrium value are expressed as a negative or positive partial pressure difference (i.e. ΔpCO₂, ΔpN₂O, ΔpCH₄) or for N₂O and CH₄, as a negative or positive “concentration anomaly”. In this chapter, positive values denote a partial pressure that is higher in the water than in the overlying air.

The fugacity of a gas is its partial pressure after correcting for any non-ideal behaviour by applying a fugacity coefficient γ (Weiss 1974). The equation for CO₂ is:

$$f\text{CO}_2 = \gamma p\text{CO}_2 \quad (3.4)$$

In practice the fugacity and partial pressure of CO₂ differ by only about 0.4 %. In this chapter we refer to fCO₂ throughout.

Box 3.3

Air-sea fluxes (F) can be quantified as the product of a gas transfer velocity (k), the gas solubility (K_0) and the difference in the gas fugacity (e.g. $f\text{CO}_2$) across the air-sea interface. For N_2O and CH_4 the difference in the partial pressure is usually applied.

$$F_{\text{CO}_2} = k_{\text{CO}_2} K_{0,\text{CO}_2} (f\text{CO}_{2\text{water}} - f\text{CO}_{2\text{air}}) \quad (3.5)$$

$$F_X = k_X K_{0,X} (pX_{\text{water}} - pX_{\text{air}}) \quad (\text{with } X = \text{N}_2\text{O or CH}_4) \quad (3.6)$$

By convention, positive flux values indicate emission from the ocean and negative flux values indicate uptake by the ocean. For CO_2 these simplified equations neglect its possible chemical enhancement, although this effect is thought to be small (Wanninkhof 1992; Matthews 1999). They further assume that away from the air-sea interface both the lower troposphere and upper ocean are well mixed, so that bulk measurements within them can be used to define a gas concentration gradient at the interface. A final assumption is that the water temperature at the interface (the skin temperature) is the same as that of the well-mixed upper ocean (Robertson and Watson 1992; Van Scoy et al. 1995).

Atmospheric CO_2 needs to equilibrate with the large pool of dissolved inorganic carbon in seawater, resulting in an equilibration time-scale of the surface ocean for gas exchange of nearly 1 year (Broecker and Peng 1982), i.e. much longer than the time-scale typically associated with upper ocean perturbations (such as by the seasonal cycle). The equilibration time-scale for CH_4 and N_2O is about 10 times shorter than for CO_2 so that the deviations of these gases from equilibrium are generally smaller unless strong sources are present.

The gas transfer velocity (k) is a function of turbulence at the sea surface and is often parameterised as a function of wind speed, as discussed in detail in Chap. 2. Several parameterisations of k as a function of wind speed have been proposed (e.g. Liss and Merlivat 1986; Wanninkhof 1992; Wanninkhof and McGillis 1999; Nightingale et al. 2000; Ho et al. 2006; Sweeney et al. 2007; Prytherch et al. 2010). The uncertainty in k , which has been estimated at 30 % (Sweeney et al. 2007), adds further uncertainty to estimates of net gas uptake and/or emission determined from surface water measurements (Sect. 3.6).

On average surface seawater dissolved inorganic carbon (DIC) (alternatively referred to as total CO_2 , ΣCO_2 and C_T) comprises about 90 % HCO_3^- , 9 % CO_3^{2-} , 1 % dissolved CO_2 and 0.001 % H_2CO_3 . Thus, in order to equilibrate across the air-sea interface, CO_2 needs to equilibrate not only with the dissolved CO_2 pool, but with all chemical species making up DIC, explaining the long equilibration time scale. The dominant presence of HCO_3^- and CO_3^{2-} are also key to explaining the large uptake capacity of the ocean with regard to the anthropogenic perturbation of tropospheric CO_2 , as it is the reaction of CO_3^{2-} with the dissolved CO_2 taken up to form two HCO_3^- ions that gives seawater its large capacity to take up CO_2 and that will enable the ocean to eventually take up nearly

80 % of total anthropogenic emissions. An important metric for this reaction is the oceanic buffer (or Revelle) factor, which is a measure of the degree to which this titration reaction occurs. The larger the concentration of the CO_3^{2-} ion, the higher this factor is, and thus the larger is the oceanic uptake capacity.

However, the current net rate of oceanic CO_2 uptake is overall set by its transport from the surface to the deep oceans (Fig. 3.2), leading to the observation that the current uptake fraction (about 30 %) is considerably smaller than the long-term potential (about 80 %).

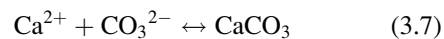
The anthropogenic perturbation occurs on top of an intense but largely internal cycling of “natural” carbon, which is the primary driver of the high spatio-temporal variability of CO_2 in the surface ocean. This natural

internal cycling is often conceptualised as a number of “pumps”, namely the solubility pump, the soft tissue or organic carbon pump and the carbonate or hard tissue pump (Volk and Hoffert 1985; Heinze et al. 1991). The reason for the pump analogy is that the associated processes act as gradient makers in that they tend to reduce the surface concentration of DIC and enhance its concentration at depth, thereby acting against the tendency for these gradients to be eliminated by transport and mixing. The net effect of these pumps on the air-sea exchange of CO₂ is controlled by the interaction and relative importance of the downward pump component relative to upward mixing and transport (Gruber and Sarmiento 2002). Regions where the downward component dominates over upward transport are sinks for tropospheric CO₂, while regions where upward transport dominates are CO₂ sources. Given the need to consider both the downward and upward components, the concept of biogeochemical loops has been proposed (Gruber and Sarmiento 2002).

The solubility pump is maximal at high-latitudes during winter when cold surface water rich in DIC (due to higher CO₂ solubility at lower temperatures) sinks to depth, resulting in a net downward transport of DIC (Fig. 3.2) (Volk and Hoffert 1985; Heinze et al 1991). In contrast, the solubility pump acts in quasi reverse order, when colder waters rich in DIC are brought to the surface and warm, giving rise to reduced CO₂ solubility.

The soft tissue pump is initiated by the photosynthetic incorporation of CO₂ as phytoplankton cellular organic carbon. As this organic carbon travels up the food chain, a fraction of it is “lost” at each trophic step by respiration, excretion and the death of organisms (Kaiser et al. 2011). Bacteria and other microorganisms are critical to the recycling of carbon in the upper ocean (Fig. 3.2). Nevertheless, a significant fraction of the photosynthetically fixed carbon leaves the upper ocean as “export production” in the form of sinking organic particles, by vertical migration of zooplankton or as dissolved organic carbon (DOC) in sinking water (Volk and Hoffert 1985; Heinze et al. 1991; Sarmiento and Gruber 2006).

The carbonate or hard tissue pump involves the biological formation of calcium carbonate (CaCO₃) in near surface waters, its downward export primarily by sinking and its subsequent dissolution in deep water. The initial step is incorporation of the CO₃²⁻ ion into the shells of calcifying organisms:



Equation 3.7 describes CaCO₃ precipitation at a physiological level; however, the uptake of CO₃²⁻ leads to a chemical re-adjustment of DIC species with the overall equation:



The precipitation of CaCO₃ leads to a shift from the HCO₃⁻ pool to the CO₂ pool and a release of CO₂ to the surrounding water. The “released” CO₂ subsequently equilibrates with HCO₃⁻, so that for each mole of CaCO₃ precipitated, less than one mole of CO₂ is “released”. The fraction for average surface sea water is 0.6 (Frankignoulle et al. 1994). Consequently, where the ratio between net organic carbon production or net community production (NCP) and calcification is below 0.6, the waters are a CO₂ source and where this ratio exceeds 0.6, they are a CO₂ sink (Suzuki and Kawahata 2004).

In coral reefs NCP is close to zero (Gattuso et al. 1998). Hence the CO₂ “released” by CaCO₃ precipitation generally exceeds the CO₂ drawdown by NCP and coral reefs tend to act as CO₂ sources to the troposphere (Gattuso et al. 1993, 1997; Frankignoulle et al. 1996; Ohde and van Woesik 1999; Bates et al. 2001). In the pelagic realm, where the vast majority of calcification is carried out by the coccolithophore component of the phytoplankton (Buitenhuis et al. 1996; Harlay et al. 2010, 2011; Suykens et al. 2010), the average ratio of NCP to net CaCO₃ precipitation is between 11 and 16 (Sarmiento et al. 2002; Jin et al. 2006). The net consequence of biological production and the export of organic carbon and CaCO₃ from the pelagic realm is a tendency towards CO₂ uptake from the troposphere.

Mineral CaCO₃ in seawater occurs in two forms: calcite and the more soluble aragonite (Mucci 1983). For both, solubility increases with increased pressure (depth) and decreased temperature. The saturation state Ω describes whether sea-water is supersaturated ($\Omega > 1$) or undersaturated ($\Omega < 1$) with respect to the solubility product, K_{sp} , of either of these two CaCO₃ forms:

$$\Omega = [\text{Ca}^{2+}] [\text{CO}_3^{2-}] / K_{\text{sp}} \quad (3.9)$$

$$K_{sp} = [\text{Ca}^{2+}]_{\text{sat}} [\text{CO}_3^{2-}]_{\text{sat}} \quad (3.10)$$

At present nearly the entire upper ocean is supersaturated with regard to both calcite and aragonite, while most of the deep ocean is undersaturated. Organisms that form CaCO₃ shells and structures therefore do so largely in waters that are supersaturated, while the exported CaCO₃ eventually sinks into regions of undersaturation and dissolves.

A reduction in ocean pH due to anthropogenic activities (Feely et al. 2004; Orr et al. 2005; Raven et al. 2005) is one consequence of increased tropospheric CO₂ and its transfer to the ocean. While the term “ocean acidification” (OA) describes a decrease in ocean pH, this is not expected to fall below 7 (Kleypas et al. 2006). The uptake of CO₂ since pre-industrial times has led to a reduction in surface seawater pH of 0.1 units relative to the pre-industrial value of about 8.2 (Orr et al. 2005). This is equivalent to a 30 % increase in the hydrogen ion (H⁺) concentration.

In situ pH measurements at the European Station for Time-series in the Ocean (ESTOC, 29°N 15°W) show a progressive reduction of pH and other changes in the carbonate chemistry of surface waters since 1995 (González-Dávila et al. 2010; Santana-Casiano and González-Dávila 2011). Figure 3.3 highlights a decrease in surface water pH_T (the pH corrected to a constant temperature of 25°C) of 0.0019 pH units year⁻¹ from 1995 to 2010, accompanied by increases in salinity normalised DIC (NC_T) and fCO₂. Similar trends in pH, DIC and fCO₂ have been observed at the Bermuda Atlantic Time-series Study, BATS (Gruber et al. 2002), and the Hawaii Ocean Time-Series site, HOT (Brix et al. 2004; Denman et al. 2007).

An important consequence of the net oceanic uptake of anthropogenic CO₂ from the troposphere is a decrease in the saturation states with regard to calcite and aragonite. This is due to the aforementioned titration of the CO₃²⁻ ion by the CO₂ taken up, which leads to a fall in the CO₃²⁻ concentration. These chemical changes are accompanied by an increase in the concentration of H⁺ and CO₂ (Feely et al. 2004; Raven et al. 2005). The ESTOC time series demonstrates how the saturation states for calcite and aragonite have decreased at rates of 0.018 ± 0.006 units year⁻¹ and 0.012 ± 0.004 units year⁻¹,

respectively, from 1995 to 2004 (Santana-Casiano and González-Dávila 2011).

Ocean acidification is suspected to lead to a reduction in calcification by calcifying organisms, such as coral reefs, coccolithophores, foraminifera, pteropods and shell fish (Sect. 3.5.2) (Raven et al. 2005). In addition, diminishing calcification would reduce net CaCO₃ transfer to the deep ocean (Feely et al. 2004; Denman et al. 2007).

3.2.3 Surface Ocean fCO₂ and Air-Sea CO₂ Fluxes in the Open Ocean

3.2.3.1 Surface Ocean fCO₂ Distribution

The seasonal cycle in surface water fCO₂ is relatively weak in tropical regions (14°S–14°N), which are strong CO₂ sources throughout the year (Takahashi et al. 2009) (Box 3.3). Surface water fCO₂ in temperate ocean regions (14–50°N and 14–50°S) has a strong seasonal cycle with high values in summer and low values in winter, as the seasonal effects of warming and cooling outweigh biological effects (Fig. 3.3) (Bates et al. 1996a; Dore et al. 2003; González-Dávila et al. 2003; Takahashi et al. 2009). The temperate Indian Ocean north of 14°N also has high fCO₂ in summer, but here seasonal upwelling in the southwest monsoon is the main driver (Takahashi et al. 2009). High latitude northern hemisphere waters have strong fCO₂ undersaturation in spring and summer as a result of biological CO₂ drawdown in the upper ocean (Takahashi et al. 2009). Biological activity equally creates a CO₂ sink in Southern Ocean waters from 50°S to 60°S during austral spring and summer (Takahashi et al. 2009). Seasonally ice covered waters south of ~60°S rapidly change from strong CO₂ supersaturation below sea ice to strong undersaturation upon ice melt, most likely driven by biological carbon uptake (Bakker et al. 2008).

Surface water fCO₂ data coverage has improved greatly over the past decade (Takahashi et al. 2009; Watson et al. 2009; Pfeil et al. 2013; Sabine et al. 2013). For example, a basin-wide network of fCO₂ measurements on Voluntary Observing Ships (VOS) and buoys has been operational in the North Atlantic Ocean since 2004, which allows the creation of basin-wide monthly fCO₂ maps, annual flux estimates and trend analyses (Schuster et al. 2009; Telszewski et al. 2009; Watson et al. 2009). Data coverage is similarly

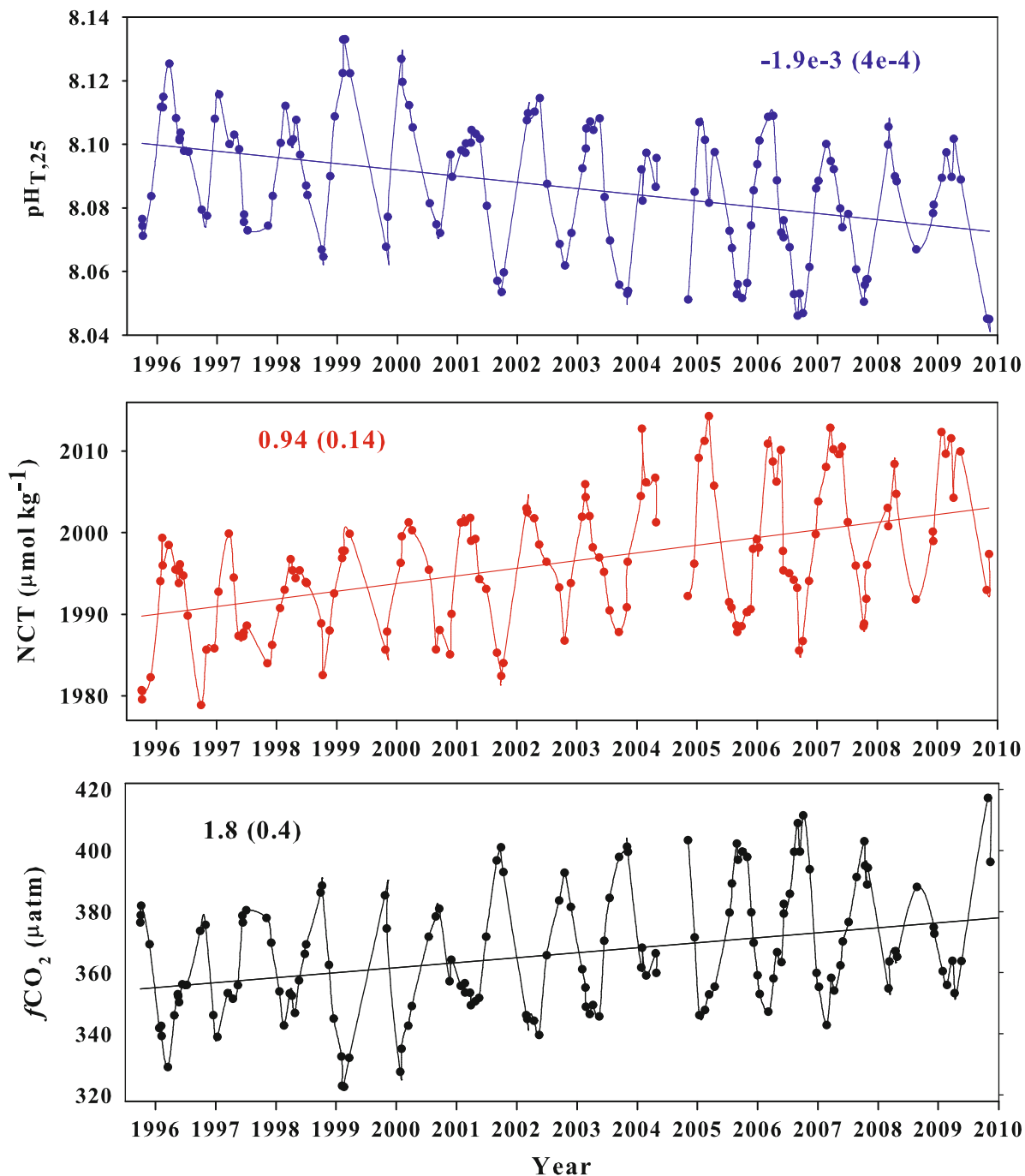


Fig. 3.3 Changes in total pH at 25 °C, salinity normalised dissolved inorganic carbon (NC_T) and $f\text{CO}_2$ from 1995 to 2010 at the European Station for Time-series in the Ocean (ESTOC, 29°N 15°W) for the full set of surface data (*upper* 10 m). The

regression lines have slopes of -0.0019 ± 0.0004 pH units year^{-1} for $\text{pH}_{T,25}$, of 0.94 ± 0.14 $\mu\text{mol kg}^{-1} \text{year}^{-1}$ for NC_T and of 1.8 ± 0.4 $\mu\text{atm year}^{-1}$ for $f\text{CO}_2$. (Figure courtesy of M González-Dávila and JM Santana-Casiano)

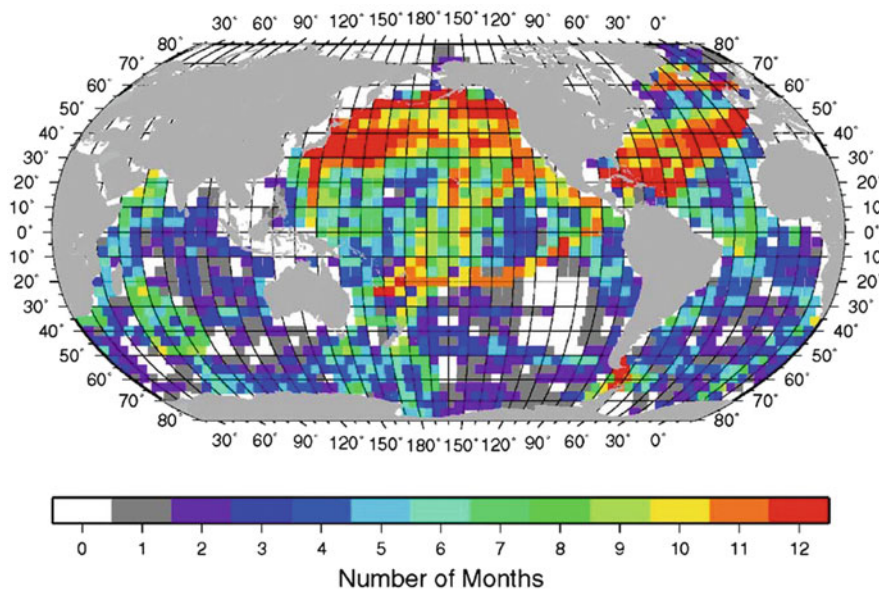


Fig. 3.4 Number of months in each 4° latitude by 5° longitude box with at least one surface water $f\text{CO}_2$ measurement between 1970 and 2007 (Reproduced from Takahashi et al. (2009) by permission of Elsevier)

high in the North Pacific (Feely et al. 2006; Ishii et al. 2009). Elsewhere data coverage has increased, but many regions remain data sparse, e.g. the Indian Ocean, the South Pacific Ocean, the South Atlantic Ocean and the Southern Ocean, notably in autumn and winter (Fig. 3.4) (Takahashi et al. 2009, 2011; Bakker et al. 2012; Pfeil et al. 2013; Sabine et al. 2013).

A variety of techniques have been applied to interpolate between surface ocean $f\text{CO}_2$ data, including a diffusion–advection based interpolation scheme (Takahashi et al. 1997, 2009), (multiple) linear regression (Boutin et al. 1999; Rangama et al. 2005; Olsen et al. 2008) and a neural network approach (Lefèvre et al. 2005; Telszewski et al. 2009). The principle of many of these methods is to correlate sparse $f\text{CO}_2$ data with more widely available parameters such as satellite-derived chlorophyll *a* concentrations, sea surface temperatures and mixed layer depths and then to use these correlations to predict $f\text{CO}_2$ where measurements are lacking.

The ‘true’ spatial distributions of surface water $f\text{CO}_2$ and air-sea CO_2 fluxes are unknown and the above methods only deliver approximations of them. Interestingly, however, Watson et al. (2009) derived similar air-sea CO_2 fluxes for the North Atlantic Ocean (10–65°N) using multiple linear regression

and a neural network. For both the standard deviation of the annual mean $f\text{CO}_2$ was $\sim 10\%$. It was concluded that if the flux uncertainty arising from uncertainty in k is ignored, the overall air-sea CO_2 flux in this region is well constrained by $f\text{CO}_2$ observations and is thus relatively insensitive to the mapping technique used. Further development and testing of interpolation methods should be a priority.

3.2.3.2 Multi-Year Changes and Trends

Analysis of the decadal evolution of $f\text{CO}_2$ provides information on the evolution of the oceanic CO_2 sink. If the rate of increase of surface ocean $f\text{CO}_2$ matches the increase in tropospheric CO_2 the oceanic CO_2 sink is at steady state, but if it is higher, then the oceanic CO_2 sink is decreasing (Schuster et al. 2009). For example, Fig. 3.3 shows $f\text{CO}_2$ from 1995 to 2010 for the upper 10 m at ESTOC (29°N 15°W). Regression of the data reveals an increase in $f\text{CO}_2$ of $1.8 \pm 0.4 \mu\text{atm year}^{-1}$.

Globally, surface water $f\text{CO}_2$ increased at a mean rate of $1.5 \mu\text{atm year}^{-1}$ from 1970 to 2007, similar to the pace of the tropospheric CO_2 increase of $1.5 \mu\text{atm year}^{-1}$ from 1972 to 2005 (Takahashi et al. 2009). Relatively low rates of increase were found in the Equatorial Pacific Ocean ($1.26 \pm 0.55 \mu\text{atm year}^{-1}$) and the North Pacific Ocean ($1.28 \pm 0.46 \mu\text{atm}$

year⁻¹), while fCO₂ increased more rapidly in the North Atlantic Ocean ($1.80 \pm 0.37 \mu\text{atm year}^{-1}$) and between 50°S and 60°S ($2.13 \pm 0.64 \mu\text{atm year}^{-1}$) (Takahashi et al. 2009). Similarly, surface water fCO₂ in the Southern Indian Ocean (south of 20°S) increased more rapidly ($2.11 \pm 0.07 \mu\text{atm year}^{-1}$) than did tropospheric CO₂ ($1.72 \mu\text{atm year}^{-1}$) between 1991 and 2007 (Metzl 2009).

Regional and temporal differences in the rate of increase of surface water fCO₂ are not well understood but have been attributed to changes in seawater buffer capacity (Thomas et al. 2007), mixing and stratification (Schuster and Watson 2007), temperature (Corbière et al. 2007), biological activity (Lefèvre et al. 2004) and lateral and vertical water transport (Takahashi et al. 2009). The expanding database for fCO₂ highlights considerable year-to-year and multi-year variations in ocean carbon cycling.

Theory and biogeochemical models predict an increase in air-sea fCO₂ disequilibrium over time in high latitude regions. Here water from the interior ocean reaches the surface. This water has a relatively low DIC content, as it equilibrated with an atmospheric CO₂ mixing ratio below the present one, when the water last was at the surface. One might expect that the increase in surface water fCO₂ of these waters lags the increase in tropospheric CO₂ (Takahashi et al. 1997, 2002), given the long equilibration time for CO₂ of almost a year. Such an increase in the air-sea fCO₂ disequilibrium would be accompanied by an increase in the net oceanic CO₂ sink. However, the observation that surface water fCO₂ in some regions of the Southern Ocean is currently increasing more rapidly than tropospheric CO₂ (Metzl 2009; Takahashi et al. 2009) runs counter to these predictions. Air-sea CO₂ flux estimates derived from the inversion of tropospheric CO₂ data suggest that this may be a more wide-spread phenomenon in the Southern Ocean, extending to the entire region south of 45°S (Le Quéré et al. 2007). This hypothesis of a weakening relative sink strength in the Southern Ocean is supported by several ocean modelling studies (Wetzel et al. 2005; Le Quéré et al. 2007; Lovenduski et al. 2007) and is attributed to a trend of increasing Southern Ocean wind speeds, which enhance the upwelling of deeper waters with high concentrations of “natural” DIC (Lovenduski et al. 2008). The changing wind regime may be related to a strengthening of the Southern Annular Mode in response to increasing greenhouse gases and the depletion of stratospheric ozone

(Lenton et al. 2009). These trends in Southern Ocean fCO₂, the strength of the oceanic CO₂ sink and the mechanisms responsible are currently topics of much scientific debate.

Recent studies provide evidence of multi-annual variation in surface water fCO₂ growth rates and CO₂ air-sea fluxes in other regions, notably the Pacific Ocean and the North Atlantic Ocean (Corbière et al. 2007; Schuster and Watson 2007; Ishii et al. 2009; Schuster et al. 2009; Watson et al. 2009). For example, the growth rates of surface water fCO₂ in the western Equatorial Pacific were different from 1985–1990 ($0.3 \pm 1.3 \mu\text{atm year}^{-1}$) to 1990–1999 ($2.2 \pm 0.7 \mu\text{atm year}^{-1}$) and 1999–2004 ($-0.2 \pm 1.0 \mu\text{atm year}^{-1}$) (Ishii et al. 2009). Annual CO₂ uptake along a shipping route between the United Kingdom and the Caribbean strongly decreased from the early 1990s to 2002–2005 (Schuster and Watson 2007; Schuster et al. 2009). Annual air-sea CO₂ fluxes varied by more than a factor two for the period 2002–2007, with values rising and falling over several years (Fig. 3.5) (Watson et al. 2009). These gradual changes suggest multi-year or possibly decadal variation that might be linked to the North Atlantic Oscillation (Thomas et al. 2008).

3.2.3.3 Comparison of Air-Sea CO₂ Flux Estimates

Independent estimates of the global oceanic uptake of anthropogenic CO₂ for the 1990s and early 2000s range from 1.8 to 2.4 Pg C year⁻¹ with model-based values often exceeding observation-based estimates (Gruber et al. 2009). An uptake of $1.8 \pm 1.0 \text{ Pg C year}^{-1}$ has been obtained by inversion of tropospheric CO₂ (Gurney et al. 2004; adjusted by Gruber et al. 2009), while a net ocean sink of $1.9 \pm 0.7 \text{ Pg C year}^{-1}$ has been estimated from a surface water CO₂ climatology (Takahashi et al. 2009; adjusted by Gruber et al. 2009). Ocean inversion of DIC has given an oceanic CO₂ sink of $2.2 \pm 0.3 \text{ Pg C year}^{-1}$, (Gruber et al. 2009) and $2.4 \pm 0.5 \text{ Pg C year}^{-1}$ has been estimated using ocean biogeochemical models (Watson and Orr 2003). Other methods give a similar range of estimates (Joos et al. 1999; Gruber and Keeling 2001; Bender et al. 2005; Manning and Keeling 2006; Jacobson et al. 2007; Gruber et al. 2009).

Measurement and modelling techniques vary in whether they quantify anthropogenic CO₂ fluxes or net contemporary CO₂ fluxes and a correction needs to be made for the outgassing of carbon from rivers and for

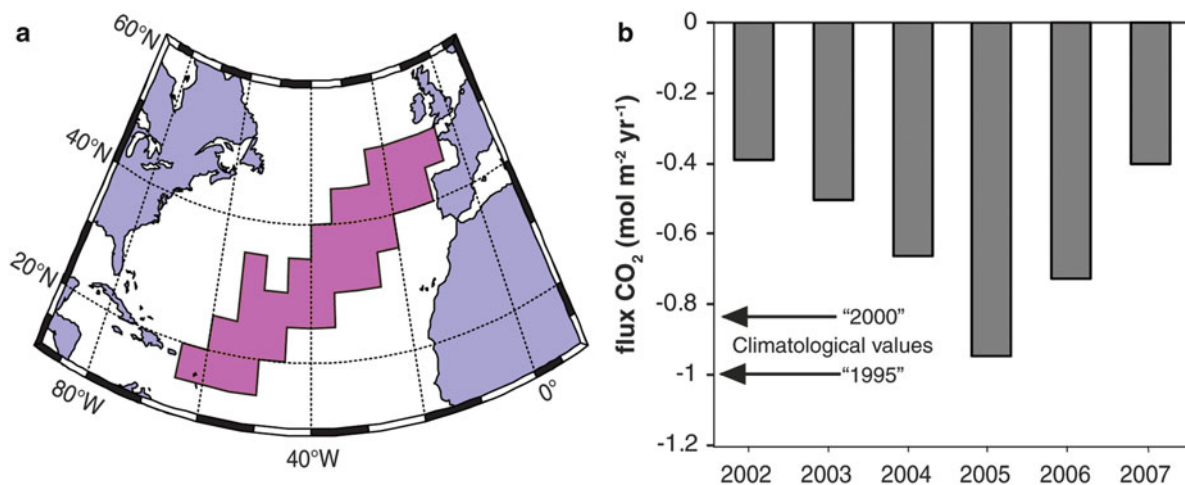


Fig. 3.5 Annual CO₂ uptake for the *pink shaded* ocean area between the UK and the Caribbean for 2002–2007. The size of climatological fluxes for the years 1995 and 2000 (Takahashi

et al. 2002, 2009) is indicated on the *left axis* of the *right figure*. (Reproduced from Watson et al. (2009) by permission of Science)

other natural CO₂ fluxes when comparing such flux estimates (Gruber et al. 2009; Takahashi et al. 2009). The open ocean source of natural CO₂ arising from river inputs has been estimated as 0.5 ± 0.2 Pg C year⁻¹ (Gruber et al. 2009, after Sarmiento and Sundquist 1992). However, this value could be too high by ~ 0.2 Pg C year⁻¹ due to the substantial outgassing of river inputs during estuarine mixing (Sect. 3.2.4).

Figures 3.6 and 3.7 show the spatial distribution of net contemporary CO₂ fluxes as determined from a pCO₂-based climatology (Takahashi et al. 2009), ocean inversion (Gruber et al. 2009), atmospheric inversion (Baker et al. 2006) and ocean biogeochemistry models (Watson and Orr 2003). The fluxes from the four methods are in reasonable agreement for most ocean regions. The notable exception is the Southern Ocean (here south of 44°S), where marine biogeochemistry models predict a much larger CO₂ sink than the other methods, mainly as a result of a weak outgassing of natural CO₂ (Mikaloff Fletcher et al. 2007). A comparison of the ocean inverse results with the pCO₂ climatology shows that while both methods indicate a similar net contemporary CO₂ sink of 0.3 Pg C year⁻¹ south of 44°S, the estimates disagree in the spatial distribution of the flux (Gruber et al. 2009). The climatology-derived flux estimates indicate a Southern Ocean sink between 44°S and 58°S and a small source south of 58°S (Takahashi et al. 2009), while the ocean inversion

suggests a more uniform CO₂ sink south of 44°S (Gruber et al. 2009). It is worth noting that the recent addition of further surface water fCO₂ data in the Southern Ocean, and in particular in seasonally ice covered waters, has led to a revision of air-sea CO₂ flux estimates for 50–62°S (from -0.34 to -0.06 Pg C year⁻¹) and south of 62°S (from -0.04 to $+0.01$ Pg C year⁻¹) in successive climatologies (Takahashi et al. 2002, 2009).

The separation of contemporary air-sea CO₂ fluxes into natural CO₂ fluxes (here excluding river-induced fluxes), river borne fluxes and anthropogenic CO₂ fluxes, using an inversion of interior ocean inorganic carbon data, is shown in Fig. 3.7 (Gruber et al. 2009). Natural CO₂ fluxes in this study vary from CO₂ sources in the tropics and the Southern Ocean to CO₂ sinks in global temperate regions and the high latitude northern hemisphere (Gruber et al. 2009). On a global scale these natural fluxes (excluding river borne fluxes) cancel out. Anthropogenic CO₂ is taken up by all ocean regions, with the largest sinks in the tropics and the Southern Ocean.

3.2.3.4 Sea Ice

Sea ice influences marine DIC cycling and the air-sea exchange of CO₂ through physical processes such as brine rejection (e.g. Anderson et al. 2004; Omar et al. 2005; Rysgaard et al. 2011) and air-ice-sea exchange (e.g. Miller et al. 2011) (Chap. 2), in addition to

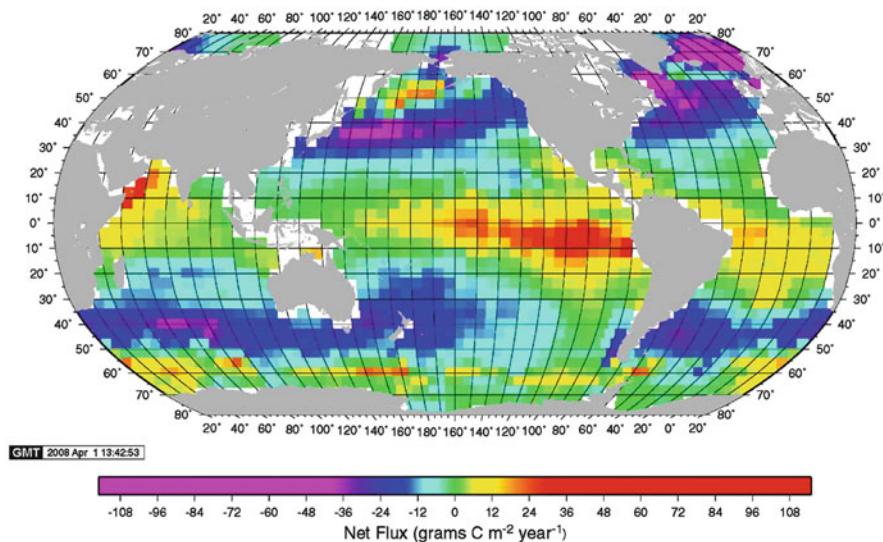


Fig. 3.6 Contemporary annual air-sea CO₂ fluxes for the year 2000 from a pCO₂ climatology (Reproduced from Takahashi et al. (2009) by permission of Elsevier)

biological and chemical processes (Delille et al. 2007; Bakker et al. 2008; Geibert et al. 2010). Although our understanding of the underlying processes is limited and quantitative estimates are scarce, the physical processes are thought to result in a net sink for tropospheric CO₂ during sea ice formation in the polar oceans. Recently, Rysgaard et al. (2011) estimated the net influx of CO₂ into the polar oceans at 33 Tg C year⁻¹, a flux resulting from the rejection of carbon from the ice crystal matrix during winter and subsequent formation of a surface layer of melt-water, undersaturated in CO₂ during summer. The sink would be much stronger (83 Tg C year⁻¹), if CaCO₃ crystals form in the sea ice. Omar et al. (2005) suggested a wintertime CO₂ sink of 5.2 g C m⁻² associated with the formation of seasonal sea ice and brine rejection in the Arctic. With a seasonal sea ice extent of 14 × 10⁶ km² (in 2005) this translated into a wintertime sink of 36 Tg C year⁻¹, which is on the higher end of estimates of 14 Tg C year⁻¹ (no CaCO₃ precipitation) and 31 Tg C year⁻¹ (with CaCO₃ precipitation) for the Arctic Ocean by Rysgaard et al. (2011). Sea ice related tropospheric CO₂ uptake was estimated as 19 Tg C year⁻¹ for the Southern Ocean, which would increase to 52 Tg C year⁻¹, if CaCO₃ crystals form in the ice (Rysgaard et al. 2011). Oceanic CO₂ uptake during the seasonal cycle of sea ice growth and decay is thus equivalent to 17–42 % of net tropospheric CO₂ uptake in ice-free polar seas (Rysgaard et al. 2011).

3.2.3.5 Coastal to Open Ocean Carbon Exchanges

Exchanges of organic and inorganic carbon between coastal shelves and the deep ocean remain poorly quantified (Biscaye et al. 1988; Monaco et al. 1990; Biscaye and Anderson 1994; Wollast and Chou 2001), even though such exchange may be an important conduit for transferring tropospheric carbon to the interior ocean (Tsunogai et al. 1999; Thomas et al. 2004). For example an efficient ‘continental shelf carbon pump’, as proposed for the East China Sea and the North Sea, critically depends on the off-shelf transport of carbon-rich subsurface water (Tsunogai et al. 1999; Thomas et al. 2004) to below the permanent pycnocline of the deep ocean (Holt et al. 2008; Huthnance et al. 2009; Wakelin et al. 2012), but these carbon transports have not been verified in situ.

3.2.4 Air-Sea CO₂ Fluxes in Coastal Areas

3.2.4.1 Continental Shelves

Contemporary air-sea exchange fluxes of CO₂ in the coastal environment have been estimated by adjusting local flux data to the global scale using procedures of varying complexity (Box 3.4; Table 3.4). These range from extrapolating a single flux estimate from a continental shelf to the global scale, such as in the East China Sea (Tsunogai et al. 1999) or the North Sea

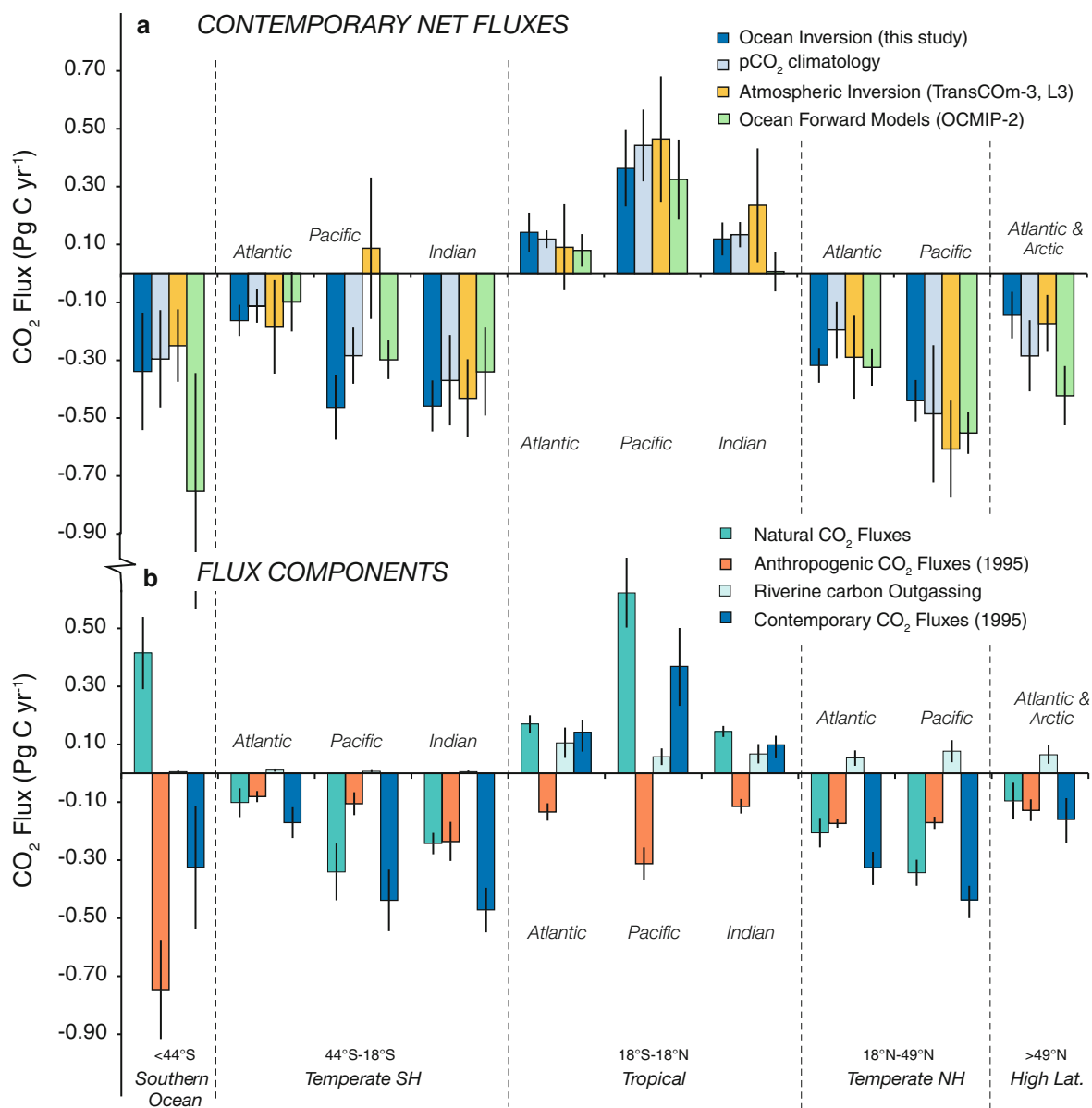


Fig. 3.7 Air-sea CO₂ fluxes for 10 regions per latitude range and per basin with positive fluxes for CO₂ leaving the ocean. (a) Net contemporary air-sea CO₂ fluxes from ocean inversion estimates (Gruber et al. 2009), a surface ocean pCO₂ climatology (Takahashi et al. 2009), mean estimates from 13 ocean biogeochemistry models (Watson and Orr 2003) and mean estimates from atmospheric inversion of CO₂ (Baker et al. 2006). Error bars for the ocean biogeochemistry model estimates are the unweighted

standard deviation of the model outputs. The uncertainties in the atmospheric inversion estimates are based on the square of the errors within and between models. (b) Natural, anthropogenic, river-induced and contemporary air-sea CO₂ fluxes by ocean inversion. Error bars indicate the cross-model weighted standard deviation of the mean. Anthropogenic and contemporary fluxes are for the nominal year 1995. (Reproduced from Gruber et al. (2009) by permission of the American Geophysical Union)

(Thomas et al. 2004), to approaches that compiled flux values for several continental shelf systems with scaling by surface area. Areas have been grouped by latitudinal bands (Borges 2005; Borges et al. 2005),

oceanic provinces (Cai et al. 2006) and surface areas derived from bathymetry (Chen and Borges 2009; Laruelle et al. 2010). The estimate of Laruelle et al. (2010) was based on a typological approach, whereby

Box 3.4

For the purpose of this work the coastal zone is defined to include near-shore systems, such as estuaries, and the continental shelf as far offshore as the 200 m depth contour (Walsh 1988; Gattuso et al. 1998; Liu et al. 2010). The continental margin consists of the coastal zone and the continental slope (from 200 to 2,000 m depth) (Liu et al. 2010). Inner estuaries are characterised by large salinity gradients, complex mixing and varying anthropogenic inputs. Laruelle et al. (2010) give a global inner estuarine area of $\sim 1 \times 10^6$ km². Outer estuaries (estuarine plumes) have restricted salinity ranges and salinities typically below 34 (Frankignoulle et al. 1998). Estuarine plumes may extend tens of km offshore and may account for considerable estuarine mixing (Naudin et al. 1997). Barnes and Upstill-Goddard (2011) estimated that European outer estuaries account for more than 75 % of the total European estuarine area, but there is no comparable global estimate. Nonetheless, estuarine plumes are generally considered as part of the continental shelf and there is a concern that the characteristic distributions of CO₂, CH₄ and N₂O in such plumes may not be sufficiently sampled.

Table 3.4 CO₂ fluxes scaled globally for continental shelves and estuaries: n is the number of data points used in the up-scaling

CO ₂ flux (Pg C year ⁻¹)	CO ₂ flux (mol m ⁻² year ⁻¹)	Surface area (10 ⁶ km ²)	n	Reference
Continental shelves globally				
-0.95	-2.90	27.0	1	Tsunogai et al. (1999)
-0.40	-1.33	25.2	1	Thomas et al. (2004)
-0.37	-1.17	25.8	15	Borges (2005)
-0.45	-1.44	25.8	17	Borges et al. (2005)
-0.22	-0.71	25.8	29	Cai et al. (2006)
-0.34	-0.92	30.0	58	Chen and Borges (2009)
-0.22	-0.71	24.7	37	Laruelle et al. (2010)
Estuaries globally				
+0.60	+36.5	1.40	13	Abril and Borges (2004)
+0.43	+38.2	0.94	16	Borges (2005)
+0.32	+28.6	0.94	16	Borges et al. (2005)
+0.36	+32.1	0.94	32	Chen and Borges (2009)
+0.27	+21.0	1.10	62	Laruelle et al. (2010)

continental shelves were defined as one of three types: enclosed, upwelling, and open. In these studies the Arctic Ocean was included in estimates for the coastal ocean, but other deep marginal seas were excluded.

The first global estimate of the continental shelf sink for CO₂, based on East China Sea data (Tsunogai et al. 1999) was 1.0 Pg C year⁻¹, whereas most recent estimates converge to a value ~ 0.3 Pg C year⁻¹ (Chen and Borges 2009; Laruelle et al. 2010; Cai 2011). While continental shelves cover less than 10 % of the total ocean surface area, their air-sea CO₂ flux density is about twice as large (Laruelle et al. 2010) as the global average for the open oceans based on the most recent CO₂ climatology (Takahashi et al. 2009). This is consistent with higher biogeochemical reaction rates on continental shelves;

rates of net primary production and export production are twice as high as in the open ocean, for example (Wollast 1998). Even so, the zonal variability in air-sea CO₂ fluxes over continental shelves (Borges 2005; Borges et al. 2005; Laruelle et al. 2010) follows the patterns of the open ocean (Takahashi et al. 2009), with low latitude continental shelves being CO₂ sources and temperate and high latitude shelves being sinks for tropospheric CO₂. This suggests that the direction of air-sea CO₂ fluxes on continental shelves is to some extent dictated by a “background” signal of “incoming” open ocean waters, and that the intensity of the flux is further modulated (enhanced) by biogeochemical processes on the continental shelf.

Lee et al. (2011) recently evaluated the anthropogenic carbon inventory in four marginal seas (Arctic Ocean, Mediterranean Sea, Sea of Okhotsk, and East/Japan Sea). These authors conclude that each of these marginal seas stores proportionally more anthropogenic CO₂ than the global open ocean and they attribute this to a dynamic over-turning circulation in these marginal seas.

3.2.4.2 Near-Shore Systems

Near-shore systems such as estuaries are known to significantly modify the fluxes of organic carbon from land to sea (e.g. Smith and Hollibaugh 1993; Gattuso et al. 1998; Battin et al. 2008) and to also emit large quantities of N₂O and CH₄ (Sects. 3.3.5 and 3.4.5) (Barnes et al. 2006; Denman et al. 2007; Upstill-Goddard 2011). Estuaries are also characterised by a net annual emission of CO₂ to the troposphere with intense flux densities (Frankignoulle et al. 1998). Various estimates of the global emission of CO₂ to the troposphere from inner estuaries are based on scaling exercises (Table 3.4) (Abril and Borges 2004; Borges 2005; Borges et al. 2005; Chen and Borges 2009; Laruelle et al. 2010). All are based on the global surface area estimate of Woodwell et al. (1973) with the exception of Laruelle et al. (2010), which is based on the typology of estuaries from Dürr et al. (2011). The first estimate by Abril and Borges (2004) of the emission of CO₂ to the troposphere was 0.6 Pg C year⁻¹ and the most recent estimates converge to ~0.3 Pg C year⁻¹ (Laruelle et al. 2010; Cai 2011). The estimate of Laruelle et al. (2010) relies on an estuarine typology with four types (small deltas and small estuaries, tidal systems and embayments, lagoons, fjords and fjårds (sea inlets, which have been subject to glacial scouring, in a rocky area of low topography)). This is an important innovation relative to previous scaling attempts, since estuarine morphology and physical structure strongly modulate the exchange of CO₂ with the troposphere (Borges 2005; Koné et al. 2009; Borges and Abril 2011). Fjords and fjårds constitute the most abundant estuarine type (~43 %), although CO₂ flux data have been reported for only one system. This highlights the limitation of using scaling approaches that are too complex with regards to the available data, and the need to obtain further data in near-shore systems to improve estimates of air-sea exchange of CO₂.

In most macro-tidal estuaries the river input of DIC can only sustain a small fraction of the observed CO₂ emission (Borges et al. 2006), implying that the bulk of estuarine CO₂ emission is sustained by the degradation

of allochthonous organic matter, in agreement with the net heterotrophic nature of these systems established from measurements of community metabolic rates (Odum and Hoskin 1958; Odum and Wilson 1962; Heip et al. 1995; Kemp et al. 1997; Gattuso et al. 1998; Gazeau et al. 2004; Hopkinson and Smith 2005). This implies that near-shore coastal environments are effective sites (or ‘bypasses’) for returning to the troposphere as CO₂, a fraction of the carbon passing from continents (through rivers) to the ocean. The removal of river borne organic carbon during estuarine transit can be roughly evaluated at ~60 % based on the above, given a global CO₂ emission of ~0.3 Pg C year⁻¹ from near shore waters (Laruelle et al. 2010; Cai 2011) and known global organic carbon river inputs of ~0.4 Pg C year⁻¹ (Schlünz and Schneider 2000). This is in general agreement with the analysis of organic carbon in estuaries (e.g. Abril et al. 2002). Such a bypass of carbon has important consequences for understanding and quantifying the global carbon cycle. For instance, the pre-industrial ocean is assumed to have been a CO₂ source driven by degradation of river borne organic carbon (Smith and Mackenzie 1987; Sarmiento and Sundquist 1992). In budget studies the contemporary ocean air-sea CO₂ flux is typically corrected for the pre-industrial air-sea CO₂ flux of 0.5 ± 0.2 Pg C year⁻¹, so as to derive the anthropogenic CO₂ flux (Sarmiento and Sundquist 1992; Gruber et al. 2009; Takahashi et al. 2009). However, if most of the degradation of river borne organic carbon occurs in near-shore coastal environments rather than in the open ocean, this correction may be overestimated by ~0.2 Pg C year⁻¹, corresponding to much of the estuarine CO₂ emissions of ~0.3 Pg C year⁻¹ (Laruelle et al. 2010; Cai 2011).

3.2.4.3 Multi-Year Changes and Trends

Based on the decadal analysis of surface water fCO₂ in a very limited number of coastal regions, the coastal CO₂ sink could be increasing in some regions (Wong et al. 2010), while decreasing elsewhere (Thomas et al. 2007). Gypens et al. (2009) used a model reconstruction of the biogeochemistry of the Southern North Sea during the last 50 years to evaluate how the change of river nutrient loads has affected the annual exchange of CO₂ with the troposphere. These authors concluded that carbon sequestration in the southern North Sea increased from the 1950s to the mid 1980s due to an increase in primary production fuelled by eutrophication with an N to P (nitrogen to phosphorus) ratio close

to Redfield of 16 to 1 (Redfield et al. 1963). In consequence, the system shifted from a source to a sink of tropospheric CO₂. During this period pH and calcite saturation increased, rather than decreased as one would have expected from ocean acidification alone (Borges and Gypens 2010). During a period of eutrophication reversal from the mid 1980s onwards, in which river borne nitrogen inputs continued to increase but phosphorus inputs were reduced, primary production in the southern North Sea decreased due to phosphorus limitation and the system shifted back to being a source of tropospheric CO₂. During this period, the carbonate chemistry changed faster than that expected from ocean acidification alone, i.e. ocean acidification was enhanced.

3.3 Marine Distribution and Air-Sea Exchange of N₂O

3.3.1 Global Tropospheric N₂O Budget

N₂O emissions from oceanic and coastal waters play a major role in the tropospheric N₂O budget (Table 3.5). According to the IPCC 4th Assessment Report (Denman et al. 2007) the oceans are a natural N₂O source of 3.8 Tg N year⁻¹ (range 1.8–5.8 Tg year⁻¹), while coastal waters, estuaries, rivers and streams together are an anthropogenic N₂O source of 1.7 Tg N year⁻¹ (range 0.5–2.9 Tg year⁻¹). These sources thus contribute 20 % and 10 % respectively, of total global N₂O emissions (Tables 3.2 and 3.5). Considerable uncertainties arise over these emission estimates for reasons that are discussed in Sects. 3.3.5 and 3.6. The quantification of oceanic N₂O emissions and the identification of the marine pathways of N₂O formation and consumption have received increased attention in recent decades (Bange 2008, 2010b).

3.3.2 Nitrous Oxide Formation Processes

Oceanic N₂O is formed exclusively by prokaryotes (bacteria and archaea) via two major processes: nitrification (i.e. oxidation of ammonium, NH₄⁺, to nitrate, NO₃⁻) and denitrification (i.e. reduction of NO₃⁻ to N₂) (Fig. 3.8). Nitrification is the dominant N₂O formation process whereas denitrification contributes about 7–35 % to the overall N₂O budget of the oceans

Table 3.5 Anthropogenic and natural sources of N₂O to the troposphere with the range of estimates between brackets (Denman et al. 2007)

	N ₂ O source (Tg N year ⁻¹)
Anthropogenic sources	
Fossil fuel combustion and industrial processes	0.7 (0.2–1.8)
Agriculture	2.8 (1.7–4.8)
Biomass burning	0.7 (0.2–1.0)
Human excreta	0.2 (0.1–0.3)
Rivers, estuaries, coastal zones	1.7 (0.5–2.9)
Atmospheric deposition	0.6 (0.3–0.9)
Total anthropogenic sources	6.7
Natural sources	
Soils under natural vegetation	6.6 (3.3–9.0)
Oceans	3.8 (1.8–5.8)
Atmospheric chemistry	0.6 (0.3–1.2)
Total natural sources	11.0
Total sources	17.7

(Bange and Andreae 1999; Freing et al. 2012). The contributions to oceanic N₂O production from other microbial processes such as dissimilatory nitrate reduction to ammonia (DNRA) are largely unknown. In general, biological N₂O production strongly depends on the availability of dissolved oxygen (O₂). Under oxic conditions, as found in the majority of oceanic waters, N₂O formation occurs via nitrification. Suboxic to anoxic conditions, which occur in about 0.1–0.2 % of the ocean volume, favour the net formation of N₂O via denitrification (Box 3.5) (Codispoti 2010).

3.3.2.1 Denitrification

During denitrification N₂O occurs as an intermediate which can be both produced and consumed. The denitrification pathway consists of the four step reduction of NO₃⁻ to N₂ (Fig. 3.8), thus it constitutes a net loss of bioavailable (or “fixed”) nitrogen (N). Denitrification is catalysed by four independent metallo-enzymes (Zumft 1997). Both bacterial and archaeal denitrifiers (Philippot 2002; Cabello et al. 2004) are able to respire NO₃⁻ when O₂ becomes limiting. Denitrification may therefore be considered the ancestor of aerobic respiration (Cabello et al. 2004). The O₂ sensitivity of the enzymes involved in denitrification increases step by step along the reduction chain. The enzymes are induced sequentially and a complete denitrification process can only take place at O₂ concentrations below 2–10 μM (Fig. 3.9) (Codispoti et al. 2005). With the observed

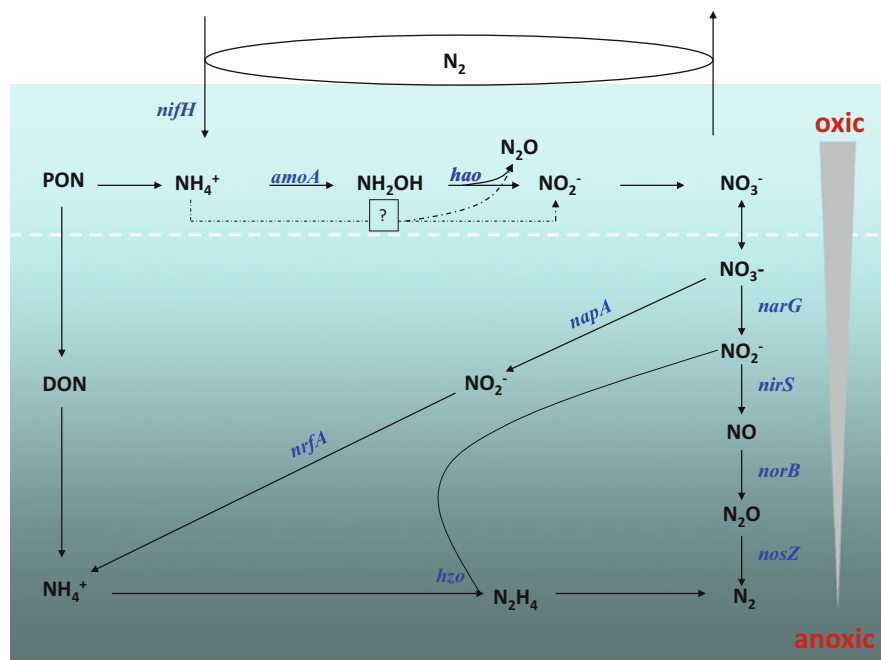


Fig. 3.8 The nitrogen cycle in the oceanic water column along a vertical oxygen gradient. Key functional genes are shown in blue italic letters for the transformations, the oxycline is

indicated by a horizontal, white dashed line, and archaeal ammonia-oxidation is indicated by a horizontal, thin, black dashed-dotted line. (Modified from Francis et al. (2007))

Box 3.5

Dissolved oxygen concentrations play an important role in N₂O and CH₄ cycling. Here we define hypoxic or low oxygen conditions as an O₂ concentration below ~60 μM, suboxic conditions as an O₂ concentration below 5 μM (Deutsch et al. 2011) and anoxic conditions where O₂ is undetectable.

expansion of Oxygen Minimum Zones (OMZs) in the open ocean (Stramma et al. 2010) and the ongoing deoxygenation of highly productive eastern boundary upwelling areas (Codispoti 2010), net N₂O formation by denitrification may increase in the future (Sect. 3.5.3).

3.3.2.2 Nitrification

Under the oxic conditions present in more than 90 % of the ocean, N₂O is formed as a metabolic by-product during nitrification, the stepwise oxidation of NH₄⁺ to nitrite (NO₂⁻) by both ammonia-oxidising bacteria (AOB) and archaea (AOA). Bacteria form N₂O during the oxidation of NH₄⁺ via hydroxylamine (NH₂OH) to NO₂⁻ (Fig. 3.8). Alternatively, N₂O can be formed during the reduction of NO₂⁻ via nitric oxide (NO) to N₂O, the so-called nitrifier-denitrification pathway (Cantera

and Stein 2007). However, the enzymes involved in the nitrifier-denitrification pathway are different from those involved in classical denitrification (Sect. 3.3.2.1). The production of N₂O during nitrification increases with decreasing O₂ concentrations (Goreau et al. 1980; Codispoti et al. 1992). This implies that a significant in situ N₂O production in the upper mixed layer is unlikely, as this layer tends to be well oxygenated.

Until recently the formation of N₂O by nitrification was regarded as an exclusive property of AOB. This view has subsequently been revised in the light of recent work showing that AOA are the key organisms for oceanic nitrification (Wuchter et al. 2006, 2007) and that AOA are able to produce N₂O in large amounts (Santoro et al. 2011; Löscher et al. 2012). Experiments using AOA enriched cultures and pure cultures of *Nitrosopumilus maritimus*, as well as onboard incubation

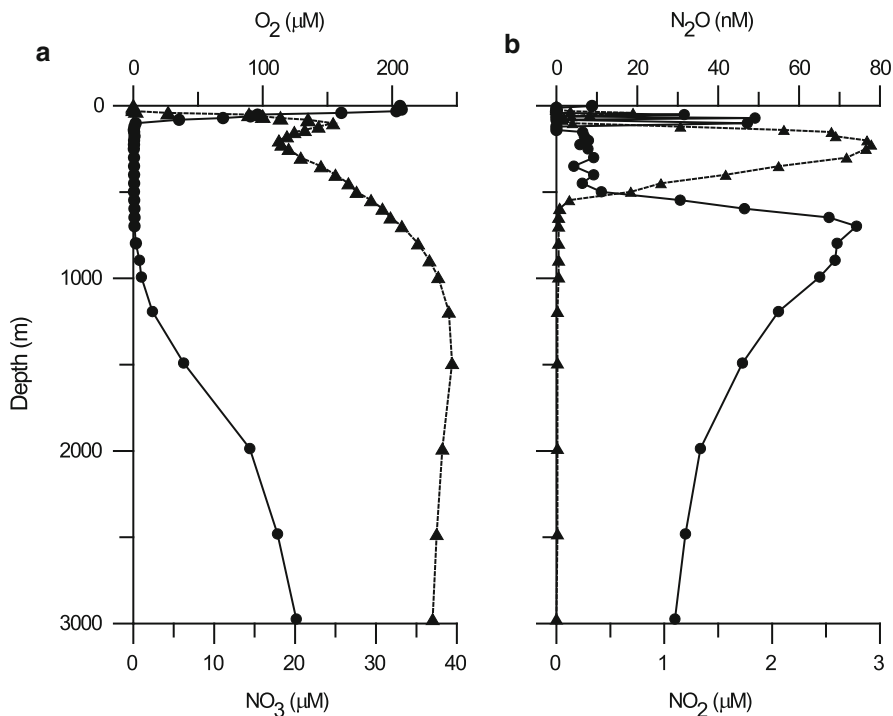


Fig. 3.9 Vertical profiles of (a) dissolved oxygen (circles) and nitrate (triangles), and (b) nitrite (triangles) and nitrous oxide (circles) at 19°N 67°E in the Arabian Sea. Note the pronounced minimum in nitrous oxide within the denitrifying zone,

characterised by a minimum in nitrate and a maximum in nitrite. Maxima in nitrous oxide are found at the peripheries of this zone. (Reproduced from Naqvi (2008) by permission of Elsevier)

experiments with the archaea inhibitor GC7 (Jansson et al. 2000), demonstrated that AOA are the key organisms for N₂O production (Löscher et al. 2012). Nevertheless, the precise metabolic pathway remains unknown. The high affinity of archaea for NH₄⁺ indicates their potential to outcompete AOB even under the nutrient depleted (oligotrophic) conditions (Martens-Habben et al. 2009) which characterise large areas of the open (surface) ocean. It can thus be hypothesised that archaeal NH₄⁺ oxidation is the major source of oceanic N₂O formation.

3.3.2.3 N₂O Formation by Dissimilatory Nitrate Reduction to Ammonium

Dissimilatory nitrate reduction to ammonium (DNRA) via NO₂⁻ is a known source of N₂O (Cole 1988), but was previously considered unimportant in the oceanic water column. However, it was recently found to significantly impact nitrogen cycling in OMZs (Lam et al. 2009) and so may be a more important source of N₂O than previously thought. A variety of bacteria (*Bacillus* sp., *Clostridium* sp., *Enterobacter* sp.) are able to carry

out DNRA (Fazzolari et al. 1990a, b) and are widespread in the ocean and in other environments. N₂O is produced during the second stage of DNRA, the reduction of NO₂⁻ to NH₄⁺ catalysed by NO₂⁻ reductase (Jackson et al. 1991). Nevertheless, information on the biochemical regulation of DNRA in oceanic environments remains sparse (Baggs and Philippot 2010).

3.3.3 Global Oceanic Distribution of Nitrous Oxide

Global maps of N₂O in the surface ocean have been computed by Nevison et al. (1995) (N95) and by Suntharalingam and Sarmiento (2000) (SS00) (Fig. 3.10). The N95 map is based on more than 60,000 measurements mainly made by the Scripps Institution of Oceanography between 1977 and 1993. Oceanic regions with no measurements were filled with a simple statistical routine. The SS00 map was derived from the same N₂O data set, but employed a multivariate adaptive regression spline method using mixed

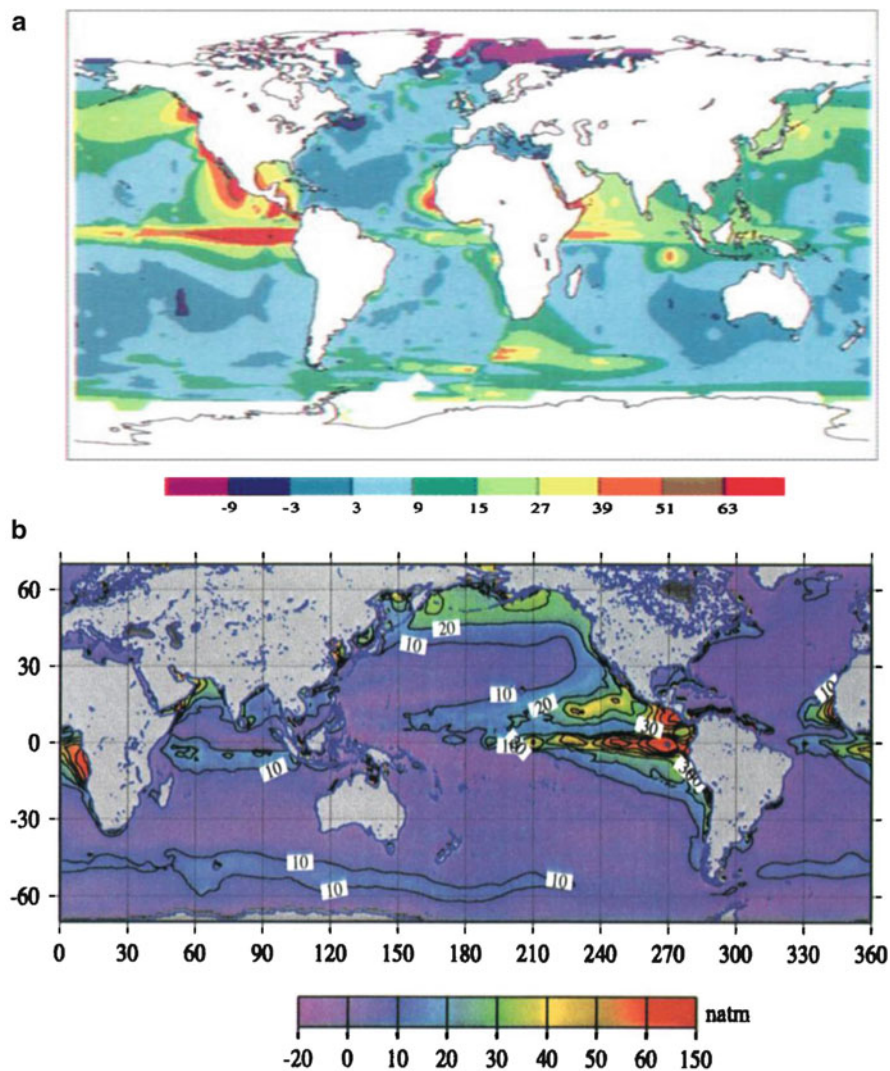


Fig. 3.10 Maps of ΔpN_2O (in natm) in the surface layer of the world's oceans: (a) map by Nevison et al. (1995) and (b) map by Suntharalingam and Sarmiento (2000). Note that the colour

coding is non-linear and different for both maps. (Reproduced from Nevison et al. (1995) and Suntharalingam and Sarmiento (2000) by permission of the American Geophysical Union)

layer depth, O₂, sea surface temperature and upwelling rate as predictor variables. Differences in the two maps result mainly from the different computation methods but they share important common features: (i) enhanced N₂O anomalies (i.e. supersaturation of N₂O) in the equatorial upwelling regions of the eastern Pacific and Atlantic Oceans and in coastal upwelling regions such as along the west coasts of North and Central America, off Peru, off Northwest Africa and in the northwestern Indian Ocean (Arabian Sea); (ii) N₂O anomalies close

to zero (i.e. near equilibrium) in the North and South Atlantic Ocean, the South Indian Ocean and the central gyres of the North and South Pacific Oceans. Both maps are biased by insufficient data coverage in some ocean regions (for example in the Indian and western Pacific Oceans). Since the studies of N95 and SS00 the number of available N₂O measurements has been steadily increasing. With this in mind the MEMENTO (MarinE MethanE and NiTrous Oxide) initiative was launched with the aim of collecting and archiving N₂O (and CH₄)

data sets and to provide surface N₂O (and CH₄) concentration fields for use in deriving emissions estimates (Bange et al. 2009) (Chap. 5).

Nevison et al. (1995) calculated a global mean N₂O surface saturation of 103.5 %, which indicates that the global ocean is a net source of N₂O to the troposphere. Apart from the spatial variability of N₂O surface concentrations described above, considerable seasonal variability has been observed in areas such as the Greenland and Weddell Seas. This seasonality can be caused by (i) rapid temperature shifts resulting in pronounced changes in solubility at a faster rate than N₂O exchange across the air-sea interface (e.g. in the Greenland Sea) and (ii) mixing of surface waters with N₂O enriched subsurface waters (e.g. in the Weddell Sea) (Nevison et al. 1995). While a biological source of N₂O in the well-oxygenated mixed layer seems unlikely, some studies suggested in situ mixed layer production based on a mismatch between the N₂O air-sea flux and the diapycnal flux into the mixed layer (Dore and Karl 1996; Morell et al. 2001). In a recent study of N₂O air-sea and diapycnal fluxes in the eastern tropical North Atlantic (including the upwelling off Mauritania, NW Africa) the mean air-sea flux, calculated using a common gas exchange approach, was about three to four times larger than the mean diapycnal flux into the mixed layer (Kock et al. 2012). Neither vertical advection nor biological production could explain this discrepancy. Kock et al. (2012) speculated that surfactants may dampen air-sea gas exchange of N₂O and other gases such as CO₂ (see for example Tsai and Liu 2003) in areas with a high biological productivity.

3.3.4 Coastal Distribution of Nitrous Oxide

During the last two decades coastal areas such as estuaries, upwelling regions, and mangrove ecosystems have received increased attention as sites of intense N₂O formation and release to the troposphere. Studies of the N₂O pathways in coastal regions have mostly been undertaken in European and North American coastal regions but the number of studies from other coastal regions (e.g. from Asia and South America) has recently been increasing. In general, strongly positive N₂O anomalies are found in nitrogen-rich estuaries (Zhang et al. 2010; Barnes and Upstill-Goddard 2011) and in

coastal upwelling systems (Nevison et al. 2004). Coastal N₂O emissions contribute significantly to the overall oceanic emission (Table 3.6).

Nitrous oxide saturations in estuaries are highly variable and can reach values up to 6,500 % (Zhang et al. 2010; Barnes and Upstill-Goddard 2011). N₂O formation in estuaries heavily depends on the availability of NH₄⁺ fuelling nitrification in the water column and/or sedimentary denitrification as major N₂O formation pathways (Bange 2006b; Barnes and Upstill-Goddard 2011). In nitrogen-rich estuarine systems, extremely high N₂O anomalies are usually only found in inner estuaries, whereas outer estuaries and adjacent shelf waters, which are not influenced by the river plumes, are close to equilibrium with the troposphere (Barnes and Upstill-Goddard 2011). In some European estuaries maximum N₂O concentrations are associated with the turbidity maximum zone at low salinities (Barnes and Upstill-Goddard 2011). The traditional view of a simple relationship between river inputs of dissolved inorganic nitrogen (the sum of NH₄⁺ and NO₃⁻) and estuarine N₂O formation has been challenged by recent findings that resuspended NH₄⁺ and/or NH₄⁺ derived from ammonification of particulate organic nitrogen in the turbidity maximum zone might dominate N₂O production (Barnes and Upstill-Goddard 2011). This implies that N₂O formation may not be related to river inputs of dissolved inorganic nitrogen in any simple way (Barnes and Upstill-Goddard 2011). High N₂O saturations in estuaries (and rivers) are also found at sites of sewage and industrial effluents.

The narrow bands of coastal upwelling systems such as those found in the northwestern Indian Ocean (Arabian Sea) and in the southeastern Pacific Ocean (off central Chile) have been identified as ‘hot spots’ of extremely high N₂O concentrations with N₂O saturations of up to 8,250 % and 2,426 %, respectively (Naqvi et al. 2005; Cornejo et al. 2007). The high N₂O saturations in coastal upwelling regions appear to be caused by the upwelling of N₂O enriched subsurface waters (Naqvi et al. 2005; Cornejo et al. 2007).

Some coastal upwelling areas show a rapid seasonal transition from oxic via suboxic to anoxic conditions and vice versa. In these systems, significant amounts of N₂O (up to several hundred nM) (Fig. 3.11) can accumulate temporarily during the short transition time, when the system is changing its oxygen regime. This phenomenon has been observed at different coastal time-series sites associated with coastal upwelling, such as off central

Table 3.6 N₂O emissions from marine waters

	Area (10 ⁶ km ²)	N ₂ O emission (Tg N year ⁻¹)	Reference
Open ocean	–	1.8–5.8	Denman et al. (2007)
	313	0.6–1.1	Rhee et al. (2009)
Total open ocean	348^a	0.6–5.8	
Coastal upwellings	1.75	0.05–0.2	Nevison et al. (2004)
	0.4 ^b	0.0015–0.0035	Rhee et al. (2009)
Estuaries	1.4 ^c	0.25	Kroeze et al. (2005)
Mangroves	0.2	0.1	Barnes et al. (2006)
Other coastal regions	10 ^d	0.08 (± >25 %)	Nevison et al. (2004)
	48 ^b	0.4–0.9	Rhee et al. (2009)
Total coastal regions (incl. upwelling, estuaries and mangroves)	13.35^e	0.4–1.45	
Total ocean (open ocean and coastal regions)	361	1.0–7.25^f	

^aEstimated as the difference between the total ocean area (361 × 10⁶ km²) and the sum of the areas (in 10⁶ km²) of coastal upwelling (1.75), continental shelves with a depth <200 m (10), estuaries (1.4) and mangroves (0.2)

^bSource not given

^cAs cited in Nevison et al. (2004)

^dContinental shelves with a depth <200 m

^eEstimated as the sum of the areas (in 10⁶ km²) of coastal upwelling (1.75), continental shelves with a depth <200 m (10), estuaries (1.4) and mangroves (0.2)

^fEstimated as the sum of the regional minimum and maximum values, respectively

Chile and off West India, and in the western Baltic Sea (Naqvi et al. 2010). During the transition stages, the accumulation of N₂O does not occur in the anoxic zones, but at the oxic to anoxic boundaries. The exact cause of this extreme accumulation of N₂O is not well understood, although inhibition of the activity of N₂O reductase through frequent incursion of O₂ into the O₂-deficient layer has been proposed as one possible explanation. In anoxic zones, N₂O is usually found at very low or even undetectable concentrations.

Another intriguing feature is the much smaller N₂O accumulation at the upper boundary of the suboxic zone of enclosed anoxic basins (Black Sea, Baltic Proper) and some anthropogenically-formed anoxic zones (Tokyo Bay and Chesapeake Bay). In the hypoxic bottom waters of the East China Sea and the Gulf of Mexico, the observed N₂O build-up is modest. Overall, these results do not show comparable N₂O build-up in the anthropogenically-formed coastal hypoxic zones to those in naturally-formed, upwelling-related coastal suboxic zones (Naqvi et al. 2010). However, a large number of anthropogenically-formed anoxic zones remain to be investigated.

Mangrove ecosystems cover ~75 % of tropical coasts and are among the world's most productive ecosystems. Their open waters cover ~0.2 × 10⁶ km²,

equivalent to ~20 % of the global estuarine area (Borges et al. 2003). The ecosystems of mangrove forests have a high potential of N₂O formation and release to the troposphere (Barnes et al. 2006). There seems to be no dominant formation process: N₂O in mangrove sediments from Puerto Rico was mainly produced by nitrification (Bauzá et al. 2002), whereas incubation experiments with mangrove soils from the east coast of Australia revealed denitrification to be the main N₂O formation pathway (Kreuzwieser et al. 2003). In a seasonal study of N₂O emissions from a pristine mangrove creek on South Andaman Island (Gulf of Bengal), Barnes et al. (2006) found that N₂O emissions were negatively correlated with tidal height, indicating that N₂O (and CH₄) is released from sediment pore waters during “tidal pumping”, i.e. during cyclic decrease and increase of the hydrostatic pressure between low and high water (Fig. 3.12; Sect. 3.4.4).

3.3.5 Marine Emissions of Nitrous Oxide

The N₂O emission estimates in Tables 3.5 and 3.6 imply that coastal areas contribute significantly to total marine N₂O emissions, which is in line with previous emission estimates (Bange 2006a). The

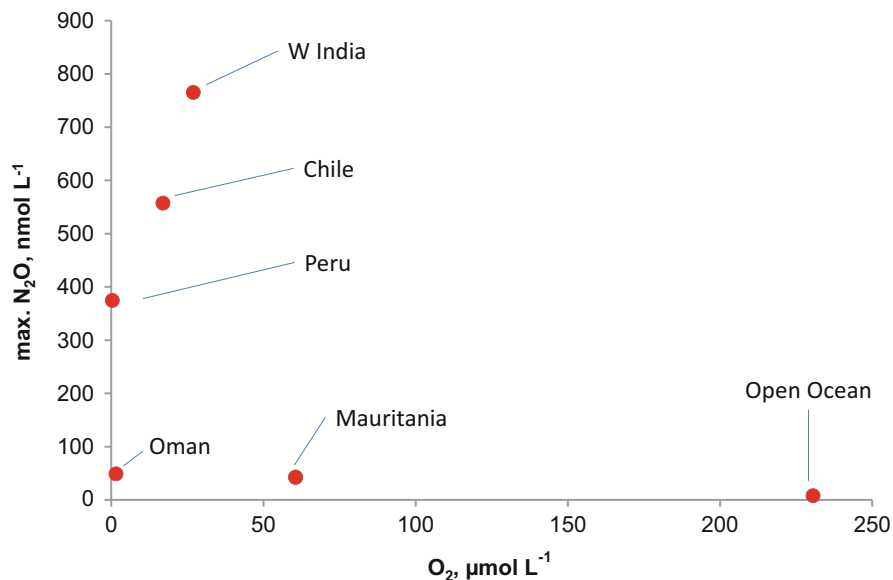


Fig. 3.11 Maximum N_2O concentrations and associated O_2 concentrations in coastal upwelling regions. A typical N_2O surface concentration in the tropical open ocean is also shown. (Data sources: W. India and Oman – S.W.A. Naqvi, pers. comm.;

Mauritania – A. Kock and H.W. Bange, unpublished; Chile – Cornejo et al. (2006); Peru – C.R. Löscher and H.W. Bange, unpublished)

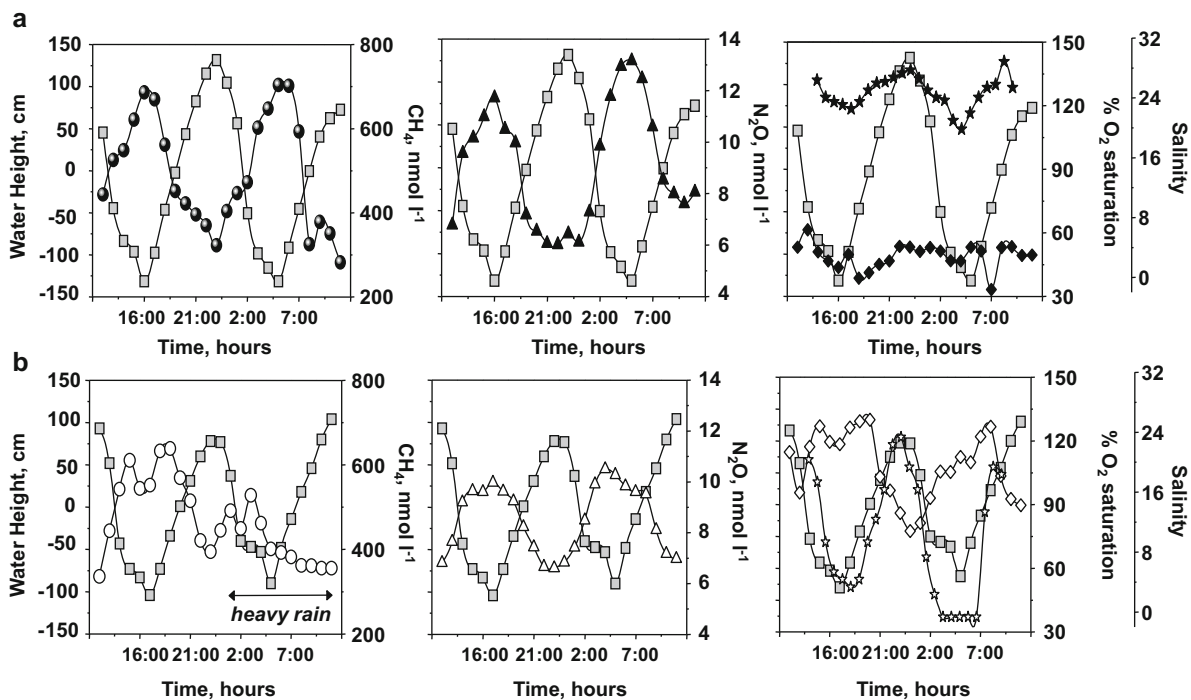


Fig. 3.12 Variation of CH_4 (circles), N_2O (triangles), tidal height (squares), O_2 saturation (stars) and salinity (diamonds) in a tropical mangrove creek (Wright Myo, Andaman Island)

during (a) the dry season (January 2004) and (b) the wet season (July 2004) (Reproduced from Barnes et al. (2006) by permission of the American Geophysical Union)

emission estimates for coastal areas (upwelling regions, shelves, estuaries and mangroves) have a large uncertainty because of the small number of available measurements. In particular, natural coastal suboxic zones are strong N₂O sources to the troposphere. The total N₂O emission from these areas could be as high as 0.56 Tg N year⁻¹ (Naqvi et al. 2010), comparable to global emissions from estuaries (0.25 Tg N year⁻¹) and continental shelves (0.4–1.45 Tg N year⁻¹) (Table 3.6) (Seitzinger and Kroeze 1998). As is the case for open ocean emissions (see below), flux estimates from coastal areas need to consider seasonal variability (Wittke et al. 2010; Zhang et al. 2010; Barnes and Upstill-Goddard 2011).

The recent open ocean estimate by Rhee et al. (2009) is considerably lower than that of the widely used IPCC 4th Assessment Report (Table 3.6) (Denman et al. 2007). However, because the estimate by Rhee et al. (2009) is based on a single meridional transect in the Atlantic Ocean, it almost certainly includes an unquantified seasonal and regional bias.

Unfortunately, the seasonality of surface water N₂O concentrations over large regions of the ocean remains unknown because ship campaigns are limited in space and time and N₂O sensors are not yet available on gliders, floats or moorings. Neglecting the seasonality of surface N₂O concentrations introduces severe bias into the N₂O flux estimates. Freing (2009) demonstrated how both N₂O concentrations in surface water and N₂O fluxes in the North Atlantic Ocean (19–42°N) follow a seasonal cycle similar to that of fCO₂ (Fig. 3.13; Sect. 3.2.3). This seasonal cycle can be described by a harmonic function and is mainly controlled by temperature. The presence of such seasonal variation renders a mean flux, if calculated from a seasonally-biased dataset, a potentially poor estimate of the true annual net flux (Freing 2009). Integrating the harmonic function over a full annual cycle gives a better estimate of the net annual flux.

In ocean regions where the upper boundary of the OMZ is shallow, minor changes in the hydrographic or meteorological conditions can lead to entrainment of N₂O from the OMZ into the surface layer, thereby enhancing N₂O sea-to-air fluxes (Naik et al. 2008). As a result of high N₂O concentrations close to the sea surface, N₂O emissions in open-ocean regions with substantial N₂O accumulation at mid-depth (associated with O₂ depletion) (e.g. in the Eastern Tropical South Pacific and the Arabian Sea), are quite high. The N₂O emissions from these regions (0.8–1.35 Tg N year⁻¹)

(Naqvi et al. 2010) make up a significant fraction of the overall N₂O emission from the oceans (Table 3.6).

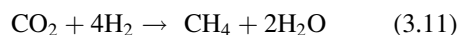
3.4 Marine Distribution and Air-Sea Exchange of CH₄

3.4.1 Global Tropospheric CH₄ Budget

In contrast to the situation for CO₂ and N₂O, the marine system plays a relatively minor role in the global tropospheric CH₄ budget, representing a small net natural contribution (Tables 3.2 and 3.3). However, in common with other global CH₄ sources, marine-derived CH₄ has proven difficult to quantify with any great certainty (Table 3.3). Although detailed CH₄ surveys in specific ocean basins have been available since the 1970s, they are comparatively limited in number and many of the early measurements were derived in the absence of reliable solubility data (Reeburgh 2007). The global marine CH₄ dataset is thus rather limited in comparison to CO₂ or N₂O. Detailed maps of the global surface ocean distribution remain to be compiled, with the recent MEMENTO initiative (Bange et al. 2009) working towards this goal (Chap. 5).

3.4.2 Formation and Removal Processes for Methane

Methanogenesis is the final stage of organic matter decomposition and is a form of anaerobic respiration carried out exclusively by single celled archaea whose growth is severely O₂-limited. The terminal electron acceptor is therefore not O₂, but carbon from low molecular weight compounds. Carbon dioxide and acetic acid (CH₃COOH) are the most familiar:



Other low molecular weight compounds acting as methanogenic substrates include formic acid (HCOOH), methanol (CH₃OH), methylamine (CH₃NH₂), dimethylsulphide (CH₃SCH₃) and methanethiol (CH₃SH). Unsurprisingly, anoxic coastal marine sediments (Middelburg et al. 1996) and strongly O₂-deficient waters (Naqvi et al.

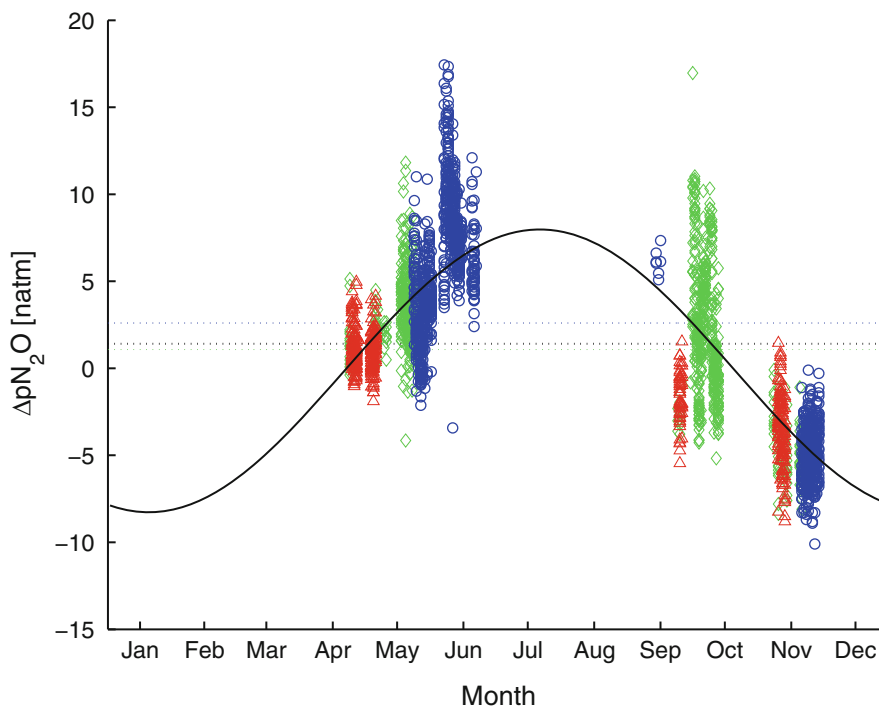


Fig. 3.13 $\Delta p\text{N}_2\text{O}$ (in natm) in the North Atlantic Ocean (19–42°N 10–66°W): Tropical (red triangles), western subtropical (green diamonds) and eastern subtropical (blue circles) regions. The solid black line denotes a fitted harmonic function.

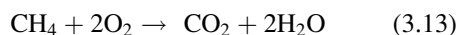
The dotted lines denote the respective annual mean for all data points (black, middle line), the western (green, bottom line) and the eastern (blue, top line) basin. (The figure is from Freing (2009))

2005) are major sites of methanogenesis. The ability of sulphate-reducing bacteria (SRB) to outcompete methanogens (Capone and Kiene 1988) means that CH₄ concentrations are generally low in near-surface sediment pore waters where sulphate reduction is active and that they are maximal below the depth where dissolved sulphate (SO₄²⁻) becomes fully depleted (Blair and Aller 1995). This can be anywhere between several centimeters and several meters below the sediment surface. The role of SRB is an important consideration in estuaries, where water column SO₄²⁻ concentrations vary from micro- to milli-molar along the salinity gradient. In these situations the depth of SO₄²⁻ depletion increases and maximal CH₄ production generally decreases seaward. Methanogenesis rates have thus been shown to decrease by up to two orders of magnitude seaward (Abril and Borges 2004). In addition to SO₄²⁻ availability and associated SRB activity, rates of organic matter sedimentation and the availability of alternative electron acceptors also influence methanogenesis rates.

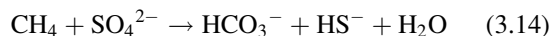
Despite inhibition of methanogenesis by both O₂ and SO₄²⁻ supply, CH₄ is typically supersaturated in the open ocean mixed layer (Sect. 3.4.3). Until recently the prevailing explanation for this so-called “marine CH₄ paradox” has been methanogenesis (Eqs. 3.11 and 3.12) within “anoxic microniches” inside zooplankton guts and suspended particles (Oremland 1979; De Angelis and Lee 1994). This notion is supported by an “oxic” methanogenic archaea isolated from coastal waters (Cynar and Yayanos 1991), the identification of methanogens in marine zooplankton guts and particles (Marty et al. 1997) and CH₄ release from sinking particles inferred from $\delta^{13}\text{C}_{\text{CH}_4}$ measurements (Sasakawa et al. 2008). Even though significant CH₄ release has been observed from mixed zooplankton-phytoplankton cultures (De Angelis and Lee 1994) and correlations of CH₄ with primary productivity indicators, such as chlorophyll *a*, have been found (Oudot et al. 2002), such correlations are weak (Upstill-Goddard et al. 1999; Holmes et al. 2000; Forster et al. 2009).

Recent investigations propose two alternative CH₄ production mechanisms, both implicating nutrient limitation in the control of mixed layer CH₄ formation. In the first hypothesis bacterioplankton successfully exploit phosphate-depleted waters, where nitrate is in excess, by deriving phosphorus from phosphonates such as methyl phosphonate (Karl et al. 2008). Methane is thus produced aerobically as a byproduct of methyl phosphonate decomposition. The second hypothesis proposes that certain microbes can catabolise dimethylsulphoniopropionate (DMSP) as a carbon source through methylotrophic methanogenesis in NO₃⁻ depleted waters, where phosphate (PO₄³⁻) is plentiful (Damm et al. 2010). Based on the conversion of DMSP to hydrogen sulphide (H₂S) and CH₃SH by DMSP-utilising bacteria (Kiene et al. 2000) and a recent proposal for the intermediate formation of CH₃SH during CH₄ oxidation (Moran et al. 2008), Damm et al. (2010) proposed a thermodynamically plausible reverse reaction for the aerobic production of CH₄ from CH₃SH. The two mechanisms are entirely compatible and raise the intriguing possibility that deviations from the Redfield N:P ratio could be indirectly responsible for the marine CH₄ paradox through planktonic succession favouring species able to exploit alternative marine phosphorus and nitrogen stores.

Whatever the mechanisms responsible for upper ocean marine CH₄ production, emission of CH₄ to the troposphere is strongly moderated by aerobic and anaerobic microbial oxidation (Boetius et al. 2000). Aerobic CH₄ oxidation occurs in oxygenated water columns and oxic sediment pore waters:



Anaerobic oxidation of methane (AOM) occurs both in anoxic sediment pore waters and in anoxic water columns and is believed to involve consortia of archaea and SRB:



In sediment pore waters the SO₄²⁻-CH₄ transition constrains upward CH₄ diffusion and leads to pore water CH₄ profiles having a concave-upward shape (Blair and Aller 1995).

3.4.3 Global Oceanic Distribution of Methane

Although CH₄ concentrations in the open ocean are generally rather low (a few nM), net mixed layer CH₄ production means that O₂-saturated near-surface waters are generally also supersaturated in CH₄, with typical values of 130–160 % and maxima near the base of the mixed layer (Oudot et al. 2002; Forster et al. 2009). Considerably higher mixed layer CH₄ supersaturation is, however, not uncommon. Figure 3.14 illustrates this for the upper 300 m of the water column on north–south Atlantic Ocean transects. In addition to upper ocean CH₄ production, lateral supply from continental margins (Sect. 3.4.4) has also been invoked to explain high mixed layer CH₄ concentrations (Reeburgh 2007).

Similar to N₂O, elevated CH₄ levels are also found in intermediate waters (~500–1,000 m depth) of the three major open ocean OMZs: the Eastern Tropical North and South Pacific and the Arabian Sea (Naqvi et al. 2010), and in the upwelling zones associated with these OMZs (Sect. 3.3.5). In these regions seasonal upwelling of nutrient-rich waters fuels primary productivity and enhances the downward flux of biogenic particles (Rixen et al. 1996), leading to O₂ consumption in the intermediate waters and subsequent methanogenesis.

Below the ocean mixed layer and away from the OMZ's, CH₄ concentrations progressively decrease through oxidation, such that CH₄ concentrations may approach undetectable levels in the deep ocean basins (Upstill-Goddard et al. 1999; Yoshida et al. 2011). Occasionally this deep water CH₄ signal impacts surface waters through oceanic upwelling, as is illustrated by the bottom panel of Fig. 3.14 where the effect of equatorial upwelling is evident as far north as ~15°N. Overall, on an annual basis the open ocean CH₄ budget is considered to be in steady-state with in situ production and vertical transport balancing CH₄ oxidation and emissions to the troposphere.

3.4.4 Coastal Distribution of Methane

3.4.4.1 Coastal Sediments

The total mass of CH₄ in shallow marine sediments remains unquantified but it is nevertheless thought to be substantial, with methanogenesis considered likely in at least 30 % of the global continental shelf area (Judd

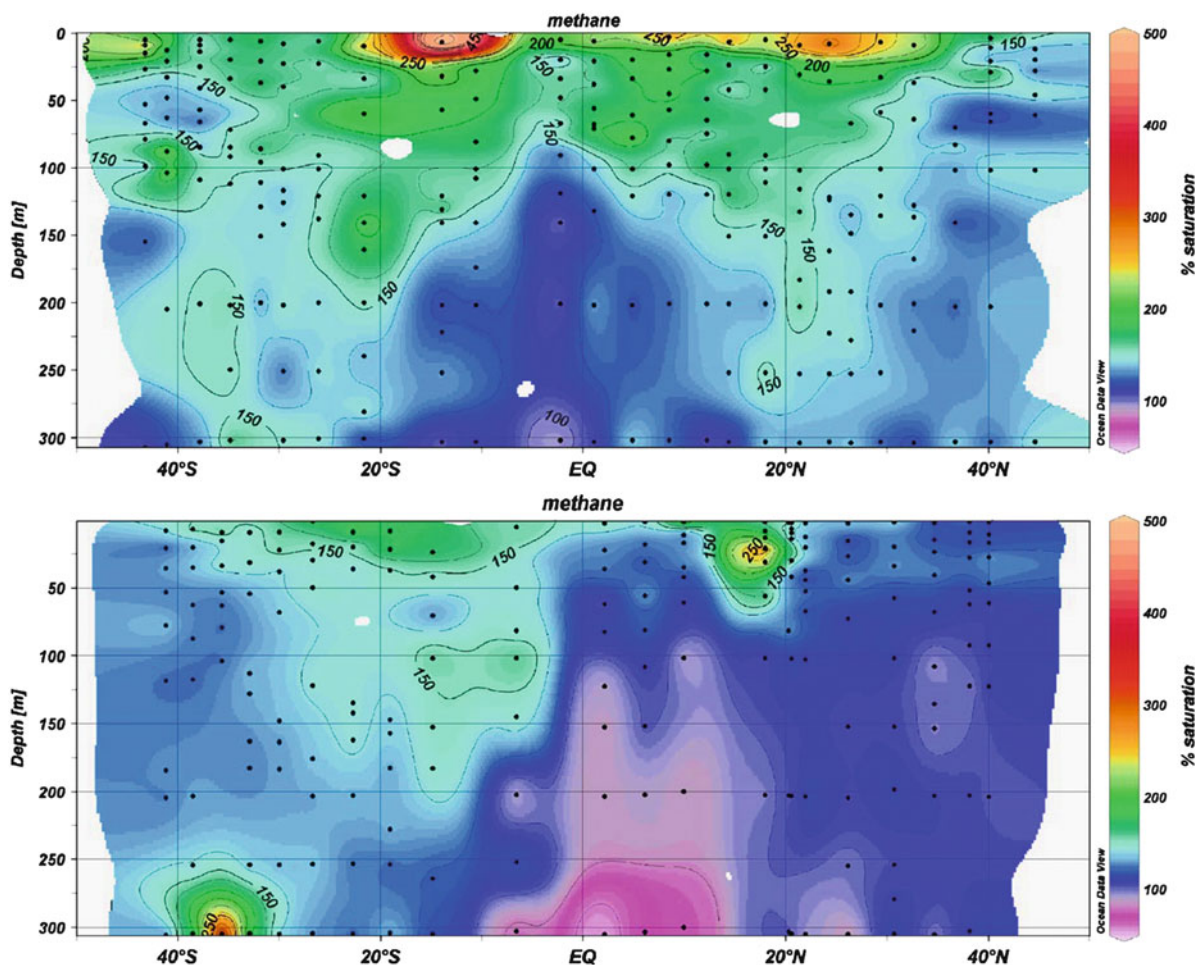


Fig. 3.14 CH₄ saturation in the upper 300 m of the Atlantic Ocean between 50°N and 52°S during 2003. *Top panel:* April–May; *bottom panel:* September–October. *Dots* represent water samples. (Reproduced from Forster et al. (2009) by permission of Elsevier)

and Hovland 2007), i.e. at least 7.4×10^6 km² (Laruelle et al. 2010). Although it is estimated that more than 90 % of the sediment CH₄ inventory may be consumed by AOM (Sect. 3.4.2) prior to sediment-water exchange (Dale et al. 2006), CH₄ emissions from individual sites can be very high per unit area (Middelburg et al. 1996; Abril and Iversen 2002) and can significantly impact the CH₄ signal in the overlying water. Figure 3.15 is an example from a UK estuary (Tyne) where the broad CH₄ maximum between salinities 5 and 20 may reflect inputs from anoxic intertidal mudflats in mid-estuary (Upstill-Goddard et al. 2000 and discussion below).

In some circumstances organic carbon burial may be sufficiently intense that the resulting rate of methanogenesis contributes to raising the total pore

water gas concentration above the hydrostatic pressure in the sediment, with the result that gas bubbles are formed (Wever et al. 1998). It has been shown that bubbles start to form at CH₄ concentrations well below its solubility (~ 1 mM) and that these may contain ~ 40 – 100 % CH₄ (Chanton et al. 1989). This results in a rapid, episodic release of CH₄ enriched bubbles to the water column (ebullition) and potentially directly to the troposphere with minimal oxidation (Dimitrov 2002). CH₄ ebullition may typically exceed the diffusional sediment CH₄ flux by more than an order of magnitude (Ostrovsky 2003; Barnes et al. 2006; Nirmal Rajkumar et al. 2008). However, ebullition is notoriously difficult to quantify because spatial and temporal variability can confound attempts to accurately capture a representative sample. Perhaps

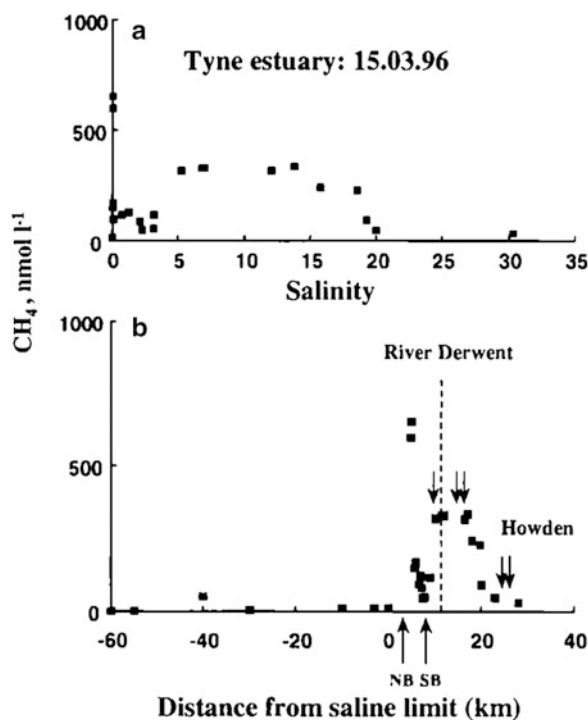


Fig. 3.15 Dissolved CH₄ in the Tyne estuary, UK. (a) CH₄ versus salinity; (b) CH₄ versus distance from the tidal limit (positive is downstream; negative is upstream). Dotted line:

location of major tributary (Derwent); arrows: locations of additional freshwater discharges (Reproduced from Upstill-Goddard et al. (2000) by permission of the American Geophysical Union)

unsurprisingly, few studies have directly studied sediment CH₄ ebullition and hence the controlling processes have not been well quantified. Temperature is clearly important through solubility effects and its control of methanogenesis rates, as is water depth. In coastal waters ~3 m deep, minimal bubble dissolution was observed during migration to the air-sea surface (Martens and Klump 1980), but in deeper waters complete bubble dissolution may occur, before the bubbles reach the sea surface (Joyce and Jewell 2003). Contamination of CH₄-enriched bubbles by surfactants can also significantly reduce their rise velocities, thereby increasing the potential for dissolution (Leifer and Patro 2002). However, surfactants on the bubble surfaces will also decrease the rate of gas exchange between the bubbles and the water (e.g. Tsai and Liu 2003). Shakhova et al. (2010) reported bubbles of CH₄ entrapped in fast sea ice in the East Siberian Arctic Shelf, which they attributed to ebullition from underlying sediment. If sea ice acts to moderate the emission of CH₄ in this way, this has clear implications for Arctic CH₄ emissions as a consequence of sea ice retreat.

Vegetation strongly impacts the distribution and transport of CH₄ in coastal sediments. It has been proposed that plant-mediated CH₄ transport and CH₄ ebullition are mutually exclusive processes in tidal marshes (Van der Nat and Middelburg 1998, 2000). Vegetation impacts CH₄ concentrations in coastal sediments via the release of labile organic compounds that may stimulate methanogenesis. Vegetation also acts as a conduit for the transport of CH₄ to the troposphere and for transport of tropospheric O₂ to the rhizosphere favouring CH₄ oxidation, both transport pathways reducing CH₄ concentrations in near-surface sediments (Van der Nat and Middelburg 1998, 2000; Biswas et al. 2006). In addition, plants promote CH₄ oxidation at depth, where methanotrophs occur adjacent to or within macrophyte roots (Gerard and Chanton 1993; King 1994). Plant-mediated CH₄ transport is both passive via molecular diffusion and active via convective flow due to pressure gradients and is maximal during daylight hours in the growing season (Van der Nat et al. 1998; Van der Nat and Middelburg 2000). In two Tanzanian mangrove systems sediment-to-air CH₄ fluxes were enhanced up to fivefold in the

presence of pneumatophores (above ground root systems) and it was estimated that transport via this pathway accounted for 38–64 % of the total sediment CH₄ source to air at low tide (Kristensen et al. 2008). In some situations both diffusive CH₄ exchange and ebullition can be enhanced by “tidal pumping” related to falling hydrostatic pressure (Sect. 3.3.4) (Barnes et al. 2006), with pressure changes of only a few percent having a large effect (Ostrovsky 2003). Figure 3.12 shows an inverse relation of CH₄ (and N₂O) concentrations with tidal height in a tropical mangrove creek. This indicates tidal pumping with CH₄-rich sediment pore waters seeping into the overlying creek waters at low tide, but remaining in the sediment as the hydrostatic pressure rises again. Barnes et al. (2006) suggested that tidal pumping is a major control of CH₄ and N₂O emissions from mangrove systems (Sect. 3.3.4).

Ancient microbial, thermogenic, and abiogenic CH₄ in coastal shelf sediments can become “geologically focussed”, which may result in episodic CH₄ ebullition on a potentially large scale (Judd and Hovland 2007). The ephemeral nature of these “seep fluxes” is well illustrated by observations at a seep site in the outer Firth of Forth (North Sea). Dissolved CH₄ concentrations in the water column strongly increased towards the shallow seabed (~1,500 % CH₄ saturation at 90 m), but 1 year later the dissolved CH₄ concentration was only mildly supersaturated (Upstill-Goddard 2011). Shallow seeps clearly influence surface water CH₄ concentrations (Damm et al. 2005; Schmale et al. 2005). The North Sea has numerous well-documented “pock marks” (Dando et al. 1991); evidence for significant past CH₄ seepage.

3.4.4.2 Coastal Waters

Inland waters (lakes, reservoirs, streams, and rivers) can be substantial CH₄ sources to the coastal zone, although they are currently not well integrated in global greenhouse gas budgets (Table 3.3) (Bastviken et al. 2011). Most rivers studied to date are highly CH₄ supersaturated, including pristine, well-oxygenated regimes with minimal sediment cover or anthropogenic disturbance (Upstill-Goddard et al. 2000). Large CH₄ inputs from adjacent forest and/or agricultural soils have been suggested (Devol et al. 1990; Yavitt and Fahey 1991). The CH₄ concentration in river water is a complex function of catchment hydrology, vegetation cover, microbial activity, and re-aeration rates. Upstill-

Goddard et al. (2000) found a general decrease in dissolved CH₄ with increasing river discharge. Their compilation of published CH₄ saturations in rivers worldwide revealed a typical range of ~1,000–40,000 %, with one extreme value for an organic-rich Amazon tributary exceeding 400,000 % (Upstill-Goddard et al. 2000). Data from 474 freshwater ecosystems point to a major CH₄ source in inland waters (Bastviken et al. 2011). Part of this contribution is almost certainly included in the source estimate for global wetlands (Table 3.3). The CH₄ source from inland waters should perhaps be formally specified as an important component in the global tropospheric CH₄ budget.

Most estuarine CH₄ data are for temperate systems. Methane saturations of up to 8,000 % have been reported for some shallow coastal embayments (Ferrón et al. 2007; Kitidis et al. 2007). A CH₄ saturation of up to 20,000 % may be typical of the mid- to upper-inner estuary (Upstill-Goddard et al. 2000; Abril and Iversen 2002; Middelburg et al. 2002). As much as 158,000 % CH₄ saturation has been reported in the Sado estuary, Portugal (Middelburg et al. 2002). The highest value recorded exceeds 3,000,000 % for the small, polluted subtropical Aydar estuary in SE India (Nirmal Rajkumar et al. 2008). This may be considered exceptional, resulting from a high organic carbon input in fresh domestic organic wastes and intense sediment methanogenesis. Indeed, methanogenesis rates were estimated to be close to maximal for the ambient temperature (Nirmal Rajkumar et al. 2008).

An important aspect of CH₄ cycling in many well-mixed macrotidal estuaries is strong tidal asymmetry with the velocity of the flood tide exceeding that of the ebb tide. This gives rise to the net transport of suspended particles upstream and retains river borne particles in a well defined turbidity maximum zone at low salinity (Uncles and Stephens 1993). High micro-organism numbers associated with the suspended particles (Plummer et al. 1987) and long particle lifetimes promote enhanced biogeochemical cycling in such regions and CH₄ concentrations can significantly exceed those in the input rivers (Fig. 3.15) (Upstill-Goddard et al. 2000). While this could result from active CH₄ release from the underlying sediments during particle resuspension (as discussed above), it could also reflect in situ water column production of CH₄ through attachment of methanogenic

archaea to tidally suspended particles in the turbid, O₂-poor waters, analogous to the “anoxic microniche” hypothesis in the open ocean (Barnes and Upstill-Goddard 2011). By contrast, Abril et al. (2007) found significant CH₄ oxidation in laboratory sediment suspensions, although at higher turbidity than measured in situ by Upstill-Goddard et al. (2000). The conflicting results may reflect competition between methanogenesis and oxidation, implying complexity in the relationship between CH₄ concentrations and estuarine turbidity.

Mangrove ecosystems are significant contributors to the marine source of tropospheric CH₄ (Fig. 3.12; Table 3.7). Typically one half of mangrove net primary production is retained within the system (Dittmar et al. 2006; Bouillon et al. 2008) and this carbon is buried and/or recycled, resulting in significant CH₄ production in heterotrophic sediments and in the overlying water. The mangrove CH₄ source appears rather constant throughout the year, possibly as a result of small annual temperature excursions in mangrove systems that give minimal variability in methanogenesis rates (Barnes et al. 2006; Ramesh et al. 2007). CH₄ saturations in waters surrounding mangroves are spatially and temporally variable. Up to ~30,000 % saturation was observed in mangrove creek waters (Barnes et al. 2006), but regionally ~2,000–3,000 % might be more typical (Biswas et al. 2007).

Coastal shelf seas are almost always supersaturated in CH₄. Data for coastal shelf seas tend to be restricted to the temperate northern hemisphere with hardly any data available for coastal waters along much of the Russian Arctic, South America, East and West Africa and Antarctica. Bange (2006b) provides the most extensive regional data compilation to date, for a European shelf area estimated at $\sim 3 \times 10^6$ km² or ~12 % of the global shelf sea area (Table 3.8). The variability between sites may partly reflect seasonal variation, but it is not straightforward to assess the extent of this seasonality due to a lack of seasonal measurements at individual locations.

Marine sediments are a major CH₄ source to coastal waters, in spite of the inhibition of methanogenesis by SRB and CH₄ oxidation by O₂ and SO₄²⁻. Indeed, substantial accumulation of dissolved CH₄ in well-oxygenated bottom waters overlying organic-rich coastal sediments is well documented (Martens and Klump 1980). Order of magnitude higher concentrations have been observed in anoxic bottom

waters overlying sediments with moderate organic carbon content in the Arabian Sea (Jayakumar et al. 2001). Production of CH₄ in sediments and its supply to bottom waters is primarily linked to biological productivity in the overlying waters, with hypoxia in the water exerting a secondary effect (Bange et al. 2010a). Most regions with high productivity are associated with coastal upwellings, the extent of which is set by Laruelle et al. (2010) at $\sim 2.3 \times 10^6$ km². While this is only ~0.6 % of the total ocean area, these regions are “hot spots” of CH₄ emissions to the troposphere, with typical surface CH₄ saturations of ~150–250 % (Naqvi et al. 2005; Kock et al. 2008). Maximal water column CH₄ accumulation occurs in sulphidic deep waters within enclosed basins, such as the Black Sea and the Cariaco Basin, but this CH₄ is largely of geological origin (Kessler et al. 2005). By contrast, over the highly productive Namibian shelf, where sulphidic bottom water is also characteristic, the large CH₄ emission from underlying organic-rich sediments is a consequence of contemporary methanogenesis (Brüchert et al. 2009). In coastal zones, where the hypoxic conditions are caused by anthropogenic activities, the CH₄ distribution is highly variable. For example, maximum CH₄ concentrations in the Gulf of Mexico (Kelley 2003) are ~15 times higher than in the Changjiang Estuary and the East China Sea (Zhang et al. 2008).

3.4.4.3 Methane Hydrates

Methane hydrate is a quasi-stable solid, resembling ice, in which CH₄ molecules are trapped within the crystalline structure of water. Hydrate stability decreases with increasing temperature and decreasing pressure (Kvenvolden 1993). Hydrate occurs extensively in buried sediments and seabed outcrops along continental margins where water depths exceed 500 m (Beauchamp 2004) and along gravitationally unstable regions of the continental slope (Fig. 3.16). The distribution and extent of stable CH₄ hydrate can be predicted from in situ temperature and pressure, such that a theoretical gas hydrate stability zone (GHSZ) can be defined. Figure 3.17 is a schematic of the GHSZs in sediments at shallow and deep marine sites. The CH₄ source may be biogenic, volcanic, hydrothermal or thermogenic. Biogenic CH₄ from sediment methanogenesis tends to dominate (Sloan 2003).

Methane hydrates can be categorised into two broad types: structural and stratigraphic. The formation of structural hydrates involves migration of CH₄ along

Table 3.7 CH₄ emissions from marine waters

	Area (10 ⁶ km ²)	CH ₄ emission (Tg C year ⁻¹)	Reference
Open ocean	334	0.3	Bates et al. (1996b)
Coastal upwellings	2.3	0.02–0.15	Naqvi et al. (2005), Kock et al. (2008)
Continental shelves	24.7	0.38–7.3	EPA (2010)
Estuaries	1.0	0.08–2.3	Upstill-Goddard (2011)
Mangroves	0.2	1.7	Barnes et al. (2006)
Continental margin seeps	?	7.5–36	Hornafius et al. (1999) Kvenvolden and Rogers (2005)
Total	362.2	10–48	

Table 3.8 CH₄ saturations in European shelf surface waters (excluding estuaries). *SD* standard deviation (Modified from Bange (2006b))

Region	Date	CH ₄ saturation (%) (range or SD)	Reference
Barents Sea	Aug 1991	120 (115–125)	Lammers et al. (1995)
Baltic Sea	1992 ^a	254 (113–395)	Bange et al. (1994)
Southern N. Sea	Nov 1980	140	Conrad and Seiler (1988)
	Aug 1993	338 (118–701)	Upstill-Goddard et al. (2000)
German Bight	Sep 1991	126 ± 8	Bange et al. (1994)
Southern Bight	Mar 1989	113 (95–130)	Scranton and McShane (1991)
Central N. Sea	May 1994	215 (120–332)	Rehder et al. (1998)
UK East coast	1995–1999	129 (112–136)	Upstill-Goddard et al. (2000)
Bay of Biscay	Nov 1980	100	Conrad and Seiler (1988)
Adriatic Sea	Aug 1996	425 (420–450) ^a	Leip (1999)
E. Ionian Sea	Jul 1993	148 ± 22	Bange et al. (1996)
N. Aegean Sea	Jul 1993	231 ± 32	Bange et al. (1996)
NW Black Sea	Jul 1995	567	Amouroux et al. (2002)
Average		222 ± 142	

^aIncludes seasonal/interannual sampling

geological faults from deep sources and subsequent crystallisation on seawater contact (O'Connor et al. 2010). This can lead to accumulation of high CH₄ concentrations in domes or underneath impermeable sediments (Archer 2007). Structural CH₄ hydrates occur at relatively shallow depths and are typically “massive”, i.e. they displace sediment to generate large hydrate chunks potentially filling tens of percent of the sediment volume (Tréhua et al. 2004). However, the majority of hydrate deposits are stratigraphic. These deposits are typically dilute, accounting for only a few percent of the sediment volume and are generally located some hundreds of metres below the sea floor. Gornitz and Fung (1994) further drew a distinction between marine hydrate synthesis in “passive” and “active” margins. Local sediment accumulation constrains hydrate formation in passive margins, whereas scavenging of organics deriving from adjacent areas leads to higher hydrate abundance

in active margins. Hydrate formation is also sensitive to the O₂ concentration in the overlying water: a 40 μM decrease in the deep water O₂ concentration may enhance the CH₄ inventory twofold (Buffett and Archer 2004).

Knowledge of the true extent of marine CH₄ hydrate remains incomplete. Direct observations from well logs (e.g. Sloan and Koh 2008) are limited in number. Interpretations based on sea floor organic carbon derived from sea surface chlorophyll *a* can be unsuccessful (Gornitz and Fung 1994) and indirect hydrate detection via seismic profiling may prove similarly inconclusive (Sloan 2003). The perceived CH₄ hydrate inventory has been downscaled by 3–4 orders of magnitude since the 1970s due to improvements in hydrate understanding and detection. An early, widely adopted global estimate of ~10⁴ Pg C in CH₄ hydrate, including a small contribution from terrestrial permafrost (Kvenvolden 1999), was more than twice the known

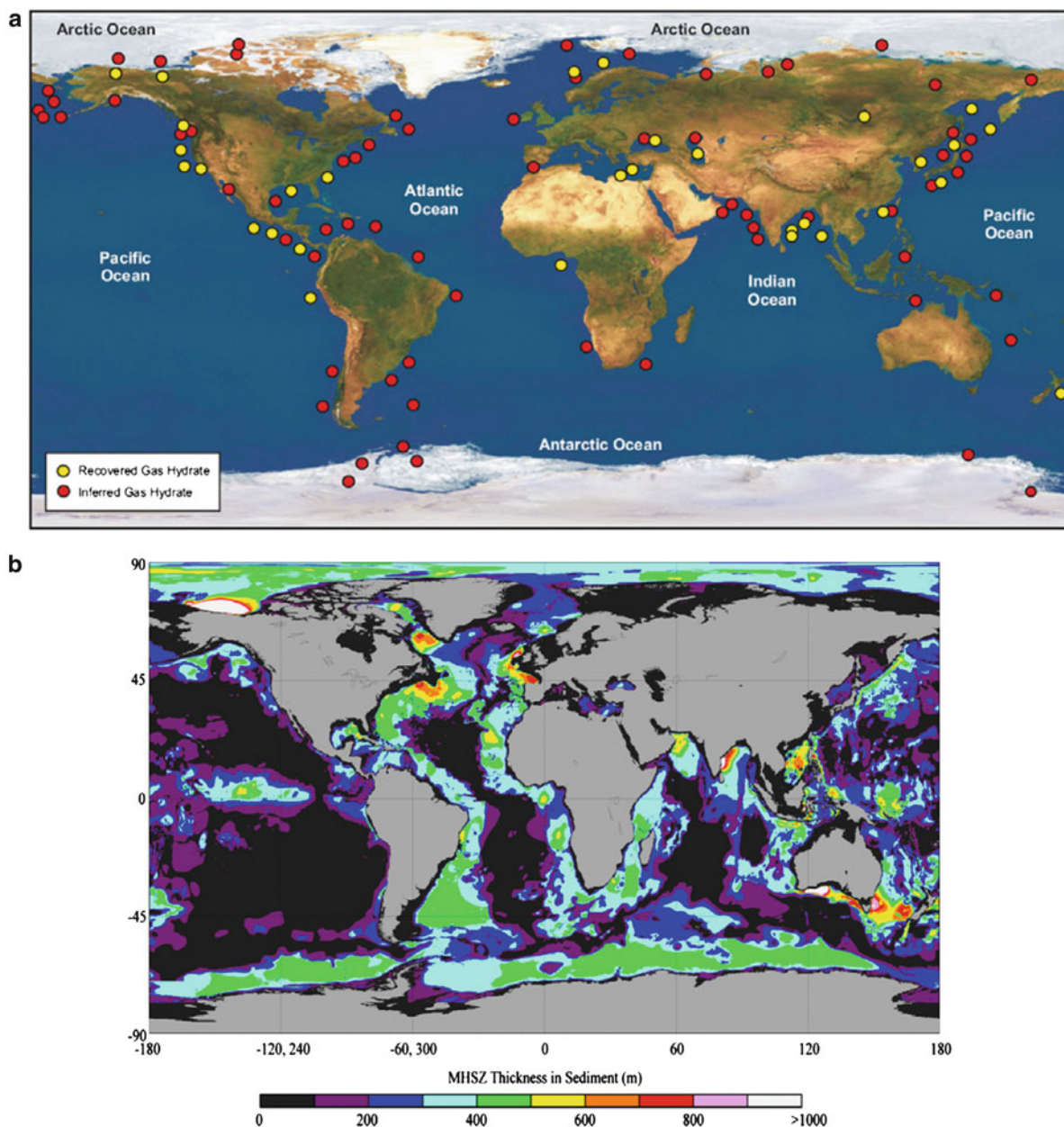


Fig. 3.16 (a) Distribution of known and inferred methane hydrate accumulations; (b) estimated thickness of the gas hydrate stability zone (GHSZ) in seafloor sediments (Reproduced from Krey et al. (2009) by permission of IOP publishing Ltd.)

fossil fuel carbon inventory. The most recent data synthesis gives a much lower estimate (170–1,000 Pg C) for marine CH₄ hydrate and a similar amount in associated free CH₄ bubbles (Archer 2007; Archer et al. 2009). O'Connor et al. (2010) set an order of magnitude uncertainty on these figures.

In excess of 250 CH₄ bubble plumes were recently observed over the GHSZ west of Spitsbergen, an area showing ~1 °C warming of bottom waters during the last 30 years (Westbrook et al. 2009). These bubble plumes were interpreted as upward migrating free gas formerly trapped below the GHSZ, implying a strong link between current warming and hydrate dissociation,

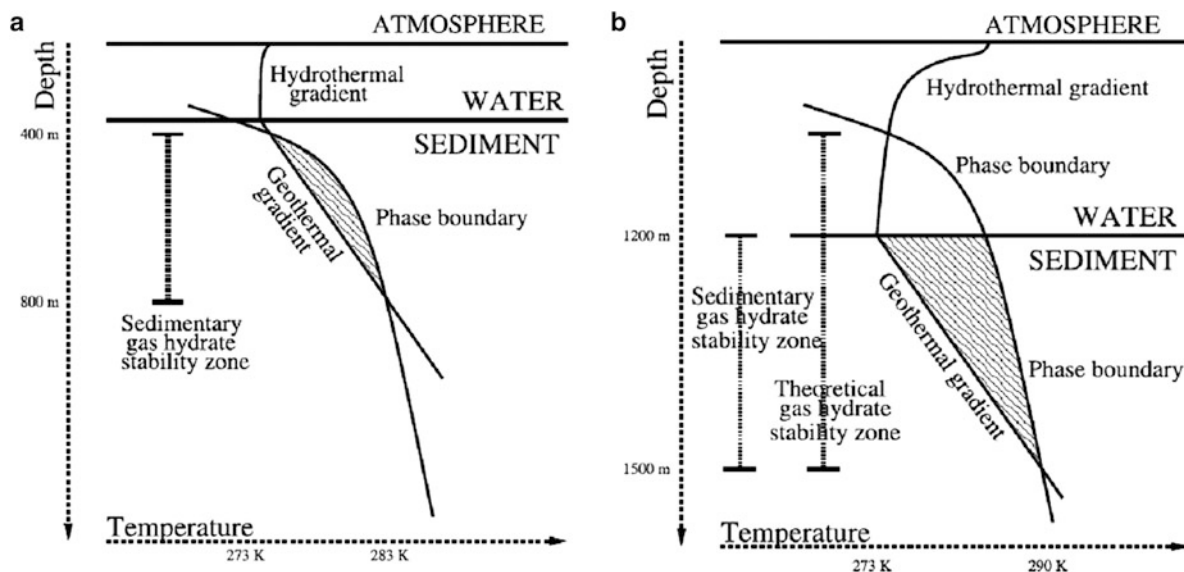


Fig. 3.17 The gas hydrate stability zone (GHSZ) associated with (a) shallow water and (b) deep water marine sediments. GHSZ volume is determined by the local geothermal gradient.

Globally this is $\sim 25\text{--}30 \text{ K km}^{-1}$, but it can show significant regional variability. (Adapted from O'Connor et al. (2010) by permission of the American Geophysical Union)

a conclusion later supported by modelling (Reagan and Moridis 2009). Lamarque (2008) calculated a potential CH₄ release at the sea floor of $420\text{--}1,605 \text{ Tg C year}^{-1}$ following hydrate destabilisation from a doubling of tropospheric CO₂. Adjusting for 1 % CH₄ leakage as observed at a large field site (Mau et al. 2007), this value was reduced to $4\text{--}16 \text{ Tg C year}^{-1}$. However these estimates do not take account of subsequent CH₄ oxidation in the water column, which can easily account for 90 % of the CH₄ released from the sea floor (Dale et al. 2006). Consequently, estimating the current tropospheric CH₄ flux from hydrate sources involves large uncertainty (Table 3.3).

3.4.5 Marine Emissions of Methane

Marine CH₄ emissions reflect the balance of rates of formation, removal and transport. Table 3.7 emphasises the dominance of coastal over open ocean waters in the marine CH₄ budget, reinforcing the conclusions of an early synthesis in which more than 75 % of marine CH₄ emissions were ascribed to coastal waters (Bange et al. 1994). The total CH₄ emission from open ocean areas, experiencing O₂ depletion in the water column, is rather small ($0.3 \text{ Tg C year}^{-1}$) (Bates et al. 1996b). Similarly, in coastal zones where hypoxia is anthropogenically

influenced, the available information suggests that these regions are currently only minor contributors to total coastal CH₄ emissions (less than $0.026 \text{ Tg C year}^{-1}$), although this estimate does not include a contribution from ebullition (Naqvi et al. 2010).

It is noteworthy that the low end of the range of total marine CH₄ emissions in Table 3.7 is at the high end of the range given in the IPCC 4th Assessment Report, as shown in Table 3.3 (Denman et al. 2007). The discrepancy can be largely accounted for by CH₄ emissions from continental margin seeps, which are not well characterised in the IPCC synthesis, but which could be the dominant contributor to the marine source of tropospheric CH₄. Such a large seep source is compatible with the notion of a “missing” fraction of fossil CH₄ ($\sim 56 \pm 11 \text{ Tg C year}^{-1}$) deduced from tropospheric ¹⁴C data (Crutzen 1991). The uncertainty in the seep estimate is compounded by the episodic nature of the seeps and by the migration of source regions on the sea floor (Kvenvolden and Rogers 2005). There is also large uncertainty in the spectrum of bubble sizes emitted and dissolution of the gas phase into seawater (Judd and Hovland 2007). Moreover, most current estimates of seep CH₄ emissions are indirect and involve large extrapolations. Overall, CH₄ emissions in seeps have a large uncertainty.

Estimating CH₄ emissions from estuaries and mangrove sites (Table 3.7) is compounded by uncertainties over ebullition rates. The importance of this mechanism is unique to CH₄ among reactive trace gases, as it results from intense methanogenesis in sediments. Importantly, although ebullition can account for more than 90 % of CH₄ emissions at some locations (Ostrovsky 2003; Barnes et al. 2006; Nirmal Rajkumar et al. 2008), it is excluded from routine air-sea emission estimates based on gas exchange relations applied to dissolved gas gradients (Upstill-Goddard 2006). In tidal estuaries and mangrove settings some fraction of the CH₄ emission occurs directly from sediments during emersion. While some progress has been made towards estimating the global surface area of estuarine water bodies (Dürr et al. 2011), no robust estimate is currently available for the global inter-tidal area. Borges and Abril (2011) made a crude estimate of estuarine inter-tidal areas and derived a global estuarine CH₄ emission ~5 Tg C year⁻¹, notably higher than the estimate of 0.1–2.3 Tg C year⁻¹ given in Upstill-Goddard (2011). Constraining marine CH₄ emissions more accurately clearly requires additional detailed studies.

3.5 Impact of Global Change

3.5.1 Future Changes in the Physics of the Oceanic Surface Layer

In order to assess the influence of global climate change on the air-sea exchange of long-lived greenhouse gases (Table 3.2), we need to separately discuss CO₂ from N₂O and CH₄, since the latter two gases have a fundamentally different global balance between the ocean and troposphere. In the case of CO₂, the ocean ultimately controls the tropospheric content of CO₂, with the CO₂ concentration in the surface layer being the immediate determinant of this ocean–atmosphere balance. This surface ocean concentration is controlled by physical, chemical, and biological processes that also create very important sources and sinks within the surface layer, causing the response of CO₂ to climate change to be complex. For N₂O and CH₄, the ocean acts as a net source of these gases to the troposphere, but their ultimate concentrations in the troposphere are on average controlled by other factors, such as their tropospheric lifetimes and terrestrial sources. Furthermore,

excluding coastal regions, N₂O and CH₄ in marine waters are mostly produced away from the surface in the ocean's interior, so that the surface layer primarily acts as a conduit between the net ocean source and the net tropospheric sink.

3.5.1.1 Carbon Dioxide in the Open Ocean

For CO₂, it is furthermore of considerable help to distinguish clearly between the climate change processes acting upon the oceanic uptake of anthropogenic CO₂, and those that influence the cycling of natural carbon (Fig. 3.18). For the former, it is essentially sufficient to consider only CO₂ induced changes in the oceanic buffer capacity and in what way ocean circulation will change the net downward transport of anthropogenic CO₂. Changes in wind regimes are essentially irrelevant because air-sea exchange is not a rate limiting step for the oceanic uptake of anthropogenic CO₂ (Sarmiento et al. 1992). Changes in sea ice will locally impact the uptake of anthropogenic CO₂ significantly, but have a relatively small effect globally. Changes in temperature also have a negligible direct effect on the uptake of anthropogenic CO₂, since the buffer factor is essentially independent of temperature (Sarmiento and Gruber 2002).

Regarding the cycling of natural CO₂, changes in temperature are very important, as they directly impact CO₂ solubility in surface water. Changes in the ocean's biogeochemical loop are of fundamental importance. This loop (Sect. 3.2.2) consists of the downward (biological) component, often referred to as the biological pump, and an upward component driven by transport and mixing, which brings carbon-rich waters from the sub-surface ocean back to the surface (Gruber and Sarmiento 2002).

One of the most consistently predicted impacts of climate change on the ocean is an increase in upper ocean stratification (e.g. Bopp et al. 2002). This will largely result from continued oceanic uptake of excess heat from the troposphere that will warm the upper ocean more than the deep ocean (at least during a transient period of several hundred years). In addition, many high-latitude regions are predicted to become fresher in response to an acceleration of the hydrological cycle (Curry et al. 2003), increasing stratification there as well. In the lower latitudes, the enhanced evaporation will actually increase salinity, but this effect is much smaller than that of the higher temperature, so that the surface ocean is predicted to become

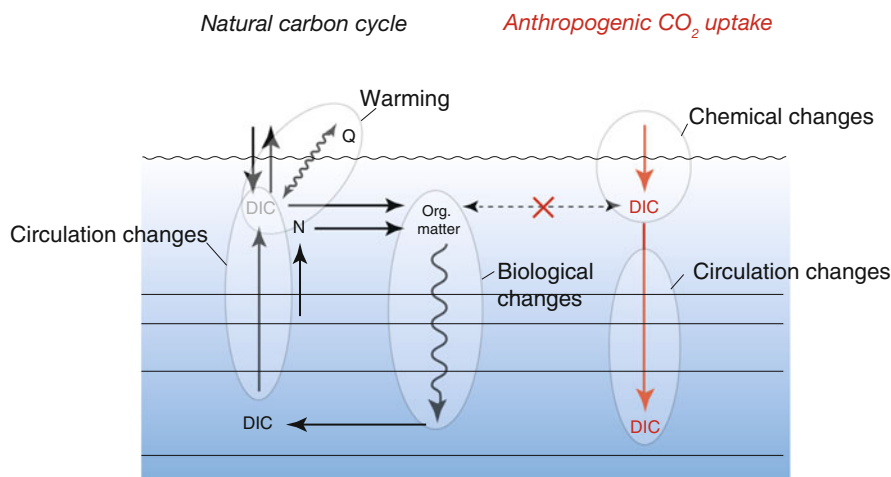


Fig. 3.18 Overview of the most important processes that affect the natural carbon cycle (left, black) and anthropogenic CO₂ uptake (right, red) in a changing world. At the center of the natural carbon cycle is the net formation of organic carbon by photosynthesis. Part of this organic matter is exported to depth, where it remineralises back to dissolved inorganic carbon (DIC). Circulation and mixing close this loop. Gas exchange through the air-sea interface connects this loop to the atmosphere. The magnitude of this exchange is governed by the balance of upward transport of DIC and downward transport of organic matter, as well as warming and cooling at the sea surface. The increase in atmospheric CO₂ has caused an

additional flux across the air-sea interface, i.e. that of anthropogenic CO₂, leading to an anthropogenic increase in DIC (red). This DIC is then further transported to depth by mixing and transport. To first order, the anthropogenic CO₂ is not interacting with the natural carbon cycle, namely it does not affect the magnitude and pattern of the organic matter production and export (red cross). When looking closer, this is not entirely correct, as there is increasing evidence that the chemical changes associated with the uptake of anthropogenic CO₂ affect ocean biology. The grey ellipses indicate the processes that are most vulnerable to climate change, leading to a change in the net ocean-atmosphere balance of CO₂

more stably stratified nearly everywhere. Important exceptions might be coastal upwelling regions, and perhaps the Southern Ocean, where increased winds may cause enhanced upwelling, partially compensating for the increased stratification.

An increase in stratification and consequently in the surface-to-depth transport will have a strongly reducing impact on the uptake of anthropogenic CO₂. In contrast, increased stratification will produce a much more complex response of the ocean's natural carbon cycle. On the one hand, the circulation (upward) component of the biogeochemical loop will be reduced, but the net effect of this will depend on how ocean biology responds. If the net export of organic matter remains unchanged, the reduction in the upward transport will lead to a substantial increase in the rate of CO₂ uptake from the troposphere. This is because the soft-tissue part of the biological pump will continue to reduce surface CO₂ by fixing it into organic matter and exporting it to depth, while the re-supply by mixing from depth will be greatly reduced. Instead, the lost CO₂ will be replaced by uptake from the troposphere,

constituting a negative feedback with regard to tropospheric CO₂. If the net export of organic matter increases, so will the uptake of CO₂ from the troposphere, but if it decreases then the net uptake of CO₂ from the troposphere will also decrease. The overall effect of expected changes in the biogeochemical loop on tropospheric CO₂ can be summarised by the efficiency of the soft-tissue pump, which describes the relative balance between the amount of (inorganic) carbon that is brought to the near-surface by mixing/transport and the amount of (organic) carbon that is exported to depth. It is currently expected that globally the efficiency of the soft-tissue pump will increase, such that the overall effect of the biogeochemical loop will be to enhance CO₂ uptake from the troposphere (Fig. 3.19). However, this conclusion critically depends on the biological response, which at present remains poorly understood.

At the same time, warming of the surface ocean will lead to a loss of CO₂ from the surface, constituting a clear positive feedback. The magnitude of this solubility-driven response is relatively well

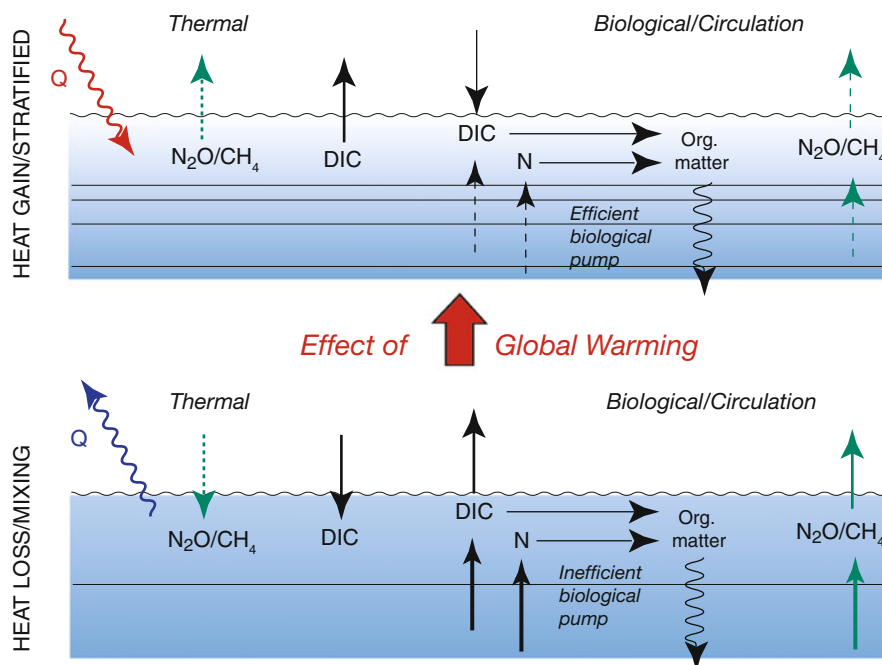


Fig. 3.19 Schematic diagram highlighting two typical situations and how they influence the exchange of natural CO_2 , N_2O , and CH_4 across the air-sea interface. The *upper panel* shows a typical low-latitude situation characterised by a net heat gain from the

atmosphere and stably stratified conditions. The *lower panel* represents a typical high latitude situation with a net loss of heat and weakly stratified conditions. Global warming will tend to make more regions of the global ocean behave like the *upper panel*

understood, and will largely depend on the magnitude of the ocean's future heat uptake. Changes in wind and sea ice extent will influence the net exchange of CO_2 across the air-sea interface as well. However this will be of secondary importance compared to the direct temperature and circulation effects, except in specific local regions where large changes in sea ice and/or winds might occur.

Based on an annual sea ice loss of $36,000 \text{ km}^2$ (mostly summer ice; Cavalieri et al. 2003), the air-sea CO_2 influx would increase by $2.0 \pm 0.3 \text{ Tg C year}^{-1}$ for the Arctic Ocean (Bates et al. 2006). Bates et al. (2006) estimated that the Arctic Ocean sink for CO_2 increased from 24 to 66 Tg year^{-1} over the past three decades due to sea ice retreat and that future sea ice melting will enhance this CO_2 uptake by 20 Tg year^{-1} by 2012. Therefore, if one considers only the physical processes through which sea ice directly impacts air-sea CO_2 exchange, the decrease of summertime sea ice extent is expected to increase CO_2 uptake in the coming decades.

Summing up, the expected changes in surface temperature and upper ocean stratification will lead to a

strong reduction of the uptake of anthropogenic CO_2 , and a mixed response on the natural carbon side with a loss of carbon driven by solubility, and perhaps a gain from the biogeochemical loop (Table 3.9). The net balance is likely to be a decrease in the net uptake of CO_2 from the troposphere in response to climate change, with current models suggesting a reduction in the net ocean uptake of about -16 to $-33 \text{ Pg } ^\circ\text{C}^{-1}$ warming until 2100 (Table 3.2) (Roy et al. 2011).

3.5.1.2 Carbon Dioxide in Coastal Seas

The potential feedbacks on increasing tropospheric CO_2 from changes in carbon flows in the coastal ocean could be disproportionately higher than in the open ocean. According to Borges (2011), the changes in carbon flows and related potential feedbacks in the coastal ocean could be driven by four main processes (Table 3.10): (i) changes in coastal physics (This section); (ii) changes in seawater carbonate chemistry (ocean acidification) (Sect. 3.5.2); (iii) changes in land use, waste water inputs and the use of agricultural fertilisers; (iv) changes in the hydrological cycle. These potential feedbacks remain largely unquantified

Table 3.9 Environmental influences on the future net ocean uptake of tropospheric CO₂. *BGC* biogeochemical

	Net ocean uptake	Magnitude	Understanding
<i>Anthropogenic CO₂</i>			
Chemical changes (buffer capacity)	Reduced	Large	High
Circulation/stratification changes	Reduced	Medium	Medium
Wind/sea ice changes	Increased/reduced	Small	Low
<i>Natural CO₂</i>			
Temperature changes	Reduced	Medium	Medium
Circulation changes affecting the BGC loop	Reduced	Medium	Low-medium
Biological changes affecting the BGC loop	Increased/reduced	Unknown	Very low
Wind/sea ice changes	Increased/reduced	Low	Low

due to a poor understanding of the underlying mechanisms, and/or a lack of data and models with which to evaluate them.

Feedbacks on increasing tropospheric CO₂ due to effects of carbon cycling in continental shelf seas related to changes in circulation or stratification could be important, but remain to be quantified (Table 3.10). The effect of changes of stratification on air-sea CO₂ fluxes are not straightforward to quantify since enhancement of stratification will depress primary production and export production due to the decrease of nutrient inputs, but at the same time will also decrease the vertical inputs of DIC and hence release of CO₂ to the troposphere. For example, on the Tasman shelf and in the adjacent open ocean the overall effect of enhanced stratification seems to be an enhancement of the CO₂ sink (Borges et al. 2008).

3.5.1.3 Nitrous Oxide and Methane

For N₂O and CH₄ the upper ocean acts mostly as a transport conduit from the ocean to the troposphere, where they are ultimately decomposed by chemical reactions. Changes in solubility are likely to exert a major effect on the exchange of these two gases in the open ocean, since their degree of supersaturation in the surface ocean is mostly determined by temperature and only to a smaller degree by the magnitude of the transport of supersaturated waters from below to the surface. Therefore, the increase in stratification induced by surface warming (and also by changes in salinity) is likely to lead to only a modest reduction in the ocean source strength of these two gases, provided that their rates of production remain about the same.

Of course, if ocean warming and enhanced stratification lead to a strong loss of O₂, then N₂O and CH₄ production in the ocean might increase substantially, which could more than offset the reduction in the deep-to-surface transport induced by stratification (Table 3.2).

3.5.2 Ocean Acidification

3.5.2.1 Carbon Dioxide

Models predict that by the end of the twenty-first century the pH of seawater will decrease by another 0.3–0.4 units (Caldeira and Wickett 2003). This decrease will be accompanied by a reduction in the CO₃²⁻ concentration and in the saturation state for calcite and aragonite (Sect. 3.2.2). Surface waters in the Southern Ocean and the Subarctic Pacific Ocean are expected to become undersaturated with respect to aragonite by the year 2100 (Orr et al. 2005).

Ocean acidification will affect organic carbon production and calcification, but exactly how it will do this is uncertain and is a topic of ongoing research in ocean acidification programmes around the world. For example, ocean acidification may impact the shells of pelagic calcifiers by reducing the ability of organisms to calcify (Comeau et al. 2011) and by dissolving calcareous shells (Orr et al. 2005). However, a few studies have found an increase in calcification on ocean acidification (e.g. Iglesias-Rodriguez et al. 2008). In particular, coral reefs are highly susceptible to increases in temperature and CO₂ concentration (Kleypas et al. 1999). Coral reefs globally may have ceased to grow and started to dissolve by the time the atmospheric mole fraction of

Table 3.10 Global change forcing of carbon cycling in the coastal ocean and associated feedback from increasing tropospheric CO₂ to the year 2100 (Adapted from Borges 2011)

Global change forcings	Feedback	Changes in CO ₂ sources and sinks (Pg C year ⁻¹)	Comment
Changes in coastal physics			
Enhanced stratification	– ?	?	1
Enhanced coastal upwelling	+ ?	?	2
Impact of expanding OMZ in coastal upwelling regions	+	?	3
Enhancement of air-sea CO ₂ fluxes related to Arctic sea-ice retreat	–	0.002	4
Changes in land use, waste water inputs, agricultural fertilisers and changes in the hydrological cycle			
Increase of river organic carbon delivery to the Arctic Ocean	+	?	
Increase of river nutrients delivery to the Arctic Ocean	–	?	
Global increase in river nutrient and organic matter delivery	–	0.200	5
Global increase in nutrient atmospheric deposition	–	?	6
Expanding hypoxic and anoxic zones	+	?	3
Changes in seawater carbonate chemistry (ocean acidification)			
Decrease of benthic calcification			
Coral reefs	–	0.015–0.026	
Other benthic environments	–	0.025–0.046	
Decrease of pelagic calcification			
Coccolithophorids	–	0.013–0.019	
Other pelagic calcifiers	–	?	
Dissolution of metastable CaCO ₃ in sediment porewaters	–	0.022	7
Enhancement of primary production and export production due to increasing [CO ₂]	–	0.108–0.216	8

1 Negative feedback only reported in Tasman shelf (Borges et al. 2008) assuming pCO₂ behaviour during warm years is representative of response to global warming, if extrapolated globally would produce a negative feed-back of the order of ~0.1 PgC year⁻¹.

2 Assuming exact opposite response of model output (Plattner et al. 2004) with decreasing upwelling favourable winds

3 Assuming enhanced denitrification leading to decreased primary production

4 Feedback computed for the next decade and not until 2100 (Bates et al. 2006)

5 The enhancement of primary production by nutrient inputs balances the additional CO₂ production by organic matter inputs (Mackenzie et al. 2004).

6 Not taking into account enhancement of acidification of surface waters by sulphur atmospheric deposition (Doney et al. 2007)

7 Based on Andersson et al. (2003)

8 Based on a single mesocosm experiment with mixed diatom and coccolithophorid assemblage (Riebesell et al. 2007)

CO₂ reaches 560 ppm (Silverman et al. 2009). Ocean acidification may well increase primary production by some phytoplankton species (Rost and Riebesell 2004) and may change ratios of carbon to nitrogen uptake by phytoplankton and subsequent carbon export (Riebesell et al. 2007).

Ocean acidification will also impact marine biogeochemical processes. These include changes in the availability of essential trace metals like iron, which are modified in speciation by pH change (Santana-Casiano et al. 2006). A decrease in pH may affect the solubility of some minerals (Liu and Millero 2002) and also the distribution of chemical species,

favouring the free dissolved forms of metals, and exerting significant physiological, ecological and toxicological effects on organisms.

On timescales of a few 100 years, a change in the hard tissue CaCO₃ pump is estimated to have a small impact on global CO₂ uptake by the oceans (Table 3.2) (Denman et al. 2007), although the effect could be very substantial on glacial to interglacial timescales (e.g. Archer et al. 2000; Matsumoto et al. 2002). The effects of ocean acidification have been estimated for coastal waters (Table 3.10). Overall, ocean acidification is likely to decrease pelagic and benthic calcification in coastal waters and to result in the dissolution of CaCO₃

in coastal sediments. These combined effects have been estimated to increase the uptake of tropospheric CO₂ by ~0.02 Pg C year⁻¹, an amount equivalent to ~10 % of the modern-day CO₂ sink in coastal seas (Tables 3.2 and 3.10). The increase in export production upon ocean acidification could also provide a significant negative feedback to increasing tropospheric CO₂, although the conclusions are based on a single perturbation experiment (Table 3.10) (Riebesell et al. 2007).

Denman et al. (2007) concluded that the combined effects of climate change and ocean acidification on the biological carbon pump are not clear and could either increase or decrease the uptake of tropospheric CO₂. What is more clear is that ocean acidification will likely result in the dissolution of CaCO₃ sediments in the interior ocean on a time scale of 40 kyear, thus creating a negative feedback on the increase in tropospheric CO₂.

3.5.2.2 Nitrous Oxide and Methane

One other important consequence of ocean acidification is a shift of the NH₃/NH₄⁺ equilibrium towards NH₄⁺ (e.g. Bange 2008). Beman et al. (2011) recently showed that nitrification rates decreased significantly when the pH was lowered to values expected to occur in the future ocean. One explanation for the pH sensitivity of nitrification rates is that the ammonia mono-oxygenase enzyme uses NH₃ and not NH₄⁺ as substrate in the first step of the nitrification sequence. On the basis of these results Beman et al. (2011) suggested that future oceanic N₂O production via nitrification might decrease by up to 44 %, although Freing et al. (2012) contend that this scenario could be an over simplification. Nitrification is part of organic matter remineralisation (i.e. oxidation of organic matter with O₂ to CO₂) and it leads to decreases in both pH and O₂ (Sect. 3.3.2). In general decreasing O₂ concentrations lead to increasing N₂O production during nitrification, such that there seems to be only a minor effect of decreasing pH on N₂O production via nitrification as part of the organic matter remineralisation process. Laboratory experiments to verify the effect of ocean acidification on N₂O production in the ocean are yet to be carried out (Table 3.2). Similarly, the potential effect of ocean acidification on oceanic CH₄ production remains to be investigated (Table 3.2).

3.5.3 Deoxygenation and Suboxia in the Open Ocean

One of the most important effects of global change on the oceans will be the deoxygenation of seawater arising from surface water warming and increased stratification of the upper ocean. These processes will lead to a decrease in O₂ solubility and its supply to subsurface waters, respectively (Keeling et al. 2010). There is compelling evidence to show that this may already be happening (Joos et al. 2003; Stramma et al. 2008; Keeling et al. 2010; Helm et al. 2011). The model-predicted decrease in the oceanic O₂ inventory ranges from 1 % to 7 % by the year 2100 (Keeling et al. 2010). The effects of such a decrease are expected to be greatest in the oceanic OMZs. For example, while a 1 °C warming of the upper ocean, which would lower the O₂ solubility by ~5 μM, may lead to an increase in the volume of hypoxic waters by 10 %, the volume of suboxic waters may increase by a factor of 3 (Deutsch et al. 2011). The ongoing expansion and intensification of the OMZs (Stramma et al. 2008) is expected to profoundly impact the biogeochemical cycling of redox-sensitive elements, especially nitrogen, and will, in conjunction with ocean acidification, adversely affect marine life (Brewer and Peltzer 2009). This may also involve modification of the oceanic source terms for climatically important gases that are sensitive to O₂ concentrations, such as N₂O and CH₄ (Sects. 3.3.2 and 3.4.2).

N₂O formation by nitrification is enhanced when O₂ concentrations are lowered (Sect. 3.3.2). Stramma et al. (2008) showed that intermediate ocean waters (300–700 m water depth) have been losing O₂ at rates ranging from 0.09 ± 0.21 μmol kg⁻¹ year⁻¹ in the eastern equatorial Indian Ocean to 0.34 ± 0.13 μmol kg⁻¹ year⁻¹ in the eastern tropical Atlantic Ocean during the last 50 years. Assuming a mean Δ[N₂O]/AOU (apparent oxygen utilisation) ratio of 10⁻⁴ (Walter et al. 2006), Bange et al. (2010) computed a maximum additional N₂O contribution from deoxygenation of 6 % above the mean N₂O background concentration in the intermediate waters of the tropical North Atlantic Ocean. It therefore seems reasonable to conclude that ongoing open ocean deoxygenation will have a minor effect on oceanic N₂O production and emissions (Table 3.2).

The total CH₄ emission from open ocean areas experiencing O₂ depletion in the water column is quite small (0.3 Tg C year⁻¹) (Table 3.7) (Bates et al. 1996b) and is unlikely to increase significantly due to the future expansion of open ocean OMZs (Table 3.2) (Naqvi et al. 2010).

3.5.4 Coastal Eutrophication and Hypoxia

Human activities related to the production of food and energy are causing the release of large quantities of nutrients, such as nitrogen and phosphorus, to the environment, a substantial fraction of which gets transported to coastal waters (Seitzinger et al. 2002; Smith et al. 2003). By 2100 changes in biological activity due to the increased nutrient delivery in rivers might cause a negative feedback on increasing tropospheric CO₂ similar in magnitude to the present-day CO₂ sink in coastal seas (0.2 Pg C year⁻¹) (Tables 3.2 and 3.10).

Stimulation of primary productivity and the degradation of photosynthesised organic matter due to nutrient over-enrichment (eutrophication) often results in dissolved O₂ depletion in the bottom waters of seasonally stratified shelf waters. Thus, over 400 hypoxic zones have developed in coastal areas all over the world in the last few decades (Diaz and Rosenberg 2008). Due to their severely detrimental ecological effects, such as the exclusion of higher animals, these hypoxic zones are often popularly referred to as “dead zones”. Although these “dead zones” differ from the naturally-formed O₂-deficient zones that occur on the continental shelves in eastern-boundary upwelling regions, there is now evidence that the latter are also intensifying as a result of anthropogenic nutrient loading and/or changes in circulation (Naqvi et al. 2000; Chan et al. 2008).

The expansion and intensification of O₂ deficiency in coastal areas is expected to affect the future cycling of N₂O and CH₄ in these regions. Currently, anthropogenic “dead zones” make a relatively insignificant (less than 0.043 Tg N year⁻¹) contribution to the total marine source of tropospheric N₂O (Naqvi et al. 2010). Nevertheless, it is likely that the comparatively large N₂O emissions from natural hypoxic zones

include an anthropogenically-enhanced component. Taken together with the sensitivity of N₂O cycling in aquatic systems to minor changes in already low O₂ concentrations, this implies that further expansion and intensification of coastal hypoxia may significantly impact the global tropospheric N₂O budget (Table 3.2).

From the limited information available on CH₄ emissions from “dead zones”, it would appear that these regions do not contribute much (less than 0.026 Tg C year⁻¹) to the total marine source of tropospheric CH₄ (Naqvi et al. 2010), although it should be noted that this estimate does not include bubble ebullition. Given the lack of evidence for a primary control of bottom water hypoxia on sedimentary CH₄ production it would appear that future intensification and/or expansion of coastal hypoxia is unlikely to significantly increase total marine emissions of CH₄ to the troposphere (Table 3.2).

3.5.5 Changes in Methane Hydrates

There is substantial debate over the role of CH₄ hydrates in potential future climate change (O'Connor et al. 2010). What is clear is that the currently estimated CH₄ hydrate inventory (Sect. 3.4.4) is sufficiently large that the release of even a modest fraction to the troposphere over a 12-year period, the tropospheric lifetime of CH₄ (Table 3.1), could enhance greenhouse forcing by an amount equivalent to increasing the tropospheric CO₂ concentration by a factor larger than 10 (Archer 2007). The global CH₄ hydrate reservoir thus has the potential to promote substantial global warming (Table 3.2).

One region in which the effects of CH₄ hydrate destabilisation are likely to be most clearly manifested is the Arctic Ocean; a marine ecosystem that is highly susceptible to global change (Doney et al. 2012). Romanovski et al. (2005) modelled the extent and temporal evolution of submarine permafrost on the shelves of the Laptev Sea and East Siberian Sea and deduced that the entire Arctic shelf is underlain by relic permafrost stable enough to support CH₄ hydrate. Much of this Arctic CH₄ hydrate is comparatively shallow structural hydrate (Sect. 3.4.4) and the gas hydrate stability zone is ~200 m below the sea surface over much of the

region. If dislodged from the sediment, for example during a submarine landslide (Brewer et al. 2002; Paull et al. 2003) or by erosion, large amounts of hydrate could potentially survive largely intact during ascent to the ocean surface. Contemporary hydrate melting is indeed apparent along the Siberian margin, due to rapid coastline recession that is exposing sub-sea floor deposits to overlying seawater at rates of $\sim 10\text{--}15\text{ km year}^{-1}$. The hydrate melting collapses further land into the sea, increasing the exposure of hydrates and leading to further melting, a process which is thought to have occurred continually over the past 7,500 years, resulting in $\sim 100\text{--}500\text{ km}$ recession of the coastline (Hubberten and Romanovski 2001). As such these CH₄ releases are not abrupt, but rather tend to modestly increase the CH₄ background over time. For example, contemporary dissolved CH₄ saturations on the East-Siberian and Laptev Sea shelves are $\sim 2,500\%$ in surface waters and in excess of $4,000\%$ in bottom waters, consistent with such seabed release (Shakhova and Semiletov 2007; Shakhova et al. 2007). Similarly, surface waters over the North Slope of Alaska are highly supersaturated in CH₄ (Kvenvolden 1999) and the release of hydrate-derived CH₄ has been clearly observed in the Beaufort Sea (Paull et al. 2008).

Notwithstanding such evidence for the ongoing release of hydrate-derived CH₄, Archer and Buffett (2005) and Archer (2007) argue that any significant climate induced hydrate melting response is likely to be on the time scale of millennia or longer, because the vast majority of CH₄ hydrate is of the stratigraphic type (Sect. 3.4.4) and is sufficiently insulated from the sediment surface by many hundreds of metres of overlying sediment. They also argue that any hydrate melting will occur below the gas hydrate stability zone, forming CH₄ bubbles whose fate is uncertain. Possibilities include their retention in the sediment, upward escape through the stability zone, or the initiation of submarine landslides through sediment column destabilisation. Although such a landslide would potentially cause abrupt CH₄ release, it is estimated that a landslide the size of the Storegga slide off Norway would typically release CH₄ sufficient only to affect climate on a scale comparable to a large volcanic eruption for ~ 10 years (Archer 2007).

Estimates of the rate at which melting hydrates are likely to increase the tropospheric CH₄ inventory over the timescale of decades (Table 3.2) are much less well constrained than changes in other CH₄ sources

such as peat decomposition in thawing permafrost, fossil fuels and agriculture, although the potential rates may be comparable (Archer 2007). Major uncertainties exist over the rate and extent of CH₄ escape to the overlying water and troposphere, which is related to sediment stability and permeability and the ability of the gas hydrate stability zone to trap CH₄ bubbles (Archer 2007). On geologic timescales, due to the relative tropospheric lifetimes of CH₄ and CO₂ (Table 3.1), the largest climate impact will likely be from CO₂ deriving from CH₄ oxidation (Schmidt and Shindell 2003; Archer and Buffett 2005; Archer 2007). Following the cessation of hydrate CH₄ release, the enhanced CO₂ concentration will persist, while tropospheric CH₄ will recover relatively rapidly to a lower steady state (Schmidt and Shindell 2003). Significant oxidation of hydrate-derived CH₄ to CO₂ in the oceans would reduce the climate impact over several decades, but on timescales of millennia or more the climate impact might be significant, because of equilibration of this oceanic CO₂ with the troposphere over several hundred years. Indeed, there may well be positive climate feedback linking tropospheric CO₂, deep ocean temperature and CO₂ production from hydrate-derived CH₄ (Archer and Buffett 2005). These authors propose that in a worst case scenario, on the timescale of millennia to hundreds of millennia, the total global CH₄ hydrate source of tropospheric CO₂ could equal that from fossil fuels.

3.6 Key Uncertainties in the Air-Sea Transfer of CO₂, N₂O and CH₄

3.6.1 Outgassing of Riverine Carbon Inputs

The error bars on carbon inputs by rivers and estuarine outgassing create considerable uncertainty when attempting to convert from net contemporary fluxes to anthropogenic fluxes (Gruber et al. 2009; Takahashi et al. 2009). If the outgassing of river borne CO₂ by the open ocean has indeed been overestimated by $\sim 0.2\text{ Pg C year}^{-1}$ as argued in Sect. 3.2.4, the anthropogenic CO₂ sink derived from CO₂ climatologies (e.g. Takahashi et al. 2009) would have been over-estimated by the same amount.

3.6.2 Heterogeneity in Coastal Systems

Obtaining meaningful air-sea gas transfer estimates for CO₂, CH₄ and N₂O in coastal systems is a substantial challenge and the ranges in Tables 3.4, 3.5 and 3.7 have large inherent uncertainties. These uncertainties reflect the heterogeneity and biogeochemical complexity of coastal systems and include: (i) gross scaling errors arising from the degree to which study sites are representative globally of each “compartment”; (ii) bias in the CO₂, N₂O and CH₄ values reflecting incomplete spatial and temporal data resolution; (iii) uncertainties in gas exchange rates arising from selected gas transfer relations and representative wind speeds (Chap. 2) (Upstill-Goddard 2006; Wanninkhof et al. 2009). Minimising gross scaling errors largely relies on the availability of accurate area determinations. General problems of defining the extent of oceanic upwellings are well documented (Nevison et al. 2004; Naqvi et al. 2005), as are the difficulties of defining representative estuarine areas (Barnes and Upstill-Goddard 2011). Minimising measurement bias has a clear seasonal aspect; production and consumption of CO₂, N₂O and CH₄ are biologically driven and as such have strong temperature dependence. Seasonality also affects the intensity of upwelling and river runoff, which affects nutrient and carbon supply. Unfortunately, most sampling campaigns take place during summer. There is also a regional aspect; most coastal regions outside the northern hemisphere are either undersampled or are not sampled at all.

Given the likelihood that coastal regions will play an important role in future trace gas budgets due to increased economic and population pressures, additional studies of CO₂, N₂O and CH₄ fluxes from key coastal regions will be required. Sampling campaigns should be spatially and temporally focused and ideally coordinated internationally. In particular CH₄ emissions by ebullition and from seeps and inland waters need more to be more accurately quantified.

3.6.3 Sea Ice

The role of sea ice in air-sea gas exchange remains poorly understood (Chap. 2). Until recently sea ice was regarded as a lid that effectively precluded air-sea gas exchange, as evidenced by under ice concentrations of dissolved gases (CFCs, O₂, CO₂) far from equilibrium

with their tropospheric contents (Gordon et al. 1984; Weiss et al. 1992; Klatt et al. 2002; Bakker et al. 2008). However, recent evidence now points to significant gas exchange between sea ice and the troposphere (Delille et al. 2007; Geilfus et al. 2012), highlighting a need for more detailed research in this area.

3.6.4 Parameterising Air-Sea Gas Transfer

The choice of turbulence-driven air-sea gas exchange relations may introduce significant bias (Chap. 2), especially where bottom-driven turbulence is a major contributor to gas exchange in shallow systems (Upstill-Goddard 2006, 2011). In addition, wind speeds in coastal systems have short spatio-temporal variability and often the appropriate wind speed distributions required for gas exchange relations are not available. Similarly, current speeds and water depths required for non-wind speed driven gas exchange relations may also be lacking (Upstill-Goddard 2006).

3.6.5 Data Collection, Data Quality and Data Synthesis

The detailed study of interannual and decadal variations and trends in regional surface water fCO₂ and air-sea CO₂ fluxes has only recently become possible. Our future understanding of these trends and of the underlying mechanisms responsible is expected to improve due to more extensive data coverage and as longer observational records become available. Future long term data collection and data synthesis will require the development of instrumentation that is more reliable and accurate while being less labour intensive. In addition the rigorous standardisation of data collection and quality control procedures will be essential. Such technical developments will require substantial and sustained funding (Borges et al. 2010; Byrne et al. 2010; Feely et al. 2010; Gruber et al. 2010; Monteiro et al. 2010).

Encouragingly, the marine CO₂ community is already making good progress towards coordinated data collection and synthesis. Notable is the agreed use of certified reference materials for the analysis of DIC and total alkalinity and traceable calibration gases for fCO₂ analysis (DOE 1994; Dickson et al. 2007). There is also agreement on recommendations for

reporting fCO₂ measurements (IOCCP 2004). The International Ocean Carbon Coordination Project (IOCCP) plays the key role in coordinating the marine carbon community and in ensuring the implementation of international agreements. By contrast, the status of marine N₂O and CH₄ research is far less mature in this regard. The N₂O and CH₄ communities have yet to progress towards discussing the adoption of either internationally agreed analytical standards or recommended analytical protocols.

Recent synthesis products for ocean carbon enable the intercomparison of model-data, the analysis of variation and trends in CO₂ air-sea fluxes, and the processes driving these. A vast and expanding global surface water fCO₂ database is now available for assessing CO₂ air-sea climatologies (Takahashi et al. 1997, 2002, 2009) and since 2011 the Surface Ocean CO₂ Atlas (SOCAT; www.socat.info) enables public access to a large CO₂ data archive for the global oceans and coastal seas (Bakker et al. 2012; Pfeil et al. 2013; Sabine et al. 2013) (Chap. 5). Other data synthesis efforts are also underway, notably MEMENTO for surface ocean N₂O and CH₄ concentrations (Chap. 5) and syntheses of carbon in the ocean interior: GLODAP (Global Ocean Data Analysis Project), CARINA (CARbon IN the Atlantic Ocean), PACIFICA (PACIFic ocean Interior Carbon) and GLODAP-2 (Key et al. 2004; Bange et al. 2009; Tanhua et al. 2010; Suzuki et al. 2013). Such data synthesis efforts, along with modelling and data-model intercomparisons (Gruber et al. 2009) are critical to improving our current understanding of the exchanges of CO₂, N₂O and CH₄ between the troposphere, coastal seas, the surface open ocean and the ocean interior.

3.7 Conclusions and Outlook

3.7.1 Carbon Dioxide

In general, the enhanced rate of change in tropospheric CO₂ observed today (Global Carbon Project 2011) will have a strong impact on future climate and environmental change. Presently it appears that neither the oceans nor terrestrial systems will absorb CO₂ as efficiently in the future as they do today. In addition, ocean acidification will become, and probably is already, an issue for ecosystems in the ocean. Both the climate and environmental effects and feedbacks make it very difficult to firmly predict future changes in ocean sources and sinks for CO₂. From time-series we can clearly identify the

rate of change in CO₂ uptake and in ocean acidification. From surface water CO₂ measurements on Voluntary Observing Ships we can make CO₂ air-sea flux maps and assess temporal and spatial variation in the oceanic uptake of CO₂. Finally, repeat hydrography elucidates the storage of carbon in the interior ocean. More important will be to predict the effect of changes in processes controlling oceanic uptake and release of carbon, notably of changes in ocean circulation, the magnitude of the biological pumps and carbon storage. This will require a comprehensive measuring system for future observations and improved modelling tools. Today, there is a clear lack of the observations required to reduce the uncertainties in air-sea CO₂ exchange and to predict its future behaviour. This in turn is very important for predicting the occurrence of levels of ocean acidification that are harmful to ecosystems. The latter also requires results from biological perturbation experiments under varying CO₂ scenarios. The future vision is:

- The design of a comprehensive network of VOS, repeat hydrographic sections and time-series. Optimisation might be obtained through modelling, statistical analysis and experience, based upon the existing network;
 - The development of automated ocean stations. Cable-based systems might be applied along coastal areas, and moored systems and buoys in open ocean situations. Remotely controlled floats and other moving platforms, such as gliders, would provide additional process information;
 - The development of data storage, data reduction, data synthesis, data assimilation and visualisation techniques, as well as continuation, automation and expansion of ongoing data synthesis efforts;
 - The development of models that can be validated by data;
- (Borges et al. 2010; Byrne et al. 2010; Feely et al. 2010; Gruber et al. 2010; Monteiro et al. 2010).

3.7.2 Nitrous Oxide and Methane

While our knowledge of the oceanic distribution, the formation pathways and the oceanic emissions of N₂O and CH₄ has increased considerably during the last four decades, we are far from having a comprehensive picture. Major questions and technical challenges remain to be solved:

- Reliable and fast, high-precision N₂O and CH₄ sensors for use at open ocean and coastal time-series stations and on ships of opportunity should be developed in order to expand the spatial and temporal coverage of oceanic N₂O and CH₄ measurements. Recently developed OA-ICOS (Off-Axis Integrated Cavity Output Spectrometer) instruments coupled to a continuously working equilibration device are a promising technology for use on VOS lines (Gülzow et al. 2011).
- We still only have a rudimentary understanding of N₂O and CH₄ cycling in coastal areas. We need to know more about seasonality in the major formation, consumption and transport pathways and the driving forces behind these. In this context, the ongoing dramatic increase in the number of coastal “dead zones” is a critical consideration because ongoing coastal eutrophication may well modify greatly, current emissions of N₂O and CH₄ from coastal areas.

Open Access This chapter is distributed under the terms of the Creative Commons Attribution Noncommercial License, which permits any noncommercial use, distribution, and reproduction in any medium, provided the original author(s) and source are credited.

References

- Abril G, Borges AV (2004) Carbon dioxide and methane emissions from estuaries. In: Tremblay A, Varfalvy L, Roehm C, Garneau M (eds) Greenhouse gas emissions: fluxes and processes, hydroelectric reservoirs and natural environments. Springer, Berlin, pp 187–207
- Abril G, Iversen N (2002) Methane dynamics in a shallow, nontidal estuary (Randers Fjord, Denmark). *Mar Ecol Prog Ser* 230:171–181
- Abril G, Nogueira E, Hetcheber H, Cabeçadas G, Lemaire E, Brogueira MJ (2002) Behaviour of organic carbon in nine contrasting European estuaries. *Estuar Coast Shelf Sci* 54:241–262
- Abril G, Commarieu MV, Guerin F (2007) Enhanced methane oxidation in an estuarine turbidity maximum. *Limnol Oceanogr* 52:470–475
- Amouroux D, Roberts G, Rapsomanikis S, Andreae MO (2002) Biogenic gas (CH₄, N₂O, DMS) emission to the atmosphere from near-shore and shelf waters of the north-western Black Sea. *Estuar Coast Shelf Sci* 54:575–587
- Anderson LG, Falck E, Jones EP, Jutterström S, Swift J (2004) Enhanced uptake of atmospheric CO₂ during freezing of seawater: a field study in Storfjorden, Svalbard. *J Geophys Res* 109, C06004. doi:10.1029/2003JC002120
- Andersson AJ, Mackenzie FT, Ver LM (2003) Solution of shallow-water carbonates: an insignificant buffer against rising atmospheric CO₂. *Geology* 31:513–516
- Archer D (2007) Methane hydrate stability and anthropogenic climate change. *Biogeosciences* 4:521–544. doi:10.5194/bg-4-521-2007
- Archer D, Buffett B (2005) Time-dependent response of the global ocean clathrate reservoir to climatic and anthropogenic forcing. *Geochim Geophys Geosyst* 6, Q03002. doi:10.1029/2004GC000854
- Archer D, Khesghi H, Maier-Reimer E (1997) Multiple timescales for neutralization of fossil fuel CO₂. *Geophys Res Lett* 24:405–408
- Archer D, Winguth A, Lea D, Mahowald N (2000) What caused the glacial/interglacial atmospheric pCO₂ cycles? *Rev Geophys* 38(2):159–189
- Archer D, Buffett B, Brovkin V (2009) Ocean methane hydrates as a slow tipping point in the global carbon cycle. *Proc Natl Acad Sci USA* 106(49):20596–20601
- Aydin M, Verhulst KR, Saltzman ES, Battle MO, Montzka SA, Blake DR, Tang Q, Prather MJ (2011) Recent decreases in fossil-fuel emissions of ethane and methane derived from firn air. *Nature* 476:198–201. doi:10.1038/nature10352
- Baggs E, Philippot L (2010) Microbial terrestrial pathways to nitrous oxide. In: Smith K (ed) Nitrous oxide and climate change. Earthscan, London, pp 36–62
- Baker DF, Law RM, Gurney KR, Rayner P, Peylin P, Denning AS, Bousquet P, Bruhwiler L, Chen Y-H, Ciais P, Fung IY, Heimann M, John J, Maki T, Maksyutov S, Masarie K, Prather M, Pak B, Taguchi S, Zhu Z (2006) TransCom 3 inversion intercomparison: impact of the transport model errors on the interannual variability of regional CO₂ fluxes, 1988–2003. *Global Biogeochem Cycle* 20, GB1002. doi:10.1029/2004GB002439
- Bakker DCE, Hoppema M, Schröder M, Geibert W, De Baar HJW (2008) A rapid transition from ice covered CO₂-rich waters to a biologically mediated CO₂ sink in the eastern Weddell Gyre. *Biogeosciences* 5:1373–1386. doi:10.5194/bg-5-1373-2008
- Bakker DCE, Pfeil B, Olsen A, Sabine CL, Metzl N, Hankin S, Koyuk H, Kozyr A, Malczyk J, Manke A, Telszewski M (2012) Global data products help assess changes to the ocean carbon sink. *Eos Trans Am Geophys Union* 93(12):125–126. doi:10.1029/2012EO120001
- Ballantyre AP, Alden CB, Miller JB, Tans PP, White JWC (2012) Increase in observed net carbon dioxide uptake by land and oceans during the past 50 years. *Nature* 488:70–73. doi:10.1038/nature11299
- Bange HW (2006a) New directions: the importance of the oceanic nitrous oxide emissions. *Atmos Environ* 40:198–199
- Bange HW (2006b) Nitrous oxide and methane in European coastal waters. *Estuar Coast Shelf Sci* 70:361–374
- Bange HW (2008) Gaseous nitrogen compounds (NO, N₂O, N₂, NH₃) in the ocean. In: Capone DG, Bronk DA, Mulholland MR, Carpenter EJ (eds) Nitrogen in the marine environment, 2nd edn. Elsevier, Amsterdam, pp 51–94
- Bange HW, Andreae MO (1999) Nitrous oxide in the deep waters of the world’s oceans. *Global Biogeochem Cycle* 13(4):1127–1135
- Bange HW, Bartell UH, Rapsomanikis S, Andreae MO (1994) Methane in the Baltic and North Seas and a reassessment of

- the marine emissions of methane. *Global Biogeochem Cycle* 8:465–480
- Bange HW, Rapsomanikis S, Andreae MO (1996) The Aegean Sea as a source of atmospheric nitrous oxide and methane. *Mar Chem* 53:41–49
- Bange HW, Bell TG, Cornejo M, Freing A, Uher G, Upstill-Goddard RC, Zhang G (2009) MEMENTO: a proposal to develop a database of marine nitrous oxide and methane measurements. *Environ Chem* 6:195–197
- Bange HW, Bergmann K, Hansen HP, Kock A, Koppe R, Malien F, Ostrau C (2010a) Dissolved methane during hypoxic events at the Boknis Eck time series station (Eckernförde Bay, SW Baltic Sea). *Biogeosciences* 7:1279–1284
- Bange HW, Freing A, Kock A, Löscher C (2010b) Marine pathways to nitrous oxide. In: Smith K (ed) *Nitrous oxide and climate change*. Earthscan, London, pp 36–62
- Barnes J, Upstill-Goddard RC (2011) N₂O seasonal distribution and air-sea exchange in UK estuaries: implications for tropospheric N₂O source from European coastal waters. *J Geophys Res* 116, G01006. doi:[10.1029/2009JG001156](https://doi.org/10.1029/2009JG001156)
- Barnes J, Ramesh R, Purvaja R, Nirmal Rajkumar A, Senthil Kumar B, Krithika K, Ravichandran K, Uher G, Upstill-Goddard RC (2006) Tidal dynamics and rainfall control N₂O and CH₄ emissions from a pristine mangrove creek. *Geophys Res Lett* 33, L15405. doi:[10.1029/2006GL026829](https://doi.org/10.1029/2006GL026829)
- Bastviken D, Tranvik LJ, Downing JA, Crill PM, Enrich-Prast A (2011) Freshwater methane emissions offset the continental carbon sink. *Science* 331:50
- Bates NR, Michaels AF, Knap AH (1996a) Seasonal and inter-annual variability of oceanic carbon dioxide species at the U.S. JGOFS Bermuda Atlantic Time-series Study (BATS) site. *Deep-Sea Res Part II* 43(2–3):347–383
- Bates TS, Kelly KC, Johnson JE, Gammon RH (1996b) A reevaluation of the open ocean source of methane to the atmosphere. *J Geophys Res* 101:6953–6961
- Bates NR, Samuels L, Merlivat L (2001) Biogeochemical and physical factors influencing seawater fCO₂ and air-sea CO₂ exchange on the Bermuda coral reef. *Limnol Oceanogr* 46(4):833–846
- Bates NR, Moran SB, Hansell DA, Mathis JT (2006) An increasing CO₂ sink in the Arctic Ocean due to sea-ice loss. *Geophys Res Lett* 33, L23609. doi:[10.1029/2006GL027028](https://doi.org/10.1029/2006GL027028)
- Battin TJ, Kaplan LA, Findlay S, Hopkinson CS, Marti E, Packman AI, Newbold JD, Sabater F (2008) Biophysical controls on organic carbon fluxes in fluvial networks. *Nat Geosci* 1:95–100
- Bauzá JF, Morrell JM, Corredor JE (2002) Biogeochemistry of nitrous oxide production in the Red Mangrove (*Rhizophora mangle*) forest sediments. *Estuar Coast Shelf Sci* 55:697–704
- Beauchamp B (2004) Natural gas hydrates: myths, facts and issues. *C R Geosci* 336:751–765. doi:[10.1016/j.crte.2004.04.003](https://doi.org/10.1016/j.crte.2004.04.003)
- Beman JM, Chow C-E, King AL, Feng Y, Fuhrman JA, Andersson A, Bates NR, Popp BN, Hutchins DA (2011) Global declines in oceanic nitrification rates as a consequence of ocean acidification. *Proc Natl Acad Sci USA* 108(1):208–213. doi:[10.1073/pnas.1011053108](https://doi.org/10.1073/pnas.1011053108)
- Bender ML, Ho DT, Hendricks MB, Mika R, Battle MO, Tans PP, Conway TJ, Sturtevant B, Cassar N (2005) Atmospheric O₂/N₂ changes, 1993–2002: implications for the partitioning of fossil fuel CO₂ sequestration. *Global Biogeochem Cycle* 19, GB4017. doi:[10.1029/2004GB002410](https://doi.org/10.1029/2004GB002410)
- Biscaye PE, Anderson R (1994) Particle fluxes on the slope of the southern Mid-Atlantic Bight: SEEP-II. *Deep-Sea Res Part II* 41:459–469
- Biscaye PE, Anderson R, Deck BL (1988) Fluxes of particles and constituents to the Eastern United States continental slope and rise: SEEP-I. *Cont Shelf Res* 8:888–904
- Biswas H, Mukhopadhyay SK, De TK, Sen S, Jana TK (2006) Methane emission from the wetland rice fields in Sagar Island, NE coast of Bay of Bengal, India. *Int J Agric Res* 1(1):78–86
- Biswas H, Mukhopadhyay SK, Sen S, Jana TK (2007) Spatial and temporal patterns of methane dynamics in the tropical mangrove dominated estuary, NE coast of Bay of Bengal, India. *J Mar Syst* 68:55–64
- Blair NE, Aller RC (1995) Anaerobic methane oxidation on the Amazon shelf. *Geochim Cosmochim Acta* 59:3707–3715
- Boetius A, Ravenschlag K, Schubert CJ, Rickert D, Widdel F, Gieseke A, Amann R, Jørgensen BB, Witte U, Pfannkuche O (2000) A marine microbial consortium apparently mediating anaerobic oxidation of methane. *Nature* 407:623–626
- Bopp L, Le Quééré C, Heimann M, Manning AC (2002) Climate-induced oceanic oxygen fluxes: implications for the contemporary carbon budget. *Global Biogeochem Cycle* 16(2):1022. doi:[10.1029/2011GB001445](https://doi.org/10.1029/2011GB001445)
- Borges AV (2005) Do we have enough pieces of the jigsaw to integrate CO₂ fluxes in the Coastal Ocean? *Estuaries* 28(1):3–27
- Borges AV (2011) Present day carbon dioxide fluxes in the coastal ocean and possible feedbacks under global change. In: Duarte PM, Santana-Casiano JM (eds) *Oceans and the atmospheric carbon content*. Springer, Berlin, pp 47–77
- Borges AV, Abril G (2011) Carbon dioxide and methane dynamics in estuaries. In: Wolanski E, McLusky DS (eds) *Treatise on estuarine and coastal science*, vol 5, *Biogeochemistry*. Elsevier, Amsterdam, pp 119–161. doi:[10.1016/B978-0-12-374711-2.00504-0](https://doi.org/10.1016/B978-0-12-374711-2.00504-0)
- Borges AV, Gypens N (2010) Carbonate chemistry in the coastal zone responds more strongly to eutrophication than to ocean acidification. *Limnol Oceanogr* 55:346–353
- Borges AV, Djenidi S, Lacroix G, Théate J, Delille B, Frankignoulle M (2003) Atmospheric CO₂ flux from mangrove surrounding waters. *Geophys Res Lett* 30(11):1558. doi:[10.1029/2003GL017143](https://doi.org/10.1029/2003GL017143)
- Borges AV, Delille B, Frankignoulle M (2005) Budgeting sinks and sources of CO₂ in the coastal ocean: diversity of ecosystems counts. *Geophys Res Lett* 32, L14601. doi:[10.1029/2005GL023053](https://doi.org/10.1029/2005GL023053)
- Borges AV, Schiettecatte L-S, Abril G, Delille B, Gazeau F (2006) Carbon dioxide in European coastal waters. *Estuar Coast Shelf Sci* 70(3):375–387
- Borges AV, Tilbrook B, Metzl N, Lenton A, Delille B (2008) Inter-annual variability of the carbon dioxide oceanic sink south of Tasmania. *Biogeosciences* 5:141–155
- Borges AV, Alin SR, Chavez FP, Vlahos P, Johnson KS, Holt JT, Balch WM, Bates N, Brainard R, Cai W-J, Chen CTA, Currie K, Dai M, Degrandpré M, Delille B, Dickson A, Evans W, Feely RA, Friederich GE, Gong G-C, Hales B, Hardman-Mountford N, Hendee J, Hernandez-Ayon JM, Hood M, Huertas E, Hydes D, Ianson D, Krasakopoulou E, Litt E, Luchetta A, Mathis J, McGillis WR, Murata A, Newton J, Ólafsson J, Omar A, Perez FF, Sabine C, Salisbury

- JE, Salm R, Sarma VVSS, Schneider B, Sigler M, Thomas H, Turk D, Vandemark D, Wanninkhof R, Ward B (2010) A global sea surface carbon observing system: inorganic and organic carbon dynamics in coastal oceans. In: Hall J, Harrison DE, Stammer D (eds) Proceedings of OceanObs'09: sustained ocean observations and information for society, vol 2, Venice, Italy, 21–25 Sept 2009, ESA publication WPP-306. doi:10.5270/OceanObs09.cwp.07
- Bouillon S, Middelburg JJ, Dehairs F, Borges AV, Abril G, Flindt MR, Ulomi S, Kristensen E (2008) Importance of intertidal sediment processes and pore water exchange on the water column biogeochemistry in a pristine mangrove creek (Ras Degen, Tanzania). *Biogeosciences* 4:311–322
- Boutin J, Etcheto J, Dandonneau Y, Bakker DCE, Feely RA, Inoue HY, Ishii M, Ling RD, Nightingale PD, Metzl N, Wanninkhof R (1999) Satellite sea surface temperature: a powerful tool for interpreting in situ pCO₂ measurements in the equatorial Pacific Ocean. *Tellus* 51B:490–508
- Brewer PG, Peltzer ET (2009) Limits to marine life. *Science* 324:347–348
- Brewer PG, Paull C, Peltzer ET, Ussler W, Rehder G, Friederich G (2002) Measurement of the fate of gas hydrates during transit through the ocean water column. *Geophys Res Lett* 29:38. doi:10.1029/2002GL014727
- Brix H, Gruber N, Keeling CD (2004) Interannual variability of the upper ocean carbon cycle at station ALOHA near Hawaii. *Global Biogeochem Cycle* 18, GB4019. doi:10.1029/2004GB002245
- Broecker WS, Peng T-H (1982) Tracers in the sea. Eldigio Press, Lamont-Doherty Geological Observatory, Columbia University, Palisades
- Brüchert V, Currie B, Peard KR (2009) Hydrogen sulphide and methane emissions on the central Namibian shelf. *Prog Oceanogr* 83:169–179
- Buffett B, Archer D (2004) Global inventory of methane clathrate: sensitivity to changes in the deep ocean. *Earth Planet Sci Lett* 227:185–199. doi:10.1016/j.epsl.2004.09.005
- Buitenhuis E, Van Bleijswijk J, Bakker DCE, Veldhuis MJW (1996) Trends in inorganic and organic carbon in a bloom of *Emiliania huxleyi* in the North Sea. *Mar Ecol Prog Ser* 143:271–282
- Byrne RH, DeGrandpre MD, Short RT, Martz TR, Merlivat L, McNeil C, Sayles FL, Bell R, Fietzek P (2010) Sensors and systems for in situ observations of marine carbon dioxide system variables. In: Hall J, Harrison DE, Stammer D (eds) Proceedings of OceanObs'09: sustained ocean observations and information for society, vol 2, Venice, Italy, 21–25 Sept 2009, ESA publication WPP-306. doi:10.5270/OceanObs09.cwp.13
- Cabello P, Roldán MD, Moreno-Vivián C (2004) Nitrate reduction and the nitrogen cycle in archaea. *Microbiology* 150 (11):3527–3546
- Cai W-J (2011) Estuarine and coastal ocean carbon paradox: CO₂ sinks or sites of terrestrial carbon incineration? *Annu Rev Mar Sci* 3:123–145
- Cai W-J, Dai MH, Wang YC (2006) Air-sea exchange of carbon dioxide in ocean margins: a province-based synthesis. *Geophys Res Lett* 33, L12603. doi:10.1029/2006GL026219
- Caldeira K, Wickett ME (2003) Anthropogenic carbon and ocean pH. *Nature* 425:365
- Cantera JLL, Stein LY (2007) Role of nitrite reductase in the ammonia-oxidizing pathway of *Nitrosomonas europaea*. *Arch Microbiol* 188(4):349–354
- Capone DG, Kiene RP (1988) Comparison of microbial dynamics in marine and freshwater sediments: contrasts in anaerobic carbon catabolism. *Limnol Oceanogr* 33(4 part 2):725–749
- Cavaliere DJ, Parkinson CL, Vinnikov KY (2003) 30-Year satellite record reveals contrasting Arctic and Antarctic decadal sea ice variability. *Geophys Res Lett* 30(18):1970. doi:10.1029/2003GL018031
- Chan F, Barth JA, Lubchenco J, Kirincich A, Weeks H, Peterson WT, Menge BA (2008) Emergence of anoxia in the California current large marine ecosystem. *Science* 319:920–920
- Chanton JP, Martens CS, Kelley CA (1989) Gas transport from methane-saturated, tidal freshwater and wetland sediments. *Limnol Oceanogr* 34(5):807–819
- Chen CTA, Borges AV (2009) Reconciling opposing views on carbon cycling in the coastal ocean: continental shelves as sinks and near-shore ecosystems as sources of atmospheric CO₂. *Deep-Sea Res Part II* 56(8–10):578–590
- Codispoti LA (2010) Interesting times for marine N₂O. *Science* 327:1339–1340
- Codispoti LA, Elkins JW, Friederich GE, Packard TT, Sakamoto CM, Yoshinari T (1992) On the nitrous oxide flux from productive regions that contain low oxygen waters. In: Desai BN (ed) *Oceanography of the Indian ocean*. Oxford-IBH, New Delhi, pp 271–284
- Codispoti LA, Flagg C, Kelly V (2005) Hydrographic conditions during the 2002 SBI process experiments. *Deep-Sea Res Part II* 52(24–26):3199–3226
- Cole JA (1988) Assimilatory and dissimilatory reduction of nitrate to ammonia. *Symp Soc Gen Microbiol* 42:281–329
- Comeau S, Gattuso JP, Nisumaa AM, Orr J (2011) Impact of aragonite saturation state changes on migratory pteropods. *Proc Royal Soc B Biol Sci*. doi:10.1098/rspb.2011.0910
- Conrad R, Seiler W (1988) Methane and hydrogen in seawater (Atlantic Ocean). *Deep-Sea Res* 35:1903–1917
- Corbière A, Metzl N, Reverdin G, Brunet C, Takahashi T (2007) Interannual and decadal variability of the oceanic carbon sink in the North Atlantic subpolar gyre. *Tellus* 59B:168–178
- Cornejo M, Fariás L, Paulmier A (2006) Temporal variability in N₂O water content and its air-sea exchange in an upwelling area off central Chile (36°S). *Mar Chem* 101:85–94
- Cornejo M, Fariás L, Gallegos M (2007) Seasonal cycle of N₂O vertical distribution and air-sea fluxes over the continental shelf waters off central Chile (36°S). *Prog Oceanogr* 75:383–395
- Crutzen PJ (1970) The influence of nitrogen oxides on the atmospheric ozone content. *Q J R Meteorol Soc* 96:320–325
- Crutzen PJ (1991) Methane's sinks and sources. *Nature* 350:380–381
- Curry R, Dickson R, Yashayaev I (2003) A change in the freshwater balance of the Atlantic Ocean over the past four decades. *Nature* 426:826–829
- Cynar FJ, Yayanos AA (1991) Enrichment and characterization of a methanogenic bacterium from the oxic upper layer of the ocean. *Curr Microbiol* 23:89–96
- Dale AW, Regnier P, Van Cappellen P (2006) Bioenergetic controls on anaerobic oxidation of methane (AOM) in coastal marine sediments: a theoretical analysis. *Am J Sci* 306:246–294. doi:10.2475/ajs.306.4.246

- Damm E, Mackensen A, Budéus G, Faber E, Hanfland C (2005) Pathways of methane in seawater: plume spreading in an Arctic shelf environment (SW Spitsbergen). *Cont Shelf Res* 25:1453–1472
- Damm E, Helmke E, Thoms S, Schauer U, Nöthig E, Bakker K, Kiene R (2010) Methane production in aerobic oligotrophic surface water in the central Arctic Ocean. *Biogeosciences* 7:1099–1108
- Dando PR, Austen MC, Burke RA, Kendall MA, Kennicutt MC, Judd AG, Moore DC, Ohara SCM, Schmaljohann R, Southward AJ (1991) Ecology of a North-Sea pockmark with an active methane seep. *Mar Ecol Prog Ser* 70:49–63
- De Angelis MA, Lee C (1994) Methane production during zooplankton grazing on marine phytoplankton. *Limnol Oceanogr* 39:1298–1308
- Delille B, Jourdain B, Borges AV, Tison J-L, Delille D (2007) Biogas (CO₂, O₂, dimethylsulfide) dynamics in spring Antarctic fast ice. *Limnol Oceanogr* 52(4):1367–1379
- Denman KL, Brasseur G, Chidthaisong A, Ciais P, Cox PM, Dickinson RE, Hauglustaine D, Heinze C, Holland E, Jacob D, Lohman U, Ramachandran S, Da Silva Dias PL, Wofsy SC, Zhang X (2007) Couplings between changes in the climate system and biogeochemistry. In: Solomon S, Qin D, Manning M, Chen Z, Marquis M, Averyt KB, Tignor M, Miller HL (eds) *Climate change 2007: The physical science basis. contribution of working group I to the fourth assessment report of the intergovernmental panel on climate change*. Cambridge University Press, Cambridge/New York, pp 499–587
- Deutsch C, Brix H, Ito T, Frenzel H, Thompson L (2011) Climate-forced variability of ocean hypoxia. *Science* 333:336–339
- Devol AH, Richey JE, Forsburg BR, Martinelli LA (1990) Seasonal dynamics in methane emissions from the Amazon river floodplain. *J Geophys Res* 95:16417–16426
- Diaz RJ, Rosenberg R (2008) Spreading dead zones and consequences for marine ecosystems. *Science* 321:926–929
- Dickson AG, Sabine CL, Christian JR (eds) (2007) *Guide to best practices for ocean CO₂ measurements, vol 3, PICES special publication*. North Pacific Marine Science Organization, Sidney, BC, Canada
- Dimitrov L (2002) Contribution to atmospheric methane by natural seepages on the Bulgarian continental shelf. *Cont Shelf Res* 22:2429–2442
- Dittmar T, Hertkorn N, Kattner G, Lara RJ (2006) Mangroves, a major source of dissolved organic carbon to the oceans. *Global Biogeochem Cycle* 20, GB1012. doi:10.1029/2005GB002570
- Dlugokencky EJ, Houweling S, Bruhwiler L, Masarie KA, Lang PM, Miller JB, Tans PP (2003) Atmospheric methane levels off: temporary pause or a new steady-state? *Geophys Res Lett* 30(19):1992. doi:10.1029/2003GL018126
- Dlugokencky EJ, Bruhwiler L, White JWC, Emmons LK, Novelli PC, Montzka SA, Masarie KA, Lang PM, Crotwell AM, Miller JB, Gatti LV (2009) Observational constraints on recent increases in the atmospheric CH₄ burden. *Geophys Res Lett* 36, L18803. doi:10.1029/2009GL039780
- DOE (1994) In: Dickson AG, Goyet C (eds) *Handbook of methods for the analysis of the various parameters of the carbon system in sea water; version 2*. ORNL/CDIAC-74, Carbon Dioxide Information Analysis Center, Oak Ridge National Laboratory, US Department of Energy, Oak Ridge, Tennessee, USA
- Doney SC, Mahowald N, Lima I, Feely RA, Mackenzie FT, Lamarque J-F, Rasch PJ (2007) Impact of anthropogenic atmospheric nitrogen and sulfur deposition on ocean acidification and the inorganic carbon system. *Proc Natl Acad Sci USA* 104(37):14580–14585
- Doney SC, Ruckelshaus M, Duffy JE, Barry JP, Chan F, English CA, Galindo HM, Grebmeier JM, Hollowed AB, Knowlton N, Polovina J, Rabalais NN, Sydeman WJ, Talley LD (2012) Climate change impacts on marine ecosystems. *Annu Rev Mar Sci* 4:11–37. doi:10.1146/annurev-marine-041911-111611
- Dore JE, Karl DM (1996) Nitrification in the euphotic zone as a source for nitrite, nitrate, and nitrous oxide at station ALOHA. *Limnol Oceanogr* 41:1619–1628
- Dore JE, Lukas R, Sadler DW, Karl DM (2003) Climate-driven changes to the atmospheric CO₂ sink in the subtropical North Pacific Ocean. *Nature* 424:754–757
- Dürr HH, Laruelle GG, Van Kempen CM, Slomp CP, Meybeck M, Middelkoop H (2011) Worldwide typology of nearshore coastal systems: defining the estuarine filter of river inputs to the oceans. *Estuar Coasts* 34:441–458
- EPA (2010) *Methane and nitrous oxide emissions from natural sources*. 430-R-10-001. Office of Atmospheric Programs (6207J), United States Environmental Protection Agency, Washington, DC
- EPICA Community Members (2004) Eight glacial cycles from an Antarctic ice core. *Nature* 429:623–628
- Fazzolari E, Mariotti A, Germon JC (1990a) Nitrate reduction to ammonia – a dissimilatory process in *Enterobacter-Annigenus*. *Can J Microbiol* 36(11):779–785
- Fazzolari E, Mariotti A, Germon JC (1990b) Dissimilatory ammonia production vs. denitrification in vitro and in inoculated agricultural soil samples. *Can J Microbiol* 36(11):786–793
- Feely RA, Sabine CL, Lee K, Berelson W, Kleypas J, Fabry VJ, Millero FJ (2004) Impact of anthropogenic CO₂ on the CaCO₃ system in the oceans. *Science* 305:362–366
- Feely RA, Takahashi T, Wanninkhof R, McPhaden MJ, Cosca CE, Sutherland SC, Carr M-E (2006) Decadal variability of the air-sea CO₂ fluxes in the equatorial Pacific Ocean. *J Geophys Res* 111, C08S90. doi:10.1029/2005JC003129
- Feely RA, Fabry VJ, Dickson AG, Gattuso J-P, Bijma J, Riebesell U, Doney S, Turley C, Saino T, Lee K, Anthony K, Kleypas J (2010) An international observational network for ocean acidification. In: Hall J, Harrison DE, Stammer D (eds) *Proceedings of OceanObs'09: sustained ocean observations and information for society, vol 2, Venice, Italy, 21–25 Sept 2009*, ESA publication WPP-306. doi:10.5270/OceanObs09.cwp.29
- Ferrón S, Ortega T, Gómez-Parra A, Forja JM (2007) Seasonal study of dissolved CH₄, CO₂ and N₂O in a shallow tidal system of the bay of Cádiz (SW Spain). *J Mar Syst* 66:244–257. doi:10.1016/j.jmarsys.2006.03.021
- Flückiger J, Blunier T, Stauffer B, Chappellaz J, Spahni R, Kawamura K, Schwander J, Stocker TF, Dahl-Jensen D (2004) N₂O and CH₄ variations during the last glacial epoch: insight into global processes. *Global Biogeochem Cycle* 18, GB1020. doi:10.1029/2003GB002122
- Forster P, Ramaswamy V, Artaxo P, Berntsen T, Betts R, Fahey DW, Haywood J, Lean J, Lowe DC, Myhre G, Nganga J, Prinn R, Raga G, Schulz M, Van Dorland R (2007) Changes in atmospheric constituents and in radiative forcing.

- In: Solomon S, Qin D, Manning M, Chen Z, Marquis M, Averyt KB, Tignor M, Miller HL (eds) *Climate change 2007: the physical science basis*. Contribution of working group I to the fourth assessment report of the intergovernmental panel on climate change. Cambridge University Press, Cambridge/New York, pp 130–234
- Forster G, Upstill-Goddard RC, Gist N, Robinson C, Uher G, Woodward EMS (2009) Nitrous oxide and methane in the Atlantic Ocean between 50°N and 52°S: latitudinal distribution and sea-to-air flux. *Deep-Sea Res Part II* 56:964–976. doi:10.1016/j.dsr2.2008
- Francis CA, Beman JM, Kuypers MM (2007) New processes and players in the nitrogen cycle: the microbial ecology of anaerobic and archaeal ammonia oxidation. *ISME J* 1(1):19–27
- Frankignoulle M, Canon C, Gattuso J-P (1994) Marine calcification as a source of carbon dioxide: positive feedback of increasing CO₂. *Limnol Oceanogr* 39(2):458–462
- Frankignoulle M, Gattuso J-P, Biondo R, Bourge I, Copin-Montégut G, Pichon M (1996) Carbon fluxes in coral reefs 2. Eulerian study of inorganic carbon dynamics and measurement of air-sea CO₂ exchanges. *Mar Ecol Prog Ser* 145:123–132
- Frankignoulle M, Abril G, Borges A, Bourge I, Canon C, Delille B, Libert E, Théate MJ (1998) Carbon dioxide emission from European estuaries. *Science* 282:434–436. doi:10.1126/science.282.5388.434
- Freing A (2009) Production and emissions of oceanic nitrous oxide. Ph.D. thesis. University of Kiel, Kiel
- Freing A, Wallace DWR, Bange HW (2012) Global oceanic production of nitrous oxide (N₂O). *Philos Trans R Soc B* 367:1245–1255
- Friedlingstein P, Houghton RA, Marland G, Hacker J, Boden TA, Conway TJ, Canadell JC, Raupach MR, Ciais P, Le Quére C (2010) Update on CO₂ emissions. *Nat Geosci* 3:811–812. doi:10.1038/ngeo1022
- Gattuso J-P, Pichon M, Delesalle B, Frankignoulle M (1993) Community metabolism and air-sea CO₂ fluxes in a coral reef ecosystem (Moorea, French Polynesia). *Mar Ecol Prog Ser* 96:259–267
- Gattuso J-P, Payri CE, Pichon M, Delesalle B, Frankignoulle M (1997) Primary production, calcification, and air-sea CO₂ fluxes of a macroalgal-dominated coral reef community (Moorea, French Polynesia). *J Phycol* 33(5):729–738
- Gattuso J-P, Frankignoulle M, Wollast R (1998) Carbon and carbonate metabolism in coastal aquatic ecosystems. *Annu Rev Ecol Syst* 29:405–433
- Gazeau F, Smith SV, Gentili B, Frankignoulle M, Gattuso J-P (2004) The European coastal zone: characterization and first assessment of ecosystem metabolism. *Estuar Coast Shelf Sci* 60(4):673–694
- Geibert W, Assmy P, Bakker DCE, Hanfland C, Hoppema M, Pichevin L, Schröder M, Schwarz JN, Stimac I, Usbeck U, Webb A (2010) High productivity in an ice melting hotspot at the eastern boundary of the Weddell Gyre. *Global Biogeochem Cycle* 24, GB3007. doi:10.1029/2009GB003657
- Geilfus N-X, Carnat G, Papakyriakou T, Tison J-L, Else B, Thomas H, Shadwick E, Delille B (2012) Dynamics of pCO₂ and related air-ice CO₂ fluxes in the Arctic coastal zone (Amundsen Gulf, Beaufort Sea). *J Geophys Res* 117, C00G10. doi:10.1029/2011JC007117
- Gerard G, Chanton J (1993) Quantification of methane oxidation in the rhizosphere of emergent aquatic macrophytes: defining upper limits. *Biogeochemistry* 23:79–97
- Global Carbon Project (2011) Carbon budget and trends 2010. www.globalcarbonproject.org/carbonbudget. Accessed 13 Jan 2012
- González-Dávila M, Santana-Casiano JM, Rueda MJ, Llinás O, González-Dávila E-F (2003) Seasonal and interannual variability of sea-surface carbon dioxide species at the European Station for Time Series in the Ocean at the Canary Islands (ESTOC) between 1996 and 2000. *Global Biogeochem Cycle* 17(3):1076. doi:10.1029/2002GB001993
- González-Dávila M, Santana-Casiano JM, Rueda MJ, Llinás O (2010) The water column distribution of carbonate system variables at the ESTOC site from 1995 to 2004. *Biogeosciences* 7:3067–3081
- Gordon AL, Huber BA (1990) Southern Ocean winter mixed layer. *J Geophys Res* 95:11655–11672
- Goreau TJ, Kaplan WA, Wofsy SC, McElroy MB, Valois FW, Watson SW (1980) Production of NO₂⁻ and N₂O by nitrifying bacteria at reduced concentrations of oxygen. *Appl Environ Microbiol* 40:526–532
- Gornitz V, Fung I (1994) Potential distribution of methane hydrates in the world's oceans. *Global Biogeochem Cycle* 8(3):335–347. doi:10.1029/94GB00766
- Gruber N, Keeling CD (2001) An improved estimate of the isotopic air-sea disequilibrium of CO₂: implications for the oceanic uptake of anthropogenic CO₂. *Geophys Res Lett* 28(3):555–558. doi:10.1029/2000GL011853
- Gruber N, Sarmiento JL (2002) Large-scale biogeochemical/physical interactions in elemental cycles. In: Robinson AR, McCarthy JJ, Rothschild BJ (eds) *The sea*, vol 12. Wiley, New York, pp 337–399
- Gruber N, Keeling CD, Bates NR (2002) Interannual variability in the North Atlantic Ocean carbon sink. *Science* 298:2374–2378
- Gruber N, Gloor M, Mikaloff Fletcher SE, Doney SC, Dutkiewicz S, Follows MJ, Gerber M, Jacobson AR, Joos F, Lindsay K, Menemenlis D, Mouchet A, Müller SA, Takahashi T (2009) Oceanic sources, sinks, and transport of atmospheric CO₂. *Global Biogeochem Cycle* 23, GB1005. doi:10.1029/2008GB003349
- Gruber N, Körtzinger A, Borges A, Claustre H, Doney SC, Feely RA, Hood M, Ishii M, Kozyr A, Monteiro P, Nojiri Y, Sabine CL, Schuster U, Wallace DWR, Wanninkhof R (2010) Plenary Paper: Toward an integrated observing system for ocean carbon and biogeochemistry at a time of change. In: Hall J, Harrison DE, Stammer D (eds) *Proceedings of OceanObs'09: sustained ocean observations and information for society*, vol 1, Venice, Italy, 21–25 Sept 2009, ESA publication WPP-306. doi:10.5270/OceanObs09. p 18
- Gülzow W, Rehder G, Schneider B, Schneider von Deimling J, Sadkowiak B (2011) A new method for continuous measurement of methane and carbon dioxide in surface waters using off-axis integrated cavity output spectroscopy (ICOS): an example from the Baltic Sea. *Limnol Oceanogr Methods* 9:168–174
- Gurney KR, Law RM, Denning AS, Rayner PJ, Pak BC, Baker D, Bousquet P, Bruhwiler L, Chen Y-H, Ciais P, Fung IY, Heimann M, John J, Maki T, Maksyutov S,

- Peylin P, Prather M, Taguchi S (2004) Transcom 3 inversion intercomparison: model mean results for the estimation of seasonal carbon sources and sinks. *Global Biogeochem Cycle* 18, GB1010. doi:[10.1029/2003GB002111](https://doi.org/10.1029/2003GB002111)
- Gypens N, Borges AV, Lancelot C (2009) Effect of eutrophication on air-sea CO₂ fluxes in the coastal Southern North Sea: a model study of the past 50 years. *Global Change Biol* 15(4):1040–1056
- Hall TM, Prather MJ (1993) Simulations of the trend and annual cycle in stratospheric CO₂. *J Geophys Res* 98:10573–10581. doi:[10.1029/93JD00325](https://doi.org/10.1029/93JD00325)
- Harlay J, Borges AV, Van Der Zee C, Delille B, Godoi RHM, Schiettecatte L-S, Roevros N, Aerts K, Lapernat P-E, Rebreanu L, Groom S, Daro M-H, Van Grieken R, Chou L (2010) Biogeochemical study of a coccolithophorid bloom in the northern Bay of Biscay (NE Atlantic Ocean) in June 2004. *Prog Oceanogr* 80:317–336. doi:[10.1016/j.pocean.2010.04.029](https://doi.org/10.1016/j.pocean.2010.04.029)
- Harlay J, Chou L, De Bodt C, Van Oostende N, Piontek J, Suykens K, Engel A, Sabbe K, Groom S, Delille B, Borges AV (2011) Biogeochemistry and carbon mass balance of a coccolithophore bloom in the northern Bay of Biscay (June 2006). *Deep-Sea Res Part I* 58:111–127
- Heinze C, Maier-Reimer E, Winn K (1991) Glacial pCO₂ reduction by the world ocean: experiments with the Hamburg carbon cycle model. *Paleoceanography* 6(4):395–430
- Heip C, Goosen NK, Herman PMJ, Kromkamp J, Middelburg JJ, Soetaert K (1995) Production and consumption of biological particles in temperate tidal estuaries. *Oceanogr Mar Biol: Annu Rev* 33:1–149
- Helm KP, Bindoff NL, Church JA (2011) Observed decreases in oxygen content of the global ocean. *Geophys Res Lett* 38, L23602. doi:[10.1029/2011GL049513](https://doi.org/10.1029/2011GL049513)
- Ho DT, Law CS, Smith MJ, Schlosser P, Harvey M, Hill P (2006) Measurements of air-sea gas exchange at high wind speeds in the Southern Ocean: implications for global parameterizations. *Geophys Res Lett* 33, L16611. doi:[10.1029/2006GL026817](https://doi.org/10.1029/2006GL026817)
- Holmes ME, Sansone FJ, Rust TM, Popp BN (2000) Methane production, consumption, and air-sea exchange in the open ocean: an evaluation based on carbon isotopic ratios. *Global Biogeochem Cycle* 14:1–10
- Holt J, Wakelin S, Huthnance J (2008) Down-welling circulation of the northwest European continental shelf: a driving mechanism for the continental shelf carbon pump. *Geophys Res Lett* 36, L14602. doi:[10.1029/2009GL038997](https://doi.org/10.1029/2009GL038997)
- Hopkinson CSJ, Smith EM (2005) Estuarine respiration: an overview of benthic, pelagic and whole system respiration. In: Del Giorgio PA, Williams PJL (eds) *Respiration in aquatic ecosystems*. Oxford University Press, Oxford
- Hornafius JS, Quigley DC, Luyendyk BP (1999) The world's most spectacular marine hydrocarbons seeps (Coal Oil Point, Santa Barbara Channel, California): quantification of emissions. *J Geophys Res* 104(C9):20703–20711
- Hubberten H-W, Romanovski NN (2001) Terrestrial and offshore permafrost evolution of the Laptev Sea region during the last Pleistocene-Holocene glacial-eustatic cycle. In: Paepe R, Melnikov V (eds) *Permafrost response on economic development, environmental security and natural resources*. Proc-NATO-ARW, Novosibirsk, 1998. Kluwer, Dordrecht, pp 43–60
- Huthnance JM, Holt JT, Wakelin SL (2009) Deep ocean exchange with west-European shelf seas. *Ocean Sci* 5:621–634
- Iglesias-Rodriguez M, Halloran PR, Rickaby REM, Hall IR, Colmenero-Hidalgo E, Gittins JR, Green DRH, Tyrrell T, Gibbs SJ, Von Dassow P, Rehm E, Armbrust EV, Boessenkool KP (2008) Phytoplankton calcification in a High-CO₂ World. *Science* 320(5874):336–340. doi:[10.1126/science.1154122](https://doi.org/10.1126/science.1154122)
- IOCCP (2004) Ocean surface pCO₂, data integration and database development workshop, National Institute for Environmental Studies, Tsukuba, Japan, 14–17 Jan 2004. IOCCP (International Ocean Carbon Coordination Project) report 2. www.ioccp.org
- IPCC (2007) In: Solomon S, Qin D, Manning M, Chen Z, Marquis M, Averyt KB, Tignor M, Miller HL (eds) *Climate change 2007: the physical science basis*. Contribution of working group I to the fourth assessment report of the intergovernmental panel on climate change. Cambridge University Press, Cambridge/New York
- Ishii M, Inoue HY, Midorikawa T, Saito S, Tokieda T, Sasano D, Nakadate A, Nemoto K, Metzl N, Wong CS, Feely RA (2009) Spatial variability and decadal trend of the oceanic CO₂ in the western equatorial Pacific warm/fresh water. *Deep-Sea Res Part II* 56(8–10):591–606
- Jackson MA, Tiedje JM, Averill BA (1991) Evidence for a no-rebound mechanism for production of N₂O from nitrite by the copper-containing nitrite reductase from *Achromobacter Cycloclastes*. *FEBS Lett* 29(1):41–44
- Jacobson AR, Mikaloff Fletcher SE, Gruber N, Sarmiento JL, Gloor M (2007) A joint atmosphere–ocean inversion for surface fluxes of carbon dioxide: 1. Methods and global-scale fluxes. *Global Biogeochem Cycle* 21, GB1019. doi:[10.1029/2005GB002556](https://doi.org/10.1029/2005GB002556)
- Jansen E, Overpeck J, Briffa KR, Duplessy J-C, Joos F, Masson-Delmotte V, Olago D, Otto-Bliesner B, Peltier WR, Rahmstorf S, Ramesh R, Raynaud D, Rind D, Solomina O, Villalba R, Zhang D (2007) Paleoclimate. In: Solomon S, Qin D, Manning M, Chen Z, Marquis M, Averyt KB, Tignor M, Miller HL (eds) *Climate change 2007: the physical science basis*. Contribution of working group I to the fourth assessment report of the intergovernmental panel on climate change. Cambridge University Press, Cambridge/New York, pp 434–497
- Jansson BPM, Malandrin L, Johansson HE (2000) Cell cycle arrest in Archaea by the hypusination inhibitor N1-Guanyl-1,7-Diaminoheptane. *J Bacteriol* 182:1158–1161. doi:[10.1128/JB.182.4.1158-1161](https://doi.org/10.1128/JB.182.4.1158-1161)
- Jayakumar DA, Naqvi SWA, Narvekar PV, George MD (2001) Methane in coastal and offshore waters of the Arabian Sea. *Mar Chem* 74:1–13
- Jin X, Gruber N, Dunne JP, Sarmiento JL, Armstrong RA (2006) Diagnosing the contribution of phytoplankton functional groups to the production and export of particulate organic carbon, CaCO₃, and opal from global nutrient and alkalinity distributions. *Global Biogeochem Cycle* 20, GB2015. doi:[10.1029/2005GB002532](https://doi.org/10.1029/2005GB002532)
- Joos F, Meyer R, Bruno M, Leuenberger M (1999) The variability in the carbon sinks as reconstructed for the last 1000 years. *Geophys Res Lett* 26:1437–1441

- Joos F, Prentice IC, Sitch S, Meyer R, Hooss G, Plattner G-K, Gerber S, Hasselmann K (2001) Global warming feedbacks on terrestrial carbon uptake under the Intergovernmental Panel on Climate Change (IPCC) emission scenarios. *Global Biogeochem Cycle* 15(4):891–907
- Joos F, Plattner G-K, Stocker TF, Körtzinger A, Wallace DWR (2003) Trends in marine dissolved oxygen: implications for ocean circulation changes and the carbon budget. *Eos Trans Am Geophys Union* 84(21):197. doi:[10.1029/2003EO210001](https://doi.org/10.1029/2003EO210001)
- Joyce J, Jewell PW (2003) Physical controls on methane ebullition from reservoirs and lakes. *Environ Eng Geosci* 9:167–178
- Judd A, Hovland M (2007) Seabed fluid flow. Impact on geology, biology and the marine environment. Cambridge University Press, Cambridge, UK
- Kai FM, Tyler SC, Randerson JT, Blake DR (2011) Reduced methane growth rate explained by decreased northern hemisphere microbial sources. *Nature* 476:194–197. doi:[10.1038/nature10259](https://doi.org/10.1038/nature10259)
- Kaiser M, Attrill M, Jennings S, Thomas DN, Barnes D, Brierley A, Hiddink JG, Kaartokallio H, Polunin NVC, Raffaelli D (2011) Marine ecology: processes, systems and impacts, 2nd edn. Oxford University Press, Oxford
- Karl DM, Beversdorf L, Björkman KM, Church MJ, Martinez A, Delong EF (2008) Aerobic production of methane in the sea. *Nat Geosci* 1:473–478
- Keeling RF, Körtzinger A, Gruber N (2010) Ocean deoxygenation in a warming world. *Annu Rev Mar Sci* 2:199–229
- Kelley C (2003) Methane oxidation potential in the water column of two diverse coastal marine sites. *Biogeochemistry* 65:105–120
- Kemp WM, Smith EM, Marvin-DiPasquale M, Boynton WR (1997) Organic carbon-balance and net ecosystem metabolism in Chesapeake Bay. *Mar Ecol Prog Ser* 150:229–248
- Kessler JD, Reeburgh WS, Southon J, Varela R (2005) Fossil methane source dominates Cariaco Basin water column methane geochemistry. *Geophys Res Lett* 32, L12609. doi:[10.1029/2005GL022984](https://doi.org/10.1029/2005GL022984)
- Key RM, Kozyr A, Sabine CL, Lee K, Wanninkhof R, Bullister J, Feely RA, Millero F, Mordy C, Peng T-H (2004) A global ocean carbon climatology: results from GLODAP. *Global Biogeochem Cycle* 18, GB4031
- Kiene RP, Linn LJ, Bruton JA (2000) New and important roles for DMSP in marine microbial communities. *J Sea Res* 43:209–224
- King GM (1994) Ecophysiological characteristics of obligate methanotrophic bacteria and methane oxidation in situ. In: Murrell JC, Kelly DP (eds) *Microbial growth on C1 compounds*. Intercept Press, Andover, pp 303–313
- Kitidis V, Tizzard L, Uher G, Judd A, Upstill-Goddard RC, Head IM, Gray ND, Taylor G, Durán R, Diez R, Iglesias J, García-Gil S (2007) The biogeochemical cycling of methane in Ria de Vigo, NW Spain: sediment processing and sea–air exchange. *J Mar Syst* 66:258–271
- Klatt O, Roether W, Hoppema M, Bulsiewicz K, Fleischmann U, Rodehacke C, Fahrback E, Weiss RF, Bullister JL (2002) Repeated CFC sections at the Greenwich Meridian in the Weddell Sea. *J Geophys Res* 107:3030. doi:[10.1029/2000JC000731](https://doi.org/10.1029/2000JC000731)
- Kleypas JA, Buddemeier RW, Archer D, Gattuso J-P, Langdon C, Opdyke BN (1999) Geochemical consequences of increased atmospheric carbon dioxide on coral reefs. *Science* 284:118–120
- Kleypas JA, Feely RA, Fabry VJ, Langdon C, Sabine CL, Robins LL (2006) Impacts of ocean acidification on coral reefs and other marine calcifiers: a guide for future research. Report of a workshop, 2005. St. Petersburg, Florida. NSF, NOAA and US Geological Survey
- Kock A, Gebhardt S, Bange HW (2008) Methane emissions from the upwelling area off Mauritania (NW Africa). *Biogeosciences* 5:1119–1125
- Kock A, Schafstall J, Dengler M, Brandt P, Bange HW (2012) Sea-to-air and diapycnal nitrous oxide fluxes in the eastern tropical North Atlantic Ocean. *Biogeosciences* 9:957–964
- Koné YJM, Abril G, Kouadio KN, Delille B, Borges AV (2009) Seasonal variability of carbon dioxide in the rivers and lagoons of Ivory Coast (West Africa). *Estuar Coasts* 32:246–260
- Kreuzwieser J, Buchholz J, Rennenberg H (2003) Emission of methane and nitrous oxide by Australian mangrove ecosystems. *Plant Biol* 5:423–431
- Krey V, Canadell JG, Nakicenovic N, Abe Y, Andrulleit H, Archer D, Grubler A, Hamilton NTM, Johnson A, Kostov V, Lamarque J-F, Langhorne N, Nisbet EG, O’Neill B, Riahi K, Riedel M, Wang W, Yakushev V (2009) Gas hydrates: entrance to a methane age or climate threat? *Environ Res Lett* 4, 034007
- Kristensen E, Flindt MR, Borges AV, Bouillon S (2008) Emission of CO₂ and CH₄ to the atmosphere by sediments and open waters in two Tanzanian mangrove forests. *Mar Ecol Prog Ser* 370:53–67
- Kroeze C, Dumont E, Seitzinger SP (2005) New estimates of global emissions of N₂O from rivers and estuaries. *Environ Sci* 2:159–165
- Kvenvolden KA (1993) Gas hydrates – geological perspective and global change. *Rev Geophys* 31(2):173–187. doi:[10.1029/93RG00268](https://doi.org/10.1029/93RG00268)
- Kvenvolden KA (1999) Potential effects of gas hydrate on human welfare. *Proc Natl Acad Sci USA* 96:3420–3426
- Kvenvolden KA, Rogers BW (2005) Gaia’s breath – global methane exhalations. *Mar Pet Geol* 22(4):579–590
- Lam P, Jensen MM, Lavik G, van de Vossenberg J, Schmid M, Woebken D, Gutierrez D, Amann R, Jetten MSM, Kuypers MMM (2009) Revising the nitrogen cycle in the Peruvian oxygen minimum zone. *Proc Natl Acad Sci USA* 106(12):4752–4757
- Lamarque J-F (2008) Estimating the potential for methane clathrate instability in the 1% CO₂ IPCC AR4 simulations. *Geophys Res Lett* 35, L19806. doi:[10.1029/2008GL035291](https://doi.org/10.1029/2008GL035291)
- Lammers S, Suess E, Hovland M (1995) A large methane plume east of Bear Island (Barents Sea): implications for the marine methane cycle. *Geol Rundsch* 84:59–66
- Laruelle GG, Dürr HH, Slomp CP, Borges AV (2010) Evaluation of sinks and sources of CO₂ in the global coastal ocean using a spatially-explicit typology of estuaries and continental shelves. *Geophys Res Lett* 37, L15607. doi:[10.1029/2010GL043691](https://doi.org/10.1029/2010GL043691)
- Le Quére C, Rödenbeck C, Buitenhuis ET, Conway TJ, Lagenfelds R, Gomez A, Labuschagne C, Ramonet M, Nakazawa T, Metz N, Gillett N, Heimann M (2007) Saturation of the Southern Ocean CO₂ sink due to recent climate change. *Science* 316:1735–1738

- Le Quéré C, Takahashi T, Buitenhuis ET, Rödenbeck C, Sutherland SC (2010) Impact of climate change and variability on the global oceanic sink of CO₂. *Global Biogeochem Cycles* 24, GB4007
- Lee K, Sabine CL, Tanhua T, Kim T-W, Feely RA, Kim H-C (2011) Roles of marginal seas in absorbing and storing fossil fuel CO₂. *Energy Environ Sci* 4:1133
- Lefèvre N, Watson AJ, Olsen A, Ríos AF, Pérez FF, Johannessen T (2004) A decrease in the sink for atmospheric CO₂ in the North Atlantic. *Geophys Res Lett* 31(7), L07306
- Lefèvre N, Watson AJ, Watson AR (2005) A comparison of multiple regression and neural network techniques for mapping in situ pCO₂ data. *Tellus* 57B:375–384
- Leifer I, Patro RK (2002) The bubble mechanism for methane transport from the shallow sea bed to the surface: a review and sensitivity study. *Cont Shelf Res* 22:2409–2428
- Leip A (1999) Nitrous oxide (N₂O) emissions from a coastal catchment in the delta of the Po river: measurements and modeling of fluxes from a Mediterranean lagoon and agricultural soils. Ph.D. thesis, University of Bayreuth, Bayreuth
- Lenton A, Cordon G, Bopp L, Metzl N, Cadule P, Tagliabue A, Le Sommer J (2009) Stratospheric ozone depletion reduces ocean carbon uptake and enhances ocean acidification. *Geophys Res Lett* 36, L12606. doi:10.1029/2009GL038227
- Liss PS, Merlivat L (1986) Air-sea exchange rates: introduction and synthesis. In: Buat-Ménard P (ed) *The role of air-sea exchange in geochemical cycling*. D. Reidel Publishing, Dordrecht, pp 113–127
- Liu X, Millero FJ (2002) The solubility of Fe(III) in seawater. *Mar Chem* 77:43–54
- Liu KK, Atkinson L, Quiñones RA, Talahue-McManus L (2010) Biogeochemistry of continental margins in a global context. In: Liu KK, Atkinson L, Quiñones RA, Talahue-McManus L (eds) *Carbon and nutrient fluxes in continental margins*. Springer, Berlin etc., pp 3–24
- Löscher CR, Kock A, Könneke, M, LaRoche J, Bange HW, Schmitz RA (2012) Production of oceanic nitrous oxide by ammonia-oxidizing archaea. *Biogeosciences* 9:2419–2429. doi:10.5194/bg-9-2419-2012
- Lovenduski NS, Gruber N, Doney SC, Lima ID (2007) Enhanced CO₂ outgassing in the Southern Ocean from a positive phase of the Southern Annular Mode. *Global Biogeochem Cycle* 21, GB2026. doi:10.1029/2006GB002900
- Lovenduski NS, Gruber N, Doney SC (2008) Toward a mechanistic understanding of the decadal trends in the Southern Ocean carbon sink. *Global Biogeochem Cycle* 22, GB3016. doi:10.1029/2007GB003139
- Lüthi D, Le Floch M, Bereiter B, Blunier T, Barnola J-M, Siegenthaler U, Raynaud D, Jouzel J, Fischer H, Kawamura K, Stocker TF (2008) High-resolution carbon dioxide concentration record 650,000–800,000 years before present. *Nature* 453:379–382. doi:10.1038/nature06949
- Mackenzie FT, Lerman A, Andersson AJ (2004) Past and present of sediment and carbon biogeochemical cycling models. *Biogeosciences* 1(1):11–32
- Manning AC, Keeling RF (2006) Global oceanic and land biotic carbon sinks from the Scripps atmospheric oxygen flask sampling network. *Tellus* 58B:95–116. doi:10.1111/j.1600-0889.2006.00175.x
- Martens CS, Klump JV (1980) Biogeochemical cycling in an organic-rich coastal marine basin – I. Methane sediment-water exchange processes. *Geochim Cosmochim Acta* 44:471–490
- Martens-Habbena WPM, Berube PM, Urakawa H, De la Torre J, Stahl DA (2009) Ammonia oxidation kinetics determine niche separation of nitrifying Archaea and Bacteria. *Nature* 461(7266):976–979
- Marty D, Nival P, Yoon WD (1997) Methanoarchaea associated with sinking particles and zooplankton collected in the Northeastern tropical Atlantic. *Oceanol Acta* 20:863–869
- Matsumoto K, Sarmiento J, Brezeinski MA (2002) Silicic acid leakage from the Southern Ocean: a possible explanation for glacial atmospheric pCO₂. *Global Biogeochem Cycle* 16(3):5. doi:10.1029/2001GB001442
- Matthews BJH (1999) The rate of air-sea CO₂ exchange: chemical enhancement and catalysis by marine microalgae. Ph.D. thesis, University of East Anglia, Norwich
- Mau S, Valentine DL, Clark JF, Reed J, Camilli R, Washburn L (2007) Dissolved methane distributions and air-sea flux in the plume of a massive seep field, Coal Oil Point, California. *Geophys Res Lett* 34, L22603. doi:10.1029/2007GL031344
- McKinley GA, Fay AR, Takahashi T, Metzl N (2011) Convergence of atmospheric and North Atlantic carbon dioxide trends on multidecadal timescales. *Nat Geosci* 4:606–609. doi:10.1038/NGEO1193
- Metzl N (2009) Decadal increase of oceanic carbon dioxide in Southern Indian Ocean surface waters (1991–2007). *Deep-Sea Res Part II* 56:607–619
- Michelsen HA, Irion FW, Manney GL, Toon GC, Gunson MR (2000) Features and trends in Atmospheric Trace Molecule Spectroscopy (ATMOS) version 3 stratospheric water vapor and methane measurements. *J Geophys Res* 105(D18):22713–22724
- Middelburg JJ, Klaver G, Nieuwenhuize J, Wielemaker A, de Haas W, Van der Nat JFWA (1996) Organic matter mineralization in intertidal sediments along an estuarine gradient. *Mar Ecol Prog Ser* 132:157–168
- Middelburg JJ, Nieuwenhuize J, Iversen N, Høgh N, De Wilde H, Helder W, Seifert R, Christof O (2002) Methane distribution in European tidal estuaries. *Biogeochemistry* 59:95–119
- Mikaloff Fletcher SE, Gruber N, Jacobson AR, Doney SC, Dutkiewicz S, Gerber M, Gloor M, Follows M, Joos F, Lindsay K, Menemenlis D, Mouchet A, Müller SA, Sarmiento JL (2007) Inverse estimates of the oceanic sources and sinks of natural CO₂ and the implied oceanic transport. *Global Biogeochem Cycle* 21, GB1010. doi:10.1029/2006GB002751
- Miller LA, Papakyriakou TN, Collins RE, Deming JW, Ehn JK, Macdonald RW, Mucci A, Owens O, Raudsepp M, Sutherland N (2011) Carbon dynamics in sea ice: a winter flux time series. *J Geophys Res* 116(C2), C02028. doi:10.1029/2009jc006058
- Monaco A, Biscay P, Soyer J, Pocklington R, Heussner S (1990) Particle fluxes and ecosystem responses on a continental margin: the 1985–1988 Mediterranean ECOMARGE Experiment. *Cont Shelf Res* 10(9–11):809–839. doi:10.1016/0278-4343(90)90061-P
- Monteiro PMS, Schuster U, Hood M, Lenton A, Metzl N, Olsen A, Rogers K, Sabine CL, Takahashi T, Tilbrook B, Yoder J, Wanninkhof R, Watson AJ (2010) Community white paper. A global sea surface carbon observing system: Assessment of changing sea surface CO₂ and air-sea CO₂ fluxes. In: Hall J,

- Harrison DE, Stammer D (eds) Proceedings of OceanObs'09: sustained ocean observations and information for society, vol 2, Venice, Italy, 21–25 Sept 2009, ESA publication WPP-306. doi:10.5270/OceanObs09.cwp.64
- Montzka SA, Dlugokencky EJ, Butler JH (2011) Non-CO₂ greenhouse gases and climate change. *Nature* 476:43–50
- Moran JJ, Beal EJ, Vrentas JM, Orphan VJ, Freeman KH, House CH (2008) Methyl sulphides as intermediates in the anaerobic oxidation of methane. *Environ Microbiol* 10:162–173
- Morell JM, Capella J, Mercado A, Bauzá J, Corredor JE (2001) Nitrous oxide fluxes in Caribbean and tropical Atlantic waters: evidence for near surface production. *Mar Chem* 74:131–143
- Mucci A (1983) The solubility of calcite and aragonite in seawater at various salinities, temperatures, and one atmosphere total pressure. *Am J Sci* 283:780–799
- Mudelsee M (2001) The phase relations among atmospheric CO₂ content, temperature and global ice volume over the past 420 ka. *Q Sci Rev* 20:583–589
- Naik H, Naqvi SWA, Suresh T, Narvekar PV (2008) Impact of a tropical cyclone on biogeochemistry of the central Arabian Sea. *Global Biogeochem Cycle* 22, GB3020. doi:10.1029/2007GB003028
- Naqvi SWA (2008) The Indian Ocean. In: Capone DG, Carpenter EJ, Bronk DA (eds) Nitrogen in the marine environment, 2nd edn. Elsevier, Amsterdam, pp 631–681
- Naqvi SWA, Jayakumar DA, Narvekar PV, Naik H, Sarma VVSS, D'Souza W, Joseph S, George MD (2000) Increased marine production of N₂O due to intensifying anoxia on the Indian continental shelf. *Nature* 408:346–349
- Naqvi SWA, Bange HW, Gibb SW, Goyet C, Hatton AD, Upstill-Goddard RC (2005) Biogeochemical ocean-atmosphere transfers in the Arabian Sea. *Prog Oceanogr* 65:116–144
- Naqvi SWA, Bange HW, Fariás L, Monteiro PMS, Scranton MI, Zhang J (2010) Marine hypoxia/anoxia as a source of CH₄ and N₂O. *Biogeosciences* 7:2159–2190
- Naudin JJ, Cauwet G, Chrétiennot-Dinet MJ, Deniaux B, Devenon JL, Pauc H (1997) River discharge and wind influence upon particulate transfer at the land-ocean interaction: case study of the Rhône river plume. *Estuar Coast Shelf Sci* 45:303–316. doi:10.1006/ecss.1996.0190
- Nevison CD, Weiss RF, Erickson DJ III (1995) Global oceanic emissions of nitrous oxide. *J Geophys Res* 100:15809–15820
- Nevison C, Lueker T, Weiss RF (2004) Quantifying the nitrous oxide source from coastal upwelling. *Global Biogeochem Cycle* 18, GB1018. doi:10.1029/2003GB002110
- Nightingale PD, Malin G, Law CS, Watson AJ, Liss PS, Liddicoat MI, Boutin J, Upstill-Goddard RC (2000) In-situ evaluation of air-sea gas exchange parameterisations using novel conservative and volatile tracers. *Global Biogeochem Cycle* 14(1):373–387
- Nirmal Rajkumar A, Barnes J, Ramesh R, Purvaja R, Upstill-Goddard RC (2008) Methane and nitrous oxide fluxes in the polluted Adyar River and estuary. *SE India Mar Pollut Bull* 56:2043–2051
- O'Connor FM, Boucher O, Gedney N, Jones CD, Folberth GA, Coppel R, Friedlingstein P, Collins WJ, Chappellaz J, Ridley J, Johnson CE (2010) Possible role of wetlands, permafrost, and methane hydrates in the methane cycle under future climate change: a review. *Rev Geophys* 48, RG4005. doi:10.1029/2010RG000326
- Odum HT, Hoskin CM (1958) Comparative studies of the metabolism of Texas bays. *Publ Inst Mar Sci Univ Tex* 5:16–46
- Odum HT, Wilson R (1962) Further studies on the reaeration and metabolism of Texas bays. *Publ Inst Mar Sci Univ Tex* 8:23–55
- Ohde S, van Woesik R (1999) Carbon dioxide flux and metabolic processes of a coral reef, Okinawa. *Bull Mar Sci* 65:559–576
- Olsen A, Brown KR, Chierici M, Johannessen T, Neill C (2008) Sea surface CO₂ fugacity in the subpolar North Atlantic. *Biogeosciences* 5:535–547. www.biogeosciences-5/535/2008/
- Omar A, Johannessen T, Bellerby RGJ, Olsen A, Anderson LG, Kivimäe C, Omar A, Johannessen T, Bellerby RGJ, Olsen A, Anderson LG, Kivimäe C (2005) Sea-ice and brine formation in Storfjorden: implications for Arctic wintertime air-sea CO₂ flux. In: Drange H, Dokken T, Furevik T, Gerdes R, Berger W (eds) The Nordic seas: an integrated perspective, vol 158, American Geophysical Union Geophysical Monograph. American Geophysical Union, Washington, DC, pp 117–187
- Oremland RS (1979) Methanogenic activity in plankton samples and fish intestines: a mechanism for in situ methanogenesis in ocean surface waters. *Limnol Oceanogr* 24:1136–1141
- Orr JC, Fabry VJ, Aumont O, Bopp L, Doney SC, Feely RA, Gnanadesikan A, Gruber N, Ishida A, Joos F, Key RM, Lindsay K, Maier-Reimer E, Matear R, Monfray P, Mouchet A, Najjar RG, Plattner G-K, Rodgers KB, Sabine CL, Sarmiento JL, Schlitzer R, Slater RD, Totterdell IJ, Weirig M-F, Yamanaka Y, Yool A (2005) Anthropogenic ocean acidification over the twenty-first century and its impact on calcifying organisms. *Nature* 437:681–686
- Ostrovsky I (2003) Methane bubbles in Lake Kinneret: quantification and temporal and spatial heterogeneity. *Limnol Oceanogr* 48:1030–1036
- Oudot C, Jean-Baptiste P, Fourré E, Mormiche C, Gueve M, Ternon J-F, Le Corre P (2002) Transatlantic equatorial distribution of nitrous oxide and methane. *Deep-Sea Res Part I* 49(7):1175–1193
- Paull CK, Brewer PG, Ussler W III, Peltzer ET, Rehder G, Clague D (2003) An experiment demonstrating that marine slumping is a mechanism to transfer methane from seafloor gas-hydrate deposits into the upper ocean and atmosphere. *Geo-Mar Lett* 22:198–203. doi:10.1007/s00367-002-0113-y
- Paull CK, Ussler W, Holbrook S, Hill TM, Keaten R, Mienert J, Hafliadao H, Johnson JE, Winters WG, Lorenson TD (2008) Origin of pockmarks and chimney structures on the flanks of the Storegga slide, offshore Norway. *Geo-Mar Lett* 28:43–51. doi:10.1007/s00367-007-0088-9
- Peters GP, Marland G, Le Quéré C, Boden T, Canadell JG, Raupach MR (2012) Rapid growth in CO₂ emissions after the 2008–2009 global financial crisis. *Nat Clim Change* 2:2–4. doi:10.1038/nclimate1332
- Petit JR, Jouzel J, Raynaud D, Barkov NI, Barnola J-M, Basile I, Bender M, Chappellaz J, Davis M, Delaygue G, Delmotte M, Kotlyakov VM, Legrand M, Lipenkov VY, Lorius C, Pépin L, Ritz C, Saltzman E, Steievenard M (1999) Climate and atmospheric history of the past 420,000 years from the Vostok ice core, Antarctica. *Nature* 399:429–436. doi:10.1038/20859

- Pfeil, B, Olsen, A, Bakker, DCE, Hankin S, Koyuk H, Kozyr A, Malczyk J, Manke A, Metz N, Sabine CL, Akl J, Alin SR, Bates N, Bellerby RGJ, Borges A, Boutin J, Brown PJ, Cai W-J, Chavez FP, Chen A, Cosca C, Fassbender AJ, Feely RA, González-Dávila M, Goyet C, Hales B, Hardman-Mountford N, Heinze C, Hood M, Hoppema M, Hunt CW, Hydes D, Ishii M, Johannessen T, Jones SD, Key RM, Körtzinger A, Landschützer P, Lauvset SK, Lefèvre N, Lenton A, Lourantou A, Merlivat L, Midorikawa T, Mintrop L, Miyazaki C, Murata A, Nakadate A, Nakano Y, Nakaoka S, Nojiri Y, Omar AM, Padin XA, Park G-H, Paterson K, Perez FF, Pierrot D, Poisson A, Ríos AF, Salisbury J, Santana-Casiano JM, Sarma VVSS, Schlitzer R, Schneider B, Schuster U, Sieger R, Skjelvan I, Steinhoff T, Suzuki T, Takahashi T, Tedesco K, Telszewski M, Thomas H, Tilbrook B, Tjiputra J, Vandemark D, Veness T, Wanninkhof R, Watson AJ, Weiss R, Wong CS, Yoshikawa-Inoue H (2013) A uniform, quality controlled Surface Ocean CO₂ Atlas (SOCAT). *Earth Syst Sci Data* 5:125–143. doi:10.5194/essd-5-125-2013
- Philippot L (2002) Denitrifying genes in bacterial and Archaeal genomes. *Biochim Biophys Acta Gene Struct Expr* 1577 (3):355–376
- Plattner G-K, Frenzel H, Gruber N, Leinweber A, McWilliams JC (2004) Changing winds and coastal carbon cycle: a case study for an upwelling region. The ocean in a high-CO₂ world. UNESCO, Paris
- Plummer DH, Owens NJP, Herbert RA (1987) Bacteria-particle interactions in turbid estuarine environments. *Cont Shelf Res* 7:1429–1433. doi:10.1016/0278-4343(87)90050-1
- Prytherch J, Yelland MJ, Pascal RW, Moat BI, Skjelvan I, Srokosz MA (2010) Open ocean gas transfer velocity derived from long-term direct measurements of the CO₂ flux. *Geophys Res Lett* 37, L23607. doi:10.1029/2010GL045597
- Ramesh R, Purvaja R, Neetha V, Divia J, Barnes J, Upstill-Goddard RC (2007) CO₂ and CH₄ emissions from Indian mangroves and surrounding waters. In: Tateda Y, Upstill-Goddard RC, Goreau T, Alongi D, Nose A, Kristensen E, Wattayakorn G (eds) Greenhouse gas and carbon balances in mangrove coastal ecosystems. Gendai Tosho, Kanagawa, pp 153–164
- Rangama Y, Boutin J, Etcheto J, Merlivat L, Takahashi T, Delille B, Frankignoulle M, Bakker DCE (2005) Variability of the net air-sea CO₂ flux inferred from shipboard and satellite measurements in the Southern Ocean south of Tasmania and New Zealand. *J Geophys Res* 110:1–17. C09005. doi: 10.1029/2004JC002619
- Raven J, Caldeira K, Elderfield H, Hoegh-Guldberg O, Liss P, Riebesell U, Shepherd J, Turley C, Watson AJ (2005) Ocean acidification due to increasing atmospheric carbon dioxide, vol 12/05, Policy document. The Royal Society, London
- Ravishankara AR, Daniel JS, Portmann RW (2009) Nitrous oxide (N₂O): the dominant ozone-depleting substance emitted in the 21st century. *Science* 326:123–125
- Reagan MT, Moridis GJ (2009) Large-scale simulation of methane hydrate dissociation along the West Spitsbergen Margin. *Geophys Res Lett* 36, L23612. doi:10.1029/2009GL041332
- Redfield AC, Ketchum BH, Richards FA (1963) The influence of organisms on the composition of seawater. In: Hill MN (ed) The sea, vol 2. Wiley Interscience, New York, pp 26–77
- Reeburgh WS (2007) Oceanic methane biogeochemistry. *Chem Rev* 107(2):486–513
- Rehder G, Keir RS, Suess E, Pohlmann T (1998) The multiple sources and patterns of methane in North Sea waters. *Aquat Geochem* 4:403–427
- Rhee TS, Kettle AJ, Andreae MO (2009) Methane and nitrous oxide emissions from the ocean: a reassessment using basin-wide observations in the Atlantic. *J Geophys Res* 114, D12304. doi:10.1029/2008JD011662
- Riebesell U, Schulz KG, Bellerby RGJ, Botros M, Fritsche P, Meyerhofer M, Neill C, Nondal G, Oschlies A, Wohlers J, Zollner E (2007) Enhanced biological carbon consumption in a high CO₂ ocean. *Nature* 450:545–548
- Rigby M, Prinn RG, Fraser PJ, Simmonds PG, Langenfelds RL, Huang J, Cunnold DM, Steele LP, Krummel PB, Weiss RF, O'Doherty S, Salameh PK, Wang HJ, Harth CM, Mühle J, Porter LW (2008) Renewed growth of atmospheric methane. *Geophys Res Lett* 35, L22805. doi:10.1029/2008GL036037
- Rixen T, Haake B, Ittekkot V, Guptha MVS, Nair RR, Schlüssel P (1996) Coupling between SW monsoon-related surface and deep ocean processes as discerned from continuous particle flux measurements and correlated satellite data. *J Geophys Res* 101:28569–28582
- Robertson JE, Watson AJ (1992) Thermal skin effect of the surface ocean and its implications for CO₂ uptake. *Nature* 358:738–740
- Romanovski NN, Hubberten H-W, Gavrillov AV, Eliseeva AA, Tipenkio GS (2005) Offshore permafrost and gas hydrate stability zone on the shelf of East Siberian Seas. *Geo-Mar Lett* 25(2–3):167–182. doi:10.1007/s00367-004-0198-6
- Rost B, Riebesell U (2004) Coccolithophores and the biological pump: responses to environmental changes. In: Thierstein HR, Young JR (eds) Coccolithophores: from molecular processes to global impact. Springer, Berlin, pp 99–125
- Roy T, Bopp L, Gehlen M, Schneider B, Cadule P, Fröhlicher TL, Segsneider J, Tjiputra J, Heinze C, Joos F (2011) Regional impacts of climate change and atmospheric CO₂ on future ocean carbon uptake: a multimodel linear feedback analysis. *J Climate* 24(9):2300–2318. doi:10.1175/2010JCLI3787.1
- Rysgaard S, Bendtsen J, Delille B, Dieckmann GS, Glud R, Kennedy H, Mortensen J, Papadimitriou S, Thomas DN, Tison JL (2011) Sea ice contribution to the air–sea CO₂ exchange in the Arctic and Southern Oceans. *Tellus* 63B (5):1–8. doi:10.1111/j.1600-0889.2011.00571.x
- Sabine CL, Feely RA, Gruber N, Key RM, Lee K, Bullister JL, Wanninkhof R, Wong CS, Wallace DWR, Tilbrook B, Millero FJ, Peng T-H, Kozyr A, Ono T, Ríos AF (2004) The oceanic sink for anthropogenic CO₂. *Science* 305:367–371
- Sabine CL, Hankin S, Koyuk H, Bakker DCE, Pfeil B, Olsen A, Metz N, Kozyr A, Fassbender A, Manke A, Malczyk J, Akl J, Alin SR, Bellerby RGJ, Borges A, Boutin J, Brown PJ, Cai W-J, Chavez FP, Chen A, Cosca C, Feely RA, González-Dávila M, Goyet C, Hardman-Mountford N, Heinze C, Hoppema M, Hunt CW, Hydes D, Ishii M, Johannessen T, Key RM, Körtzinger A, Landschützer P, Lauvset SK, Lefèvre N, Lenton A, Lourantou A, Merlivat L, Midorikawa T, Mintrop L, Miyazaki C, Murata A, Nakadate A, Nakano Y, Nakaoka S, Nojiri Y, Omar AM, Padin XA, Park G-H,

- Paterson K, Perez FF, Pierrot D, Poisson A, Ríos AF, Salisbury J, Santana-Casiano JM, Sarma VVSS, Schlitzer R, Schneider B, Schuster U, Sieger R, Skjelvan I, Steinhoff T, Suzuki T, Takahashi T, Tedesco K, Telszewski M, Thomas H, Tilbrook B, Vandemark D, Veness T, Watson AJ, Weiss R, Wong CS, Yoshikawa-Inoue H (2013) Gridding of the Surface Ocean CO₂ Atlas (SOCAT) Gridded data products. *Earth Syst Sci Data* 5:145–153. doi:[10.5194/essd-5-145-2013](https://doi.org/10.5194/essd-5-145-2013)
- Santana-Casiano JM, González-Dávila M (2011) pH decrease and effects on the chemistry of seawater. In: Duarte P, Santana-Casiano JM (eds) *Oceans and the atmospheric carbon content*. Springer, Berlin, pp 95–114
- Santana-Casiano JM, González-Dávila M, Millero FJ (2006) The role of Fe(II) species on the oxidation of Fe(II) in natural waters in the presence of O₂ and H₂O₂. *Mar Chem* 99:70–82
- Santoro AE, Buchwald C, McIlvin MR, Casciotti KL (2011) Isotopic signature of N₂O produced by marine ammonia-oxidizing archaea. *Science* 333(6047):1282–1285. doi:[10.1126/science.1208239](https://doi.org/10.1126/science.1208239)
- Sarmiento JL, Gruber N (2002) Sinks for anthropogenic carbon. *Phys Today* 55:30–36
- Sarmiento JL, Gruber N (2006) *Ocean biogeochemical dynamics*. Princeton University Press, Princeton
- Sarmiento JL, Sundquist ET (1992) Revised budget for the oceanic uptake of anthropogenic carbon dioxide. *Nature* 356:589–593
- Sarmiento JL, Orr JC, Siegenthaler U (1992) A perturbation simulation of CO₂ uptake in an ocean general circulation model. *J Geophys Res* 97(C3):3621–3646
- Sarmiento JL, Dunne J, Gnanadesikan A, Key RM, Matsumoto K, Slater R (2002) A new estimate of the CaCO₃ to organic carbon export ratio. *Global Biogeochem Cycle* 16(4):1107. doi:[10.1029/2002GB001919](https://doi.org/10.1029/2002GB001919)
- Sasakawa M, Tsunogai U, Kameyama S, Nakagawa F, Nojiri Y, Tsuda A (2008) Carbon isotopic characterization for the origin of excess methane in subsurface seawater. *J Geophys Res* 113, C03012. doi:[10.1029/2007JC004217](https://doi.org/10.1029/2007JC004217)
- Schlünz B, Schneider RR (2000) Transport of terrestrial organic carbon to the oceans by rivers: re-estimating flux and burial rates. *Int J Earth Sci* 88:599–606
- Schmale O, Greinert J, Rehder G (2005) Methane emission from high intensity marine gas-seeps in the Black Sea into the atmosphere. *Geophys Res Lett* 32, L07609. doi:[10.1029/2004GL021138](https://doi.org/10.1029/2004GL021138)
- Schmidt GA, Shindell DT (2003) Atmospheric composition, radiative forcing, and climate change as a consequence of a massive methane release from gas hydrates. *Paleoceanography* 18(1):1004. doi:[10.1029/2002PA000757](https://doi.org/10.1029/2002PA000757)
- Schuster U, Watson AJ (2007) A variable and decreasing sink for atmospheric CO₂ in the North Atlantic. *J Geophys Res* 112(C11), C11006
- Schuster U, Watson AJ, Bates NR, Corbière A, González-Dávila M, Metz N, Pierrot D, Santana-Casiano M (2009) Trends in North Atlantic sea-surface fCO₂ from 1990 to 2006. *Deep-Sea Res Part II* 56(8–10):620–629
- Scranton MI, McShane K (1991) Methane fluxes in the southern North Sea: the role of European rivers. *Cont Shelf Res* 11:37–52
- Seitzinger SP, Kroeze C (1998) Global distribution of nitrous oxide production and N inputs in freshwater and coastal marine ecosystems. *Global Biogeochem Cycle* 12:93–113
- Seitzinger SP, Kroeze C, Bouwman AE, Caraco N, Dentener F, Styles RV (2002) Global patterns of dissolved inorganic and particulate nitrogen inputs to coastal systems. *Estuaries* 25:640–655
- Shakhova N, Semiletov I (2007) Methane release and coastal environment in the East Siberian Arctic shelf. *J Mar Syst* 66:227–243
- Shakhova N, Semiletov I, Salyuk AN, Belcheva N, Kosmach D (2007) Methane anomalies in the near-water atmospheric layer above the shelf of East Siberian Arctic Shelf. *Trans Russ Acad Sci* 415:764–768
- Shakhova N, Semiletov I, Salyuk A, Yusupov V, Kosmach D, Gustafsson O (2010) Extensive methane venting to the atmosphere from sediments of the East Siberian Arctic Shelf. *Science* 327:1246–1250. doi:[10.1126/science.1182221](https://doi.org/10.1126/science.1182221)
- Silverman J, Lazar B, Cao L, Caldeira K, Erez J (2009) Coral reefs may start dissolving when atmospheric CO₂ doubles. *Geophys Res Lett* 36, L05606. doi:[10.1029/2008GL036282](https://doi.org/10.1029/2008GL036282)
- Sloan ED (2003) Fundamental principles and applications of natural gas hydrates. *Nature* 426:353–363. doi:[10.1038/nature02135](https://doi.org/10.1038/nature02135)
- Sloan ED, Koh CA (2008) *Clathrate hydrates of natural gases*, 3rd edn. CRC Press, Boca Raton
- Smith SV, Hollibaugh JT (1993) Coastal metabolism and the oceanic carbon balance. *Rev Geophys* 31:75–89
- Smith SV, Mackenzie FT (1987) The ocean as a net heterotrophic system: implications from the carbon biogeochemical cycle. *Global Biogeochem Cycles* 1:187–198
- Smith SV, Swaney DP, Talaue-McManus L, Bartley JD, Sandhei PT, McLaughlin CJ, Dupra VC, Crossland CJ, Buddemeier RW, Maxwell BA, Wulff F (2003) Humans, hydrology, and the distribution of inorganic nutrient loading to the ocean. *Bioscience* 53:235–245
- Sowers TA, Alley R, Jubenville J (2003) Elemental and isotopic records of atmospheric nitrous oxide covering the last 106,000 years from the GISP II and Taylor Dome ice cores. *Science* 301:945–948
- Spahni R, Chappellaz J, Stocker TF, Loulergue L, Hausamann G, Kawamura K, Flückiger J, Schwander J, Raynaud D, Masson-Delmotte V, Jouzel J (2005) Atmospheric methane and nitrous oxide of the late Pleistocene from Antarctic ice cores. *Science* 310(5752):1317–1321
- Stramma L, Johnson GC, Sprintall J, Mohrholz V (2008) Expanding oxygen-minimum zones in the tropical oceans. *Science* 320:655–658
- Stramma L, Schmidtko S, Levin A, Johnson GC (2010) Ocean oxygen minima expansions and their biological impacts. *Deep-Sea Res Part I* 57(4):587–595
- Suntharalingam P, Sarmiento JL (2000) Factors governing the oceanic nitrous oxide distribution: simulations with an ocean general circulation model. *Global Biogeochem Cycle* 14:429–454
- Suykens K, Delille B, Chou L, De Bodt C, Harlay J, Borges AV (2010) Dissolved inorganic carbon dynamics and air-sea carbon dioxide fluxes during coccolithophore blooms in the northwest European continental margin (northern Bay of Biscay). *Global Biogeochem Cycle* 24, GB3022. doi:[10.1029/2009GB003730](https://doi.org/10.1029/2009GB003730)
- Suzuki A, Kawahata K (2004) Reef water CO₂ system and carbon production of coral reefs: topographic control of system-level performance. In: Shiyomi M, Kawahata H,

- Koizumi H, Tsuda A, Awaya Y (eds) Global environmental change in the ocean and on land. Terrapub, Tokyo, pp 229–248
- Suzuki T, Ishii M, Aoyama M, Christian JR, Enyo K, Kawano T, Key RM, Kosugi N, Kozyr A, Miller LA, Murata A, Nakano T, Ono T, Saino T, Sasaki K, Sasano D, Takatani Y, Wakita M, Sabine CL (2013) PACIFICA Data Synthesis Project. ORNL/CDIAC-159, NDP-092. Carbon Dioxide Information Analysis Center, Oak Ridge National Laboratory, U.S. Department of Energy, Oak Ridge, Tennessee, USA. doi:10.3334/CDIAC/OTG.PACIFICA_NDP092
- Sweeney C, Gloor E, Jacobson AR, Key RM, McKinley G, Sarmiento JL, Wanninkhof R (2007) Constraining global air-sea gas exchange for CO₂ with recent bomb ¹⁴C measurements. *Global Biogeochem Cycle* 21, GB2015. doi:10.1029/2006GB002784
- Takahashi T, Feely RA, Weiss RF, Wanninkhof RH, Chipman DW, Sutherland SC, Takahashi TT (1997) Global air-sea flux of CO₂: an estimate based on measurements of sea-air pCO₂ difference. *Proc Natl Acad Sci USA* 94:8292–8299
- Takahashi T, Sutherland SC, Sweeney C, Poisson A, Metzl N, Tilbrook B, Bates N, Wanninkhof RH, Feely RA, Sabine CL, Olafsson J, Nojiri Y (2002) Global sea-air CO₂ flux based on climatological surface ocean pCO₂, and seasonal biological and temperature effects. *Deep-Sea Res Part II* 49:1601–1622
- Takahashi T, Sutherland SC, Wanninkhof R, Sweeney C, Feely RA, Chipman DW, Hales B, Friederich G, Chavez F, Sabine C, Watson AJ, Bakker DCE, Schuster U, Metzl N, Inoue HY, Ishii M, Midorikawa T, Nojiri Y, Koertzing A, Steinhoff T, Hoppema J, Olafsson J, Arnarson TS, Tilbrook B, Johannessen T, Olsen A, Bellerby R, Wong CS, Delille B, Bates NR, de Baar HJW (2009) Climatological mean and decadal change in surface ocean pCO₂, and net sea-air CO₂ flux over the global oceans. *Deep-Sea Res Part II* 56:544–577. doi:10.1016/j.dsr2.2008.12.009
- Takahashi T, Sutherland SC, Kozyr A (2011) Global ocean surface water partial pressure of CO₂ database: Measurements performed during 1957–2010 (Version 2010). ORNL/CDIAC-159, NDP-088(V2010). Carbon Dioxide Information Analysis Center, Oak Ridge Nat. Lab., US Department of Energy, Oak Ridge, Tenn, doi:10.3334/CDIAC/otg.ndp088(V2010)
- Tanhua T, van Heuven S, Key RM, Velo A, Olsen A, Schirnack C (2010) Quality control procedures and methods of the CARINA database. *Earth Syst Sci Data* 2:35–49. doi:10.5194/essd-2-35-2010
- Telszewski M, Chazottes A, Schuster U, Watson AJ, Moulin C, Bakker DCE, González-Dávila M, Johannessen T, Körtzinger A, Lüger H, Olsen A, Omar A, Padin XA, Ríos A, Steinhoff T, Santana-Casiano M, Wallace DWR, Wanninkhof RH (2009) Estimating the monthly pCO₂ distribution in the North Atlantic using a self-organizing neural network. *Biogeosciences* 6:1405–1421. <http://www.biogeosciences.net/6/1405/2009>
- Thomas H, Bozec Y, Elkalay K, de Baar HJW (2004) Enhanced open ocean storage of CO₂ from shelf sea pumping. *Science* 304(5673):1005–1008
- Thomas H, Prowe F, van Heuven S, Bozec Y, de Baar HJW, Schiettecatte L-S, Suykens K, Koné M, Borges AV, Lima ID, Doney SC (2007) Rapid decline of the CO₂ buffering capacity in the North Sea and implications for the North Atlantic Ocean. *Global Biogeochem Cycle* 21, GB4001. doi:10.1029/2006GB002825
- Thomas H, Prowe AEF, Lima I, Doney SC, Wanninkhof R, Greatbatch RJ, Schuster U, Corbière A (2008) Changes in the North Atlantic Oscillation influence CO₂ uptake in the North Atlantic over the past 2 decades. *Global Biogeochem Cycle* 22, GB4027. doi:10.1029/2007GB003167
- Tréhu AM, Long PE, Torres ME, Bohrmann G, Rackd FR, Collette TS, Goldberg DS, Milkov AV, Riedel M, Schultheiss P, Bangsj NL, Barr SR, Borowski WS, Claypool GE, Delwiche ME, Dickson GR, Graciar E, Guerin G, Holland M, Johnson JE, Leer Y-J, Lius C-S, Sut X, Teichert B, Tomaruv H, Vannestew M, Watanabe M, Weinberg JL (2004) Three-dimensional distribution of gas hydrate beneath southern Hydrate Ridge: constraints from ODP Leg 204. *Earth Planet Sci Lett* 222:845–862
- Tsai W, Liu K-K (2003) An assessment of the effect of sea surface surfactant on global atmosphere–ocean CO₂ flux. *J Geophys Res* 108:3127. doi:10.1029/2000JC000740
- Tsunogai S, Watanabe S, Sato T (1999) Is there a “continental shelf pump” for the absorption of atmospheric CO₂? *Tellus* 51B(3):701–712
- Uncles RJ, Stephens JA (1993) The freshwater-saltwater interface and its relationship to the turbidity maximum in the Tamar estuary, United Kingdom. *Estuaries* 16:126–141. doi:10.2307/1352770
- Upstill-Goddard RC (2006) Air-sea exchange in the coastal zone. *Estuar Coast Shelf Sci* 70:388–404
- Upstill-Goddard RC (2011) The production of trace gases in the estuarine and coastal environment. In: Wolanski E, McLusky DS (eds) *Treatise on estuarine and coastal science*, vol 2, *Geochemistry of estuaries and coasts*. Elsevier, Amsterdam, pp 271–309
- Upstill-Goddard RC, Owens NJP, Barnes J (1999) Nitrous oxide and methane during the 1994 SW monsoon in the Arabian Sea/northwestern Indian Ocean. *J Geophys Res* 104:30067–30084
- Upstill-Goddard RC, Barnes J, Frost T, Punshon S, Owens NJP (2000) Methane in the southern North Sea: low-salinity inputs, estuarine removal, and atmospheric flux. *Global Biogeochem Cycle* 14:1205–1217
- Van der Nat F-JWA, Middelburg JJ (1998) Seasonal variation in methane oxidation by the rhizosphere of *Phragmites australis* and *Scirpus lacustris*. *Aquat Bot* 61(2):95–110
- Van der Nat F-JWA, Middelburg JJ (2000) Methane emission from tidal freshwater marshes. *Biogeochemistry* 49(2):103–121
- Van der Nat F-JWA, Middelburg JJ, Van Meteren D, Wielemakers A (1998) Diel methane emissions patterns from *Scirpus lacustris* and *Phragmites australis*. *Biogeochemistry* 41:1–22
- Van Scoy KA, Morris KP, Robertson JE, Watson AJ (1995) Thermal skin effect and the air-sea flux of carbon dioxide: a seasonal high-resolution estimate. *Global Biogeochem Cycle* 9(2):253–262
- Volk T, Hoffert MI (1985) Ocean carbon pumps: analysis of relative strengths and efficiencies in ocean-driven atmospheric CO₂ changes. In: Sundquist E, Broecker WS (eds) *The carbon cycle and atmospheric CO₂: natural variations Archean to present*, vol 32, *American Geophysical Union*

- Geophysical Monograph. American Geophysical Union, Washington, DC, pp 99–110
- Wakelin SL, Holt JT, Blackford JC, Allen JI, Butenschön M, Artioli Y (2012) Modeling the carbon fluxes of the northwest European continental shelf: validation and budgets. *J Geophys Res* 117, C05020. doi:10.1029/2011JC007402
- Walsh JJ (1988) On the nature of continental shelves. Academic Press, San Diego
- Walter S, Bange HW, Breitenbach U, Wallace DWR (2006) Nitrous oxide in the North Atlantic Ocean. *Biogeosciences* 3:607–619
- Wanninkhof RH (1992) Relationship between wind speed and gas exchange over the ocean. *J Geophys Res* 97(C5):7373–7382
- Wanninkhof RH, McGillis WR (1999) A cubic relationship between air-sea CO₂ exchange and wind speed. *Geophys Res Lett* 26(13):1889–1892
- Wanninkhof RH, Asher WE, Ho DT, Sweeney C, McGillis WR (2009) Advances in quantifying air-sea gas exchange and environmental forcing. *Annu Rev Mar Sci* 1:213–244
- Watson AJ, Orr JC (2003) Carbon dioxide fluxes in the global ocean. In: Fasham MJR (ed) *Ocean biogeochemistry: a JGOFS synthesis*, Global change. IGBP series. Springer, Berlin, pp 123–143
- Watson AJ, Schuster U, Bakker DCE, Bates N, Corbière A, González-Dávila M, Friedrich T, Hauck J, Heinze C, Johannessen T, Körtzinger A, Metzl N, Olafsson J, Oschlies A, Pfeil B, Olsen A, Oschlies A, Santano-Casiano JM, Steinhoff T, Telszewski M, Ríos A, Wallace DWR, Wanninkhof RH (2009) Tracking the variable North Atlantic sink for atmospheric CO₂. *Science* 326(5958):1391–1393
- Wayne RP (2000) *Chemistry of atmospheres*, 3rd edn. Oxford University Press, Oxford, 775 pp
- WDCGG (2012) World Meteorological Organization (WMO) Global Atmosphere Watch (GAW) Data. Greenhouse gases and other atmospheric gases. WMO WDCGG (World Data Centre for Greenhouses Gases) 36(4). Japan Meteorological Agency and the WMO, Tokyo, p. 100
- Weiss RF (1974) Carbon dioxide in water and seawater: the solubility of a non-ideal gas. *Mar Chem* 2:203–205
- Weiss RF, Van Woy FA, Salameh PK (1992) Surface water and atmospheric carbon dioxide and nitrous oxide observations by shipboard automated gas chromatography: Results from expeditions between 1977 and 1990. Scripps Institution of Oceanography reference 92–11, ORNL/CDIAC-59, NDP-044, Carbon Dioxide Information Analysis Center, Oak Ridge National Laboratory, US Department of Energy, Oak Ridge, Tennessee, USA
- Westbrook GK, Thatcher KE, Rohling EJ, Piotrowski AM, Palike H, Osborne AH, Nisbet EG, Minshull TA, Lanoiselle M, James RH, Huhnerbach V, Green D, Fisher RE, Crocker AJ, Chabert A, Bolton C, Beszczynska-Moller A, Berndt C, Aquilina A (2009) Escape of methane gas from the seabed along the West Spitsbergen continental margin. *Geophys Res Lett* 36, L15608. doi:10.1029/2009GL039191
- Wetzel P, Winguth A, Maier-Reimer E (2005) Sea-to-air fluxes CO₂ fluxes from 1948 to 2003: a model study. *Global Biogeochem Cycle* 19, GB2005. doi:10.1029/2004GB002339
- Wever TF, Abegg F, Fiedler HM, Fechner G, Stender IH (1998) Shallow gas in the muddy sediments of Eckernförde Bay, Germany. *Cont Shelf Res* 18:1715–1739
- Wittke F, Kock A, Bange HW (2010) Nitrous oxide emissions from the upwelling off Mauritania (NW Africa). *Geophys Res Lett* 37, L12601. doi:10.1029/2010GL042442
- Wollast R (1998) Evaluation and comparison of the global carbon cycle in the coastal zone and in the open ocean. In: Brink KH, Robinson AR (eds) *The global coastal ocean*. Wiley, New York, pp 213–252
- Wollast R, Chou L (2001) The carbon cycle at the ocean margin in the northern Gulf of Biscay. *Deep-Sea Res Part II* 48:3265–3293
- Wong CS, Christian JR, Wong S-KE, Page J, Xie L, Johannessen S (2010) Carbon dioxide in surface sea water of the eastern North Pacific Ocean (Line P), 1973–2005. *Deep-Sea Res Part I* 57:687–695
- Woodwell GM, Rich PH, Hall CAS (1973) Carbon in estuaries. In: Woodwell GM, Pecan EV (eds) *Carbon and the biosphere*. United States Atomic Energy Commission, Springfield, pp 221–240
- Wuchter C, Abbas B, Coolen MJL, Herfort L, van Bleijswijk J, Timmers P, Strous M, Teira E, Herndl GJ, Middelburg JJ, Schouten S, Damste JSS (2006) Archaeal nitrification in the ocean. *Proc Natl Acad Sci USA* 103(33):12317–12322
- Wuchter C, Abbas B, Coolen MJL, Herfort L, van Bleijswijk J, Timmers P, Strous M, Teira E, Herndl GJ, Middelburg JJ, Schouten S, Damste JSS (2007) Archaeal nitrification in the ocean (vol 103, pg 12317, 2006). *Proc Natl Acad Sci USA* 104(13):5704–5704
- Yavitt JB, Fahey TJ (1991) Production of methane and nitrous oxide by organic soils within a northern hardwood forest ecosystem. In: Oremland RS (ed) *Biogeochemistry of global change: radiatively active trace gases*. Chapman and Hall, New York, pp 261–277
- Yoshida O, Inoue HY, Watanabe S, Suzuki K, Noriki S (2011) Dissolved methane distribution in the South Pacific and the Southern Ocean in austral summer. *J Geophys Res* 116, C07008. doi:10.1029/2009JC006089
- Zhang G-L, Zhang J, Liu SM, Ren J-L, Xu J, Zhang F (2008) Methane in the Changjiang (Yangtze River) Estuary and its adjacent marine area: riverine input, sediment release and atmospheric fluxes. *Biogeochemistry* 91:71–84
- Zhang G-L, Zhang J, Liu S-M, Ren J-L, Zhao Y-C (2010) Nitrous oxide in the Changjiang (Yangtze River) estuary and its adjacent marine area: riverine input, sediment release and atmospheric fluxes. *Biogeosciences* 7:3505–3516
- Zumft WG (1997) Cell biology and molecular basis of denitrification. *Microbiol Mol Biol Rev* 61:533–616